

# Development of a topical ocular drug delivery system using polymeric nanoparticles

by

Shengyan Liu

A thesis  
presented to the University of Waterloo  
in fulfillment of the  
thesis requirement for the degree of  
Doctor of Philosophy  
in  
Chemical Engineering

Waterloo, Ontario, Canada, 2016

©Shengyan Liu 2016

## **AUTHOR'S DECLARATION**

I hereby declare that I am the sole author of this thesis. This is a true copy of the thesis, including any required final revisions, as accepted by my examiners.

I understand that my thesis may be made electronically available to the public.

## Abstract

Common eye diseases such as dry eye syndrome affect 15% of the population. Although eye drops are the most common treatment for these diseases, over 95% of the drugs applied through eye drops are quickly cleared away due to blinking and tear turnover. Consequently, patients struggle with the multiple daily applications required and the resulting side effects.

Nanoparticle (NP) drug carriers have gained significant traction recently because of several advantages they provide over conventional eye drop delivery methods. NP surfaces can be tuned to achieve specific properties such as binding affinity towards the ocular surface. NPs can also carry a large amount of drugs and release them in a sustained manner over a long period. Due to their small size, NPs do not cause abrasive sensations on the eye upon patient application. With these unique advantages, NP drug carriers may drastically improve patient compliance while reducing side effects.

The thesis focuses on developing an ocular drug delivery platform using NPs to improve retention of ocular therapeutics on the precorneal surface. We developed a method to synthesize an amphiphilic block copolymer composed of poly(D,L-lactide) (PLA) and dextran (Dex) that can self-assemble into NP drug carriers. The size of the NPs can be tuned between 15 and 70 nm by adjusting the molecular weights of PLA and/or Dex. The PLA-b-Dex NPs form the foundation of the ocular drug delivery platform developed in this thesis.

A targeted delivery system is crucial for ocular drug delivery due to the rapid clearance by tear drainage on the corneal surface. The PLA-b-Dex NPs were surface modified with phenylboronic acid (PBA) molecules, which can undergo covalent binding with the mucous membrane to circumvent the rapid clearance. Due to the abundance of functional groups on the dextran, we were able to tune the density of PBA on the NP surface to optimize the binding affinity between the NPs and the mucin. While maximizing the PBA density on the NP surface improved the covalent interaction between the NPs and the mucin, it also compromised the NP colloidal stability. The PBA modified NPs demonstrated encapsulation of Cyclosporine A (CsA), a dry eye treatment drug, and sustained release for up to 5 days *in vitro*, showing their potential as a long-term eye drop delivery platform.

We then performed biocompatibility and efficacy studies on these NPs using animal models. Biocompatibility is of the utmost importance in developing new drug delivery formulations. During the 12 weeks of study, no physical signs of irritation or discomfort were detected nor was any inflammatory response or ocular tissue damage observed in the eyes administered with NPs. Topical administration

of CsA-loaded NPs on dry eye induced mice using once a week dosing demonstrated complete elimination of the inflammatory response as well as full recovery of the integrity of the ocular tissues. In the same study, the commercial eye drop form of CsA, Restasis®, administered thrice daily only eliminated the inflammatory infiltrates without recovering ocular goblet cells. By delivering CsA through PLA-b-Dex-g-PBA NPs, we can significantly reduce the dose and the frequency of eye drop administration without compromising the treatment efficacy.

*In vitro* mucoadhesion as a result of PBA's on NP surfaces was demonstrated. We proceeded to further demonstrate this mucoadhesion using *in vivo* models. Indocyanine green (ICG), a near-infrared fluorescent dye, was encapsulated in the NPs and administered to rabbit eyes to track its ocular retention. ICG delivered via PBA modified NPs showed ocular retention beyond 24 hours on rabbit eyes, whereas free ICG or ICG delivered via unmodified NPs were mostly cleared within the first 3 hours. When the weekly dosing of CsA loaded PLA-b-Dex-g-PBA NPs was repeated for 4 weeks on dry eye induced mice, we observed the same elimination of inflammatory infiltrates but also the damaged ocular tissue structures. When the concentration of the CsA in the weekly dosing of NPs was further reduced 5 times, the treatment effect was much more pronounced, showing both the elimination of the inflammation and the full recovery of the ocular surface tissues. Overall, by using mucoadhesive nanoparticle drug carriers, we reduced the dosage of CsA at least 50-fold compared with the commercial product, Restasis®, without compromising the dry eye treatment efficacy.

Finally, we developed a scalable method to synthesize PLA-b-Dex-g-PBA block copolymers using a semi-solid state reaction chemistry. The previous method of conjugating PBA to the Dex required long reaction hours with multiple reaction and purification steps. In contrast, the new method combines the quickness of a semi-solid state reaction with the simplicity of a Williamson ether chemistry to graft PBA to Dex. The results showed that the new method achieved a similar range of tunability of PBA density onto Dex using reaction times as short as 10 minutes.

This thesis demonstrates the development process of a polymeric NP as a topical ocular drug delivery system. The PLA-b-Dex-g-PBA NPs demonstrated delivery of a clinically relevant dosage of dry eye therapeutics, controlled release of therapeutics over prolonged period of time, and mucoadhesive properties resulting in prolonged ocular surface retention of drugs. These mucoadhesive NPs show remarkable promise as a long-term topical ocular drug delivery system that significantly reduces the dose and the administration frequency of the eye drops while minimizing side effects.

## Acknowledgements

First of all, I would like to express my deepest gratitude to my supervisor, Professor Frank Gu, for his advice, mentorship, and support. I was extremely lucky to have landed myself in his research group; that I was given the opportunity to perform the type of research that I did was far beyond my expectations. He not only helped me become an effective researcher and a project leader, but he also helped me become a better human being. I am immensely indebted to him for all his support and belief in my career. I would also like to extend my deepest gratitude to my external mentor Professor Lyndon Jones who has gone above and beyond to support me with his incredible amount of knowledge and intellectual resources. He has been instrumental in shaping the focus and direction of my research.

I also would like to acknowledge my thesis committee members, Professor Pu Chen, Professor Vivek Maheshwari, and Professor Neil McManus, for their constructive feedback, guidance and encouragement of my research. I am also grateful to my external committee member Professor Przemyslaw (Mike) Sapiiha for participating in the thesis defense.

I would like to acknowledge the help that I received from various research groups and individuals who have positively influenced the execution of my thesis research. I would like to thank Dr. Parisa Sadatmousavi and Frank (Yong) Ding from Professor Pu Chen's group for training and helping me with zeta potential measurements and fluorescence spectrometry. I would like to thank Miriam Heynen from Professor Lyndon Jones group for helping me with high-performance liquid chromatography (HPLC). I would also like to thank Dr. Ulli Stahl, Dr. Jill Woods, and Alex Muntz, also from Professor Lyndon Jones' group for training and helping me with slit-lamp examination experiments. I would like to thank Dr. Denise Hileeto for performing histopathology analysis for my *in vivo* experiments. My *in vivo* experiments would not have been possible at all if not for the endless support provided by the animal care committee members from University of Waterloo: Dr. Maureen Nummelin, Nancy Gibson, Jean Flanagan, Martin Ryan, and Cindy Futher. I would also like to thank Dr. Shelley Boyd's group, Dr. Shelley Boyd, Huiyuan Liang, and Matthew-Mina Reyad at Keen Research Centre (St. Michael's Hospital, Toronto) for their help with the ocular retention study of nanoparticle drug carriers. Last but not least, I would like to also thank Dr. Ariel Chan for her guidance on the development of semi-solid state reactions to enhance the block copolymer synthesis for topical ocular drug delivery applications.

From within our research group, I am forever indebted to the support from all lab members who have helped me with numerous experiments throughout my PhD career. My gratitude goes to the co-op

students who worked with me: Matthew Dozois, Chu Ning Chang, Mostafa Saquib, Rajan Anderson, Deborah Ng, Kristen Blowes, Aya Tsugimatsu, Paul Chen, Yih Yang Chen, Ameena Meerasa, and Farzana Yusafali, and to my fellow graduate students: Jasper Huang, Mohit Verma, Sarah LeBlanc, Erin Bedford, Timothy Leshuk, Stuart Linley, Jiang Xu, Peter Lin, Benjamin Lehtovaara, Drew Davidson, David Wulff, and Aaminah Ahmad.

I could not have asked for better friends and family who have shown me unwavering faith in my career. I am forever indebted to their support and compassion.

Finally, I would like to acknowledge the numerous organizations and their financial support for my thesis: Natural Sciences and Engineering Research Council of Canada (NSERC) Postgraduate Scholarship, Ontario Graduate Scholarship (OGS), Waterloo Institute of Nanotechnology (WIN) fellowship, University of Waterloo Faculty of Engineering President's Graduate Scholarship. I also want to thank 20/20 NSERC- Ophthalmic Materials Network and AmorChem for financial support for the research and development.

## Dedication

To my mother, Shunfu Jin, and my father, Zhongjiu Liu.

## Table of Contents

AUTHOR'S DECLARATION.....	ii
Abstract.....	iii
Acknowledgements.....	v
Dedication.....	vii
Table of Contents.....	viii
List of Figures.....	xii
List of Tables.....	xvi
Chapter 1 INTRODUCTION.....	1
1.1 Overview.....	1
1.2 Research objectives.....	2
1.3 Thesis outline.....	3
Chapter 2 LITERATURE REVIEW.....	5
2.1 The field of ocular drug delivery.....	5
2.2 Challenges of conventional ocular drug delivery system.....	7
2.3 Contact lenses in ocular drug delivery.....	9
2.4 Nanomaterials in ocular drug delivery.....	10
2.5 Nanomaterial-based ophthalmic formulation currently in the clinical stages.....	11
2.6 Recent developments of nanomaterials in ophthalmic formulations.....	14
2.6.1 Polymeric micelles.....	14
2.6.2 Hydrogels.....	17
2.6.3 Liposomes.....	18
2.6.4 Niosomes.....	20
2.6.5 Dendrimers.....	21
2.6.6 Cyclodextrins.....	22
2.7 Future perspectives.....	23
Chapter 3 Development of nanoparticle drug carriers using PLA-Dex block copolymers.....	24
3.1 Summary.....	24
3.2 Introduction.....	24
3.3 Experimental Section.....	25
3.3.1 Materials.....	25
3.3.2 Synthesis of PLA-Dex block copolymer.....	26



3.3.3 Characterization of PLA-Dex NPs .....	27
3.3.4 Doxorubicin encapsulation in PLA-Dex NPs.....	28
3.3.5 <i>In vitro</i> release of Doxorubicin from PLA-Dex NPs.....	28
3.4 Results and Discussion.....	29
3.4.1 <sup>1</sup> H NMR characterization of PLA-Dex.....	29
3.4.2 Size and morphology of the PLA-Dex NPs.....	29
3.4.3 Drug encapsulation and release .....	30
3.5 Conclusion.....	31
Chapter 4 Mucoadhesive nanoparticles for topical ocular drug delivery .....	32
4.1 Summary .....	32
4.2 Introduction .....	32
4.3 Experimental Section.....	33
4.3.1 Materials .....	33
4.3.2 Surface functionalization of PLA-Dex NPs with PBA.....	34
4.3.3 Characterization of PLA-Dex_PBA .....	34
4.3.4 Cyclosporine A encapsulation and <i>in vitro</i> release.....	34
4.3.5 <i>In vitro</i> mucoadhesion .....	34
4.4 Results and Discussion.....	35
4.4.1 Synthesis and characterization of PBA functionalized PLA-Dex NPs .....	35
4.4.2 Cyclosporine A encapsulation and <i>in vitro</i> release.....	36
4.4.3 <i>In vitro</i> Mucoadhesion.....	38
4.5 Conclusion.....	39
Chapter 5 Phenylboronic acid modified mucoadhesive nanoparticle drug carriers facilitate weekly treatment of experimentally-induced dry eye syndrome .....	40
5.1 Summary .....	40
5.2 Introduction .....	40
5.3 Experimental .....	42
5.3.1 Materials .....	42
5.3.2 Synthesis of PLA-b-Dex and surface modification with PBA .....	42
5.3.3 Characterization of PLA-b-Dex-g-PBA NPs .....	43
5.3.4 Animal studies.....	43
5.3.5 <i>In vivo</i> ocular irritancy test .....	43

5.3.6 Histopathology .....	44
5.3.7 Experimental dry eye model – <i>in vivo</i> efficacy test .....	44
5.4 Results and Discussion .....	45
5.4.1 Characterization of PLA-b-Dex-g-PBA NPs .....	45
5.4.2 <i>In vivo</i> ocular irritancy test .....	47
5.4.3 <i>In vivo</i> efficacy test – experimental dry eye.....	52
5.5 Conclusion .....	58
Chapter 6 Cyclosporine A loaded mucoadhesive nanoparticle eye-drop formulation enhances long term treatment of experimental dry eye in mice using a weekly dosing regimen.....	59
6.1 Summary .....	59
6.2 Introduction.....	60
6.3 Experimental.....	62
6.3.1 Materials .....	62
6.3.2 Nanoparticle formulation, and encapsulation and <i>in vitro</i> release of Cyclosporine A.....	63
6.3.3 Animal studies .....	64
6.3.4 Ocular surface retention study on NZW rabbits .....	64
6.3.5 Dry eye induction and nanoparticle administration on C57BL/6 mice.....	65
6.3.6 Tear production measurement.....	65
6.3.7 Corneal fluorescein staining.....	66
6.3.8 Histopathology analysis .....	66
6.4 Results.....	66
6.4.1 Nanoparticle formulation .....	66
6.4.2 Ocular surface retention study .....	67
6.4.3 Tear production and corneal fluorescein clearance on C57BL/6 mice .....	69
6.4.4 Histopathology analysis .....	71
6.5 Discussion .....	74
6.6 Conclusion .....	76
Chapter 7 A novel method for chemically modifying carbohydrates using a semi-solid state reaction .....	77
7.1 Summary .....	77
7.2 Introduction.....	77
7.3 Experimental.....	78

7.3.1 Materials .....	78
7.3.2 A semi-solid state chemistry to chemically modify dextran with 4-(bromomethyl)phenylboronic acid .....	79
7.4 Application of the semi-solid state chemistry in synthesizing BPBA modified dextran based nanoparticles.....	80
7.5 Results and discussion.....	80
7.5.1 Conjugation of BPBA onto dextran using semi-solid state chemistry .....	80
7.5.2 Effect of the reaction time and the temperature.....	81
7.5.3 Effect of the ratio of the reactants .....	82
7.5.4 Application of the semi-solid state chemistry in synthesizing BPBA modified dextran based nanoparticles.....	84
7.6 Conclusion.....	86
Chapter 8 Conclusions and Future Work .....	87
8.1 Summary .....	87
8.2 Conclusions .....	87
8.3 Recommendations for future work.....	89
Appendix A Covalent linkage between phenylboronic acid and sialic acid for mucoadhesive targeting .....	91
Bibliography .....	92

## List of Figures

Figure 1. A schematic illustration of different nanomaterial-based ocular drug delivery systems. Polymeric micelles are nanoparticles self-assembled from amphiphilic copolymers with the ability to encapsulate hydrophobic drugs in the core of the particles. Hydrogel colloids are 3D network of water-soluble polymers which have the ability to incorporate hydrophilic drugs in the 3D network. Liposomes/niosomes are vesicle structures with both lipophilic and hydrophilic phases, and therefore can encapsulate both hydrophobic and hydrophilic drug components. Dendrimers are 3D highly branched tree-structured macromolecules that can encapsulate hydrophobic drug molecules since they possess internal empty cavities and open conformations for low generation dendrimers. Cyclodextrins are a family of cyclic oligosaccharides, composed of 6 to 8 glucose units which have been shown to improve pharmacokinetic properties of many drugs through formation of inclusion complex.[1] ..... 6

Figure 2. The anatomy of the eye illustrating various ocular barriers and various mechanisms of drug delivery: 1. Topical administration, 2. Intravitreal injection, 3. Periocular injections (3a. sub-conjunctival, 3b. peribulbar, 3c. sub-tenon, 3d. retrobulbar), and 4. Systemic administration.[1] ..... 8

Figure 3. Schematic of nanoparticle-laden lens inserted in the eye (Reproduced with permission from[2])..... 10

Figure 4. Schematic representation of the interaction between the thiolated NLCs and mucus (Reproduced with permission from [3])..... 17

Figure 5. Synthesis of Dex-*b*-PLA block copolymers. a) Synthesis of Dextran-NH-Et-NH-Boc. Conditions: NaCNBH<sub>3</sub> in Borate buffer (pH 8.2) for 72 hr at RT in dark. b): Synthesis of Dextran-NH-Et-NH<sub>2</sub>. Conditions: HCl/TEA in DI-H<sub>2</sub>O for 1hr each at RT. c): Synthesis of Dextran-NH-Et-NH-PLA. Conditions: EDC/Sulfo-NHS RT for 4hrs..... 27

Figure 6. <sup>1</sup>H NMR of I. Dextran (10 kDa), II. Dextran-Ethylenediamine-Boc, III. Dextran-Ethylenediamine, IV. PLA (20 kDa), V. PLA-Dex (PLA20-Dex10).[4] ..... 29

Figure 7. Particle size and morphology of PLA-Dex NPs: a) Effect of MW's of PLA and Dextran on the sizes of the NPs formed from nine different polymers; b) TEM image of PLA20-Dex6 (MW<sub>PLA</sub> = 20 kDa, MW<sub>DEX</sub> = 6 kDa).[4] ..... 30

Figure 8. Drug encapsulation and release: Doxorubicin loading in PLA-Dex and PLGA-PEG NPs (left), and Doxorubicin in vitro release profiles (right).[4]..... 31

Figure 9. <sup>1</sup>H NMR characterization of PLA-Dex\_PBA. .... 35

Figure 10. TEM imaging of PLA-Dex\_320PBA NPs. .... 36

Figure 11. a) CycA loading and b) In vitro release from PBA modified and unmodified NPs. .... 38

Figure 12. Schematic illustration of the self-assembly process to form Cyclosporine A loaded PLA-b-Dex-g-PBA nanoparticles, and the mucoadhesion mechanism of the grafted PBA's. .... 46

Figure 13. TEM image of PLA-b-Dex-g-PBA NPs. .... 47

Figure 14. In vivo acute ocular irritancy test grading obtained through slit-lamp examination. .... 48

Figure 15. Histopathology analysis of both NP administered and control eyes in in vivo acute ocular irritancy test reveal no significant differences in the corneal and conjunctival morphological characteristics and architecture. The scale bars (black) are 500  $\mu\text{m}$  in length. .... 49

Figure 16. In vivo chronic ocular irritancy test for weekly administration of NP formulation for up to 12 weeks (each data point shown as mean  $\pm$  s.e.m. (standard errors of mean); n = 5). .... 50

Figure 17. In vivo chronic ocular irritancy test of weekly administration of NP+CycA formulation for up to 12 weeks (each data point shown as mean  $\pm$  s.e.m.; n = 4). .... 51

Figure 18. Histopathology study after in vivo chronic ocular irritancy tests with weekly administration of NP and NP+CycA. NP (-) and NP+CycA (-) represent the contralateral control eyes of the rabbits administered with NP or NP+CycA formulations. The scale bars (black) are 500  $\mu\text{m}$  in length unless otherwise specified. .... 52

Figure 19. Tear volume measurements of 7 different treatment groups at 4 time points: before dry eye (DE) induction (day 1), before 1st administration (day 5), before 2nd administration (day 8), and before histopathology (day 12). Each data point is shown as mean  $\pm$  s.e.m., n = 6. Statistical symbols for t-test: † for  $0.05 < p \leq 0.1$ , \* for  $0.01 < p \leq 0.05$ , \*\* for  $0.001 < p \leq 0.01$ , and \*\*\* for  $p < 0.001$ . .... 54

Figure 20. Corneal fluorescein staining images of 7 different treatment groups obtain at 4 time points: before dry eye (DE) induction (day 1), before 1st administration (day 5), before 2nd administration (day 8), and before histopathology (day 12). The images were obtained 10 minutes after the application of sodium fluorescein. Note that the corneal fluorescein present on the edges of the lids were due to the local structure and has little to do with the tear production or ocular surface damage, thus they were not taken into consideration for the fluorescein clearance analysis. .... 55

Figure 21. Histopathology analysis of ocular tissues of mice after 7 different treatment types: A) Healthy, experimental dry eye treated with B) Saline (1/wk), C) Saline (2/wk), D) Blank NPs, E) NP+CycA (1/wk), F) NP+CycA (2/wk), and G) RESTASIS. The scale bars (black) are 300  $\mu\text{m}$  in length. The arrows (red) represent some of the inflammatory infiltrates such as lymphocytes, polymorphonuclears and eosinophils observed. .... 57

Figure 22. Preparation of mucoadhesive nanoparticle drug carriers as eye drop formulation. .... 62

Figure 23. Fluorescence images of NZW rabbit eyes treated with ICG and ICG-NP taken using confocal Scanning Laser Ophthalmoscopy (cSLO).....	68
Figure 24. ImageJ analysis of the fluorescence images taken from rabbit eyes treated with ICG and NP-ICG (n = 4; mean $\pm$ s.e.m.). I: mean fluorescence intensity measured using ImageJ software; I <sub>0</sub> : initial fluorescence (at 0 hr). .....	69
Figure 25. Tear production measurement of mice with different treatment groups. The tear volumes (T) were normalized with respect to their initial tear volume (T <sub>0</sub> ). The arrows represent the weekly dosing regimen of Saline, Blank NPs, NP-CsA 0.005-0.01% and NP-CsA 0.025% groups. ....	70
Figure 26. Corneal fluorescein staining analysis of mice with different treatment groups. The arrows represent the weekly dosing regimen of Saline, Blank NPs, NP-CsA 0.005-0.01% and NP-CsA 0.025% groups. Note that the analysis does not take into account the fluorescein on the lid margins of the eyes. ....	71
Figure 27. Histopathology analysis of ocular tissues of mice with different treatments: A) Healthy, B) Saline, C) Blank NPs, D) NP-CsA 0.005-0.01%, E) NP-CsA 0.025%, and F) Restasis®. The scale bars are 100 $\mu$ m in length. The red arrows represent some of the inflammatory infiltrates such as lymphocytes, polymorphonuclears and eosinophils observed. ....	73
Figure 28. Reaction scheme for the Williamson ether synthesis between dextran and 4-bromomethylphenylboronic acid (BPBA), using sodium tert-butoxide (tBuONa) as the catalyst. Note that the BPBA is shown to have reacted with the hydroxyl group on C2 of the dextran repeating unit, but BPBA may also attach to the hydroxyl groups on C3 and C4. ....	79
Figure 29. <sup>1</sup> H NMR analysis of the semi-solid state chemistry on BPBA modified dextran in D <sub>2</sub> O after purification of unreacted BPBA and tBuONa.....	81
Figure 30. Effect of reaction time and temperature on the BPBA:dextran conjugation efficiency. ....	82
Figure 31. Effect of the molar ratio of BPBA to dextran repeating unit on the BPBA:dextran conjugation efficiency. The molar ratio of tBuONa to dextran repeating unit is kept constant at 1. ....	83
Figure 32. Effect of the molar ratio of tBuONa to dextran repeating unit on the BPBA:dextran conjugation efficiency. The molar ratio of BPBA to dextran repeating unit is kept constant at 1. ....	83
Figure 33. Reaction scheme: application of the semi-solid state method in synthesizing a block copolymer between BPBA modified dextran and poly(D,L-lactide) (PLA). ....	85
Figure 34. <sup>1</sup> H NMR analysis of the all 4 steps on the PLA-Dex block copolymer synthesis with BPBA grafted dextran. Note that D <sub>2</sub> O was used for analysis on the products of steps 1 to 3, and DMSO-d <sub>6</sub> was used for the analysis of product on step 4.....	85

Figure 35. Verification of covalent complexation between the phenylboronic acid (PBA) on the PLA-Dex NPs with sialic acid. The intrinsic fluorescence of PBA (excitation: 288 nm; emission 376 nm) is quenched in the presence of sialic acid (SA) due to the covalent complexation between PBA and sialic acid. .... 91

## List of Tables

Table 1. List of preclinical and clinical studies using nanomaterials in ocular drug delivery system .	13
Table 2. PBA conjugation efficiency and mucin adsorption of PLA-Dex NPs. ....	36
Table 3. PLA-b-Dex-g-PBA characterization: PBA surface functionalization, Cyclosporine A loading, and diameter. ....	46
Table 4. Seven different treatment groups applied to the mice for experimental dry eye treatment study in mice. ....	53
Table 5. Six different groups applied to the mice for treatment of experimental dry eye .....	65
Table 6. Nanoparticle diameters and their polydispersity measured using dynamic light scattering (DLS). ....	67



# Chapter 1

## INTRODUCTION

### 1.1 Overview

A significant population of the world suffers from some form of eye disease. The severity of eye diseases ranges from daily complications to blindness. Dry eye syndrome is one of the milder forms of eye diseases that cause dryness in the eye as a result of a reduced rate of lacrimation or increased rate of tear film evaporation. This condition affects about 4.9 million individuals in the United States alone, causing ocular surface irritation and inflammation [5]. Although its symptoms may be mild, if left untreated, dry eye syndrome can lead to various infectious diseases on the ocular surface.

Topical administration, typically in the form of eye drop formulations, is the most common delivery method employed for treating diseases associated with anterior segments of the eye. Although simple to use, topical administrations suffer from low ocular surface retention as a result of rapid drainage through the naso-lacrimal duct, near-constant dilution by tear turnover, and low drug permeability across the corneal epithelium [6]. Therefore, eye drops are normally administered multiple times daily in order to achieve therapeutic efficacy – this, however, also leads to an increased risk of side effects and lowered patient compliance.

Nanomedicine—the fusion of nanotechnology and medicine—has been a focal point of research in the field of ocular drug delivery in the past decades [1, 7-10]. Nanoparticle (NP) drug carriers have the potential to overcome challenges posed by current eye drop formulations. NPs are particles with sub-100 nm sizes that can encapsulate and deliver therapeutic agents. They have high surface area-to-volume ratios and the surfaces of the NPs can be tuned to achieve specific surface properties such as adhesion to ocular mucous membranes for prolonged retention. NPs can also release the encapsulated therapeutics in a sustained manner for prolonged treatment of the ocular diseases. Because of their small size, NPs do not cause abrasive sensations on the surface of the eye, improving patient comfort.

The thesis explores the application of NPs as a drug delivery platform to enhance the delivery of therapeutics to the ocular surface. A polymeric NP self-assembled from a block copolymer was developed as the ocular drug delivery platform. The surfaces of these NPs were chemically modified with phenylboronic acid (PBA), which can covalently target the sialic acid moieties that are abundant on the ocular mucous membrane. Cyclosporine A, a commercially used drug for the treatment of dry eye, was used as a model drug to determine the capability of the PBA-modified NPs to encapsulate and

release the drugs. In preclinical studies, the safety of the Cyclosporine A-loaded NPs was evaluated in animal models and their dry eye treatment efficacy was also tested. Further animal studies were used to analyze the mucoadhesive properties of the NPs to calculate their ocular retention time, and the dosage of the Cyclosporine A in the NP formulation was tuned for the long term treatment of dry eye. Finally, an improved methodology was developed to process the PBA-modified block copolymers in a scalable way. Some of the avenues to explore in the future to advance this NP drug delivery platform into clinical trials include developing a good manufacturing practice (GMP) process for the NP drug delivery platform and good laboratory practice (GLP) studies to further investigate the safety and efficacy of the NP formulation.

## **1.2 Research objectives**

The overall objective of the proposed project is to develop a nanoparticle drug delivery system capable of enhancing the therapeutic efficacy of topical formulations targeting anterior segments of the eye. To develop a nanoparticle drug delivery system, we start by designing a block copolymer that can self-assemble into nano-sized micelles capable of encapsulating and controlling the release of therapeutics. The nanoparticles are characterized for mucoadhesion, drug encapsulation, and release *in vitro* before performing *in vivo* tests. Subsequent *in vivo* tests involve testing the biocompatibility and efficacy of the nanoparticle formulations. Finally, a scalable process for synthesizing the block copolymer must be developed to demonstrate the feasibility of the formulation for clinical trials. The specific objectives of the study are as follows:

1. Develop a polymeric nanoparticle drug delivery system
  - Synthesize a block copolymer, through conjugation of hydrophobic poly(D,L-lactide) (PLA) and hydrophilic dextran, that self-assembles into nanoparticles
  - Characterize the size, morphology, and drug delivery capacity of the nanoparticles formed from PLA and Dex
2. Develop a mucoadhesive nanoparticle drug carrier for topical ocular delivery applications
  - Demonstrate the mucoadhesion properties of the phenylboronic acid (PBA) functionalized nanoparticle carriers
  - Demonstrate the capability of the nanoparticles to encapsulate and delivery ocular therapeutic agents

3. Demonstrate the *in vivo* biocompatibility and efficacy of the nanoparticles as a platform delivery system to target the anterior eye
  - Demonstrate the biocompatibility and non-irritancy of the nanoparticle formulation in rabbit models
  - Demonstrate the treatment efficacy by delivering Cyclosporine A using mucoadhesive nanoparticles to mice with experimentally induced dry eye
4. Demonstrate the prolonged ocular retention of nanoparticles and adjust the dosage of Cyclosporine A in the nanoparticles for long-term treatment of dry eye in mice
  - Investigate the ocular retention time of the nanoparticles on the ocular surface
  - Determine the optimal dosage of Cyclosporine A in the nanoparticles for the long-term treatment of dry eye in mice
5. Develop a scalable synthesis process for PBA modified PLA-Dex block copolymers using semi-solid state reaction mechanisms
  - Develop a fast, simple, and scalable process for synthesizing PBA-modified PLA-Dex copolymers

### 1.3 Thesis outline

This thesis is comprised of eight chapters: the introduction, a literature review, five experimental research based chapters, and a final chapter featuring the conclusion and recommended future work. Chapter 1 introduces the key challenges to be addressed in the thesis, the hypothesis, and the specific objectives to test this hypothesis.

Chapter 2 reviews the current status of the field of ocular drug delivery. Various types of nanomaterials currently being investigated in the field of ocular drug delivery are discussed and their advantages and disadvantages are outlined. The future outlook of nanomaterial-based ocular drug delivery vehicles is also highlighted.

Chapter 3 describes the method of the synthesis of an amphiphilic block copolymer and the *in vitro* characterization of the nanoparticles formed from the self-assembly process. The block copolymer is an initial building block of the nanoparticle drug carriers, which then becomes the delivery platform for us to explore various ocular treatment options.

Chapter 4 presents the method of modifying the surface of PLA-Dex nanoparticles with PBA to achieve mucoadhesive targeting. This is a crucial step in prolonging the retention of drugs delivered to the ocular surface. This study demonstrates the potential of the nanoparticle drug carrier system to serve as an enhanced drug delivery platform for treating ocular diseases.

Chapter 5 follows the *in vitro* characterizations of Chapter 4 with the *in vivo* characterization of the biocompatibility and the treatment efficacy of this mucoadhesive nanoparticle formulation. This study provides the foundation for the further advancement of this platform delivery system into clinical trials, after demonstrating both the preliminary biocompatibility and treatment efficacy in preclinical settings.

Chapter 6 further explores the *in vivo* examination of the mucoadhesive properties of the nanoparticles as well as the dosage-dependent dry eye treatment efficacy of the nanoparticles carrying Cyclosporine A. The chapter investigates the ocular retention time of drugs delivered by the nanoparticles using live imaging of the drug molecule on animals, as opposed to more commonly used methods of post-euthanasia analyses. Due to the mucoadhesive nature of the delivery system, the dose and the dosing frequency of the formulation must also be carefully controlled to prevent any side effects.

Chapter 7 revisits the discussion from Chapters 3 and 4 to improve the synthesis process for the PBA-modified block copolymer. One of the key milestones to meet before proceeding to clinical trials is to develop a scalable manufacturing process for the formulation. Chapter 7 explores a novel semi-solid state reaction mechanism to achieve a simple, fast, and scalable way of producing the block copolymers.

Chapter 8 highlights the conclusions drawn from the research described in Chapters 3 to 7 and recommendations for future work based on these conclusions. While Chapter 7 discusses the importance of a scalable process for the copolymer building block, another important step before proceeding to clinical trial is to also provide a manufacturing process for the nanoparticle-drug formulation. Finally, an important future goal is to explore the flexibility of the nanoparticle drug delivery platform to treat other common ocular diseases in addition to dry eye syndrome, such as glaucoma and allergic conjunctivitis.

## **Chapter 2**

### **LITERATURE REVIEW**

#### **2.1 The field of ocular drug delivery**

Ocular drug delivery remains a challenging task due to the nature of the ocular structures and the unique ocular physiology. The eye is a small and complex organ that is separated from the rest of the body by multiple layers of biological barriers. Moreover, the eye tissue is protected from the external environment by the tight junctions of the corneal epithelium and the mucosal surface. Therefore, the primary challenge of ocular drug delivery is to circumvent these protective barriers in order to achieve therapeutically effective concentrations of drugs in the intraocular tissues. The objective of ocular drug administration is to treat diseases in a localized manner as opposed to serving as an intermediate route to achieve systemic drug activity.

There are a plethora of vision-threatening ocular diseases that require therapeutic treatment, and most of these diseases are associated with intraocular structures such as the retina, retinal pigment epithelium (RPE), or choroid.[11] Typically, anti-inflammatory drugs, anti-microbial agents, and angiogenesis inhibitors are used to treat various types of local infections or disorders such as chronic uveitis, glaucoma, endophthalmitis and choroid neovascularization among many; nevertheless, the efficiency with which these substances are successfully delivered has largely been limited by the presence of ocular barriers. To date, most common ophthalmic drugs are administered topically in the form of eye drops on the corneal surface. However, topically administered drugs suffer from low bioavailability due to clearance mechanisms such as tear turnover. Alternative delivery methods such as intravitreal or periocular injections have been developed to improve the bioavailability of the therapeutic agents, but due to the invasive nature of these methods, side effects such as retinal detachment or intravitreal hemorrhage have been observed. The challenges affiliated with these conventional methods of ocular drug delivery have lead scientists to contribute significant effort into developing advanced drug delivery systems.

At present, nanocarrier-based ocular drug delivery systems appear to be the most promising tool to meet the primary requirements of an ideal ocular delivery system. Nanocarriers, due to their small sizes, are likely to have high diffusivity across membranes such as the corneal epithelium: a significant number of studies have already demonstrated that the use of such nanomaterials via topical administration improved the corneal permeability of drugs.[12-15] Similarly, due to their high surface-

area-to-volume ratio, nanocarriers may also show improved interaction with the mucous membrane of the corneal surface to prolong the retention of the topically administered drug formulations. Ongoing advances in developing improved nanocarrier-based ocular drug delivery system may also provide new possibilities of effectively delivering therapeutic agents to intraocular tissues such as the retina or choroid using non-invasive delivery methods. The following literature review highlights some of the most recent findings in the utilization of nanomaterials, such as polymeric micelles, hydrogels, liposomes, niosomes, dendrimers, and cyclodextrins, for enhanced ocular drug delivery performance (Figure 1).

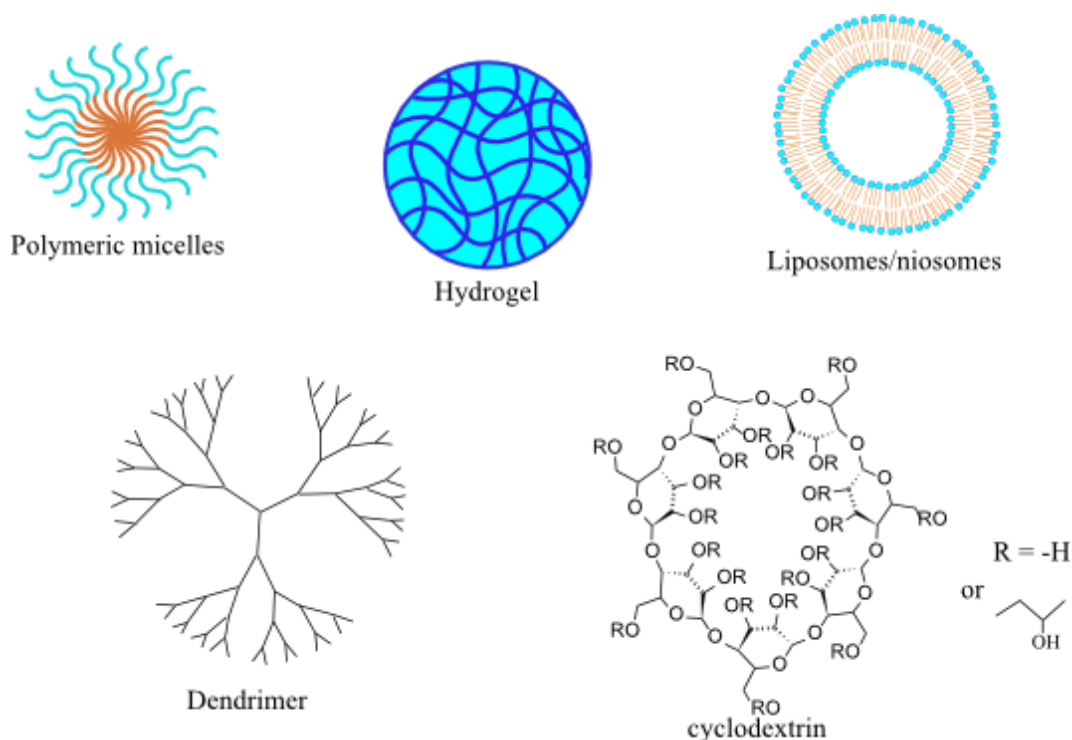


**Figure 1. A schematic illustration of different nanomaterial-based ocular drug delivery systems.**

**Polymeric micelles are nanoparticles self-assembled from amphiphilic copolymers with the ability to encapsulate hydrophobic drugs in the core of the particles. Hydrogel colloids are 3D network of water-soluble polymers which have the ability to incorporate hydrophilic drugs in the 3D network. Liposomes/niosomes are vesicle structures with both lipophilic and hydrophilic phases, and therefore can encapsulate both hydrophobic and hydrophilic drug components.**

**Dendrimers are 3D highly branched tree-structured macromolecules that can encapsulate hydrophobic drug molecules since they possess internal empty cavities and open conformations for low generation dendrimers. Cyclodextrins are a family of cyclic oligosaccharides, composed**

**of 6 to 8 glucose units which have been shown to improve pharmacokinetic properties of many drugs through formation of inclusion complex.[1]**

## **2.2 Challenges of conventional ocular drug delivery system**

Difficulties in delivering drugs through the ophthalmic route arise from the anatomy and the physiology of the eye, an organ which is divided into anterior and posterior segments (Figure 2). Topical drug administrations, such as eye drops, suspensions, or ointments, are the most preferred route of delivery to the anterior segment of the eye due to the ease of administration and low cost. However, local drug administration to the anterior portion of the eye by topical application is significantly limited by the clearance mechanisms of the corneal surface, which include lacrimation, tear dilution, and tear turnover.[6] In addition, topically administered drugs are generally absorbed either through the corneal route (cornea → aqueous humor → intraocular tissues) or non-corneal route (conjunctiva → sclera → choroid/RPE),[6] which further limits the amount of drug that is ultimately absorbed in the intraocular tissues. Due to these clearance mechanisms and ocular barriers, less than 5% of the total administered drug reaches the aqueous humor.[16] For example, after administration of a common eye-drop solution containing 0.05% cyclosporine to treat dry eye syndrome, more than 95% of the drug reaches systemic circulation through transnasal or conjunctival absorption.[17]

The administration of drugs to the posterior portion of the eye is even more challenging due to the lack of cellular components in the vitreous body which reduces the convection of molecules to the posterior segments. Efficient drug delivery to the posterior segment of the eye is a challenge faced by many pharmaceutical researchers, as most blindness-inducing diseases are associated with the posterior segment.[18] Systemic administration has also been used to deliver therapeutic agents to the posterior segment of the eye; however, this route of administration requires large administration doses because of the inner and outer blood-retinal barriers that separate the retina and the vitreous humor from the systemic circulation:[19] studies to date have shown that less than 2% of systemically administered drugs reaches the vitreous cavity. High administration doses or frequent administration directly translates to poor patient compliance and increased risk of systemic side effects.

Recently, intravitreal injections and vitreal implants have been investigated in order to achieve therapeutic concentrations at the posterior segment, although both intravitreal injections and vitreal implants are very invasive methods with high degrees of risk.[12] Frequent administration through the intravitreal route is associated with short-term adverse effects such as retinal detachment,

endophthalmitis, intravitreal hemorrhage, and increased risk of cataract development.[6, 14] More recently, periocular drug delivery has been investigated as a less invasive method, compared to intravitreal administration, in order to achieve high drug concentrations in the vitreous cavity.[22] Periocular administration refers to the injection of the drug in the vicinity of the ocular organ, such as the sub-conjunctival, sub-tenon, or parabolbar regions, so that the drugs can reach the vitreous cavity by crossing the sclera, choroid, and RPE barriers.[22] However, periocular drug administration is not without side effects: rise in intraocular pressure, cataract development, hyphema, strabismus, and corneal decompensation have been observed for some patients following periocular injections.[6] As a result, topical drug delivery carriers that possess enhanced permeability across corneal membranes and prolonged retention of the carriers in the ocular moiety are still largely preferred over intravitreal or periocular injections due to the invasive nature of the latter methods.

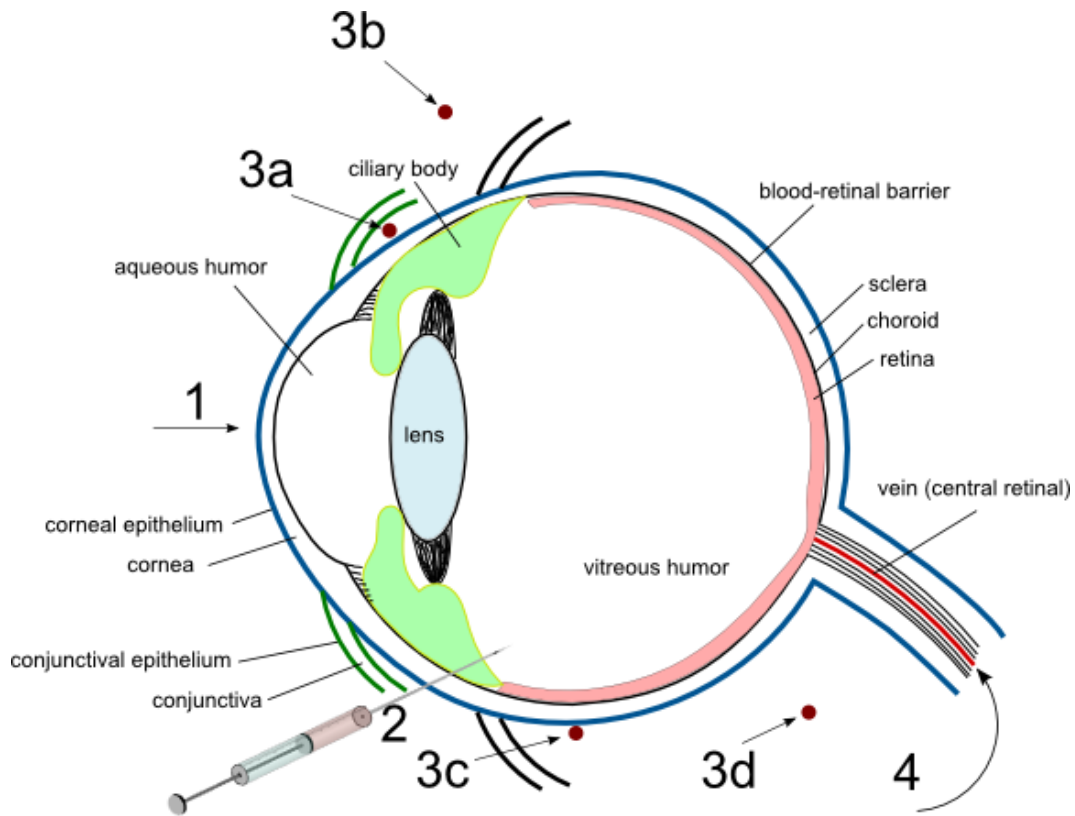


**Figure 2. The anatomy of the eye illustrating various ocular barriers and various mechanisms of drug delivery: 1. Topical administration, 2. Intravitreal injection, 3. Periocular injections (3a.**



**sub-conjunctival, 3b. peribulbar, 3c. sub-tenon, 3d. retrobulbar), and 4. Systemic administration.[1]**

### **2.3 Contact lenses in ocular drug delivery**

Earlier advancement in ocular drug delivery came from the idea of using contact lenses as sustained drug delivery system.[6, 23-25] In 2007, there were about 35 million contact lens wearers in North America alone, and the number is expected to have risen continuously to date.[26] The idea of using contact lenses as drug delivery tools, therefore, has been considered very practical. The contact lens drug delivery systems are typically prepared by soaking commercial lens products, such as silicone-hydrogel, in a drug solution, allowing retention of drugs in the hydrogel matrix. Subsequently, the drug is allowed to be released at the corneal surface upon application of the lens on the eye. The purpose of using a contact lens drug delivery system is to increase the residence time of drugs on the corneal surface, compared to topical applications, so as to increase the amount of corneal absorption of these drugs. A mathematical model was used to postulate that as much as 50% of the drug released from contact lens could be absorbed by the cornea, but *in vivo* studies have yet to confirm the hypothesis.[27] The drug release from the lens is governed by a diffusional mechanism, which may often result in burst release of drugs for initial few hours.[28] Therefore, several studies have focused on using additional components in the contact lenses to control the release rate of the drugs.

Ciolino et al. used the formulation of poly(lactic-co-glycolic) acid (PLGA) film, which is an FDA approved biocompatible polymer that has shown to be able to control drug-release kinetics, coated with poly(hydroxyethyl methacrylate) (pHEMA) hydrogel layers to control the release of ciprofloxacin.[28] The formulation resulted in steady zero-order release of ciprofloxacin up to 4 weeks. When the PLGA film was not present, ciprofloxacin released at a rate more than 3 times faster from pHEMA hydrogel than from the PLGA-pHEMA combination. Several of more recent studies examined the usage of nanomaterial-laden hydrogel contact lenses to achieve controlled drug release phenomena.[2, 29-31] Nevertheless, nanomaterial-laden contact lens drug delivery systems still face challenges in practical applications. The obvious challenge is that with the controlled release mechanism, the duration of the therapeutic window is also prolonged. This means that the patient must wear the lenses for a longer period of time which may cause discomfort in the eyes. Another challenge is that the diffusional-based drug release mechanism still causes some of the drugs to be released in the pre-lens tear film, as opposed to the post-lens tear film (i.e. between the cornea and the lens), which are also exposed to clearance mechanisms similar to topical administration. Lastly, the nanomaterials that allow slow release

mechanism may also trap the drugs permanently in the hybrid hydrogel matrix, which is shown in PLGA-pHEMA layers: only about 10% of the total drug from the contact lens was released during the sustained release phase. [28] This implies that the drug shelf-life must be long enough so that efficient amount of drug will be absorbed by cornea before losing its therapeutic efficacy. In general, the incorporation of nanomaterials in the contact lens must also not compromise some of the key properties of the lens itself such as biocompatibility, transparency, comfort and wettability. Much progress has been made in applying contact lenses as drug delivery system in order to overcome the challenges outlined previously. With the advent of nanomaterials, the contact lenses are potentially one of the more convenient ways of delivering ocular drugs.

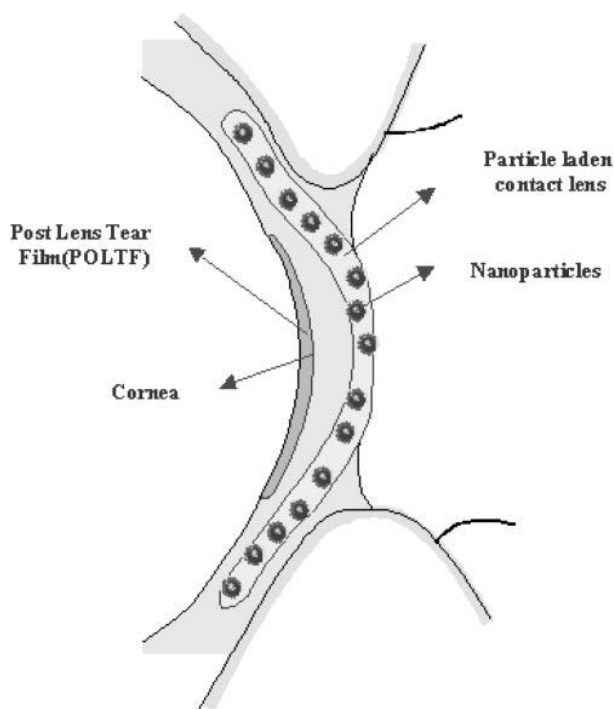


**Figure 3. Schematic of nanoparticle-laden lens inserted in the eye (Reproduced with permission from[2]).**

## **2.4 Nanomaterials in ocular drug delivery**

Much research has been carried out on using different types of nanomaterials for the ophthalmic delivery of drugs. Sahoo et al. have outlined three major goals for ocular drug delivery nanocarriers: 1) enhancing drug permeation, 2) controlling the release mechanisms of drugs, and 3) modifying the surfaces of the nanocarriers with specific targeting moieties.[32] Due to the small size of these

nanocarriers, the permeability of these drug carriers through the vitreous barrier is greatly enhanced, which in turn improves the delivery rate of the drugs to the posterior tissues. Moreover, with the mucoadhesive properties exhibited by certain types of nanoparticles, drug carrier retention may be significantly prolonged in the targeted tissues. The nanocarrier-drug complex can be administered as eye drop solutions requiring less frequent administration due to the higher retention of the drugs, reducing the cost of administration and increasing patient compliance. Zimmer et al. have suggested that the sizes of administered particles for ophthalmic applications must be less than 10  $\mu\text{m}$  in order to avoid the sensation of scratching upon administration.[33] The potential advantages of using nanoparticles (NPs) for ocular drug delivery have been reviewed elsewhere.[34]

The field of ocular drug delivery has been significantly impacted in the past decade by advances in technology, especially the development of nanostructured drug carriers. It was proposed that microspheres and nanoparticles used for the encapsulation of drugs would enhance the overall performance of ocular drug delivery systems.[33] The application of nanotechnology in the field of ocular drug delivery has been extensively reviewed by several groups. Gaudana et al. have highlighted recent advances in nanotechnology applications for ocular drug delivery, listing numerous nanostructure carriers as potential ocular drug carriers.[6] Ludwig has discussed the use of mucoadhesive polymer based nanostructures for the ophthalmic delivery of drugs, reporting the enhancement of targeting and retention of the drugs at the tissue site of interest such as corneal surface.[35] Nagarwal et al. have focused more on polymer-based nanoparticles, exploiting the application of the block copolymer micelles in the field of ocular drug delivery.[12]

## **2.5 Nanomaterial-based ophthalmic formulation currently in the clinical stages**

The studies discussed thus far have focused on the initial proof-of-concept stage of nanomaterials in the field of ocular drug delivery. Table 1 below summarizes the progress of nanomaterial-based ocular drug delivery system in the clinical stages. The past few decades has seen significant increase in the number of journal articles published dealing with developing advanced ocular drug delivery system. Among these delivery systems, eye-drop formulations incorporated with various drug release-controlling excipients (i.e. Polycarbophil) are currently available in the market.[36] A number of products in the form of intravitreal implant, inserts or punctal plug in the micro- or milli-scale are also currently being developed by various pharmaceutical companies.[36] Although numerous nanomaterial-based ocular drug delivery systems have already progressed onto the preclinical studies (i.e. *in vivo* animal studies) to characterize their pharmacokinetic properties in physiological

environment, very few of them have been analyzed in the clinical studies. Hydrogel carriers of timolol formulation showed improved control over the individual variation of timolol concentration in the aqueous humor among human patients compared to the pure drug suspension.[37] The lowered variation in drug concentration reduces the probability of having insufficient local drug concentration, and it also reduces the risk of toxic effects caused by an excessive amount of drug. Another interesting delivery method for trans-scleral iontophoresis was also studied in human patients using a hydrogel formulation.[38] Iontophoresis uses a small electric current to deliver charged therapeutic agents across biological membranes, and it has been extensively studied in ocular drug delivery due to the various ocular barriers.[25, 39-43] The hydrogel-iontophoresis delivery method in randomized human study demonstrated that total charge less than 60 mA•min were well tolerated by patients, rendering itself as a promising ocular drug delivery method for targeting both anterior and posterior segments of the eye. In addition to hydrogel ophthalmic delivery systems, incorporation of ophthalmic drugs with cyclodextrin has shown efficacy in lowering intraocular pressure in human patients.[44, 45] On the other hand, evaluations of nanomaterials such as micelles, liposomes/niosomes, and dendrimers are currently limited to the preclinical animal studies. However, these nanomaterials are also expected to be involved in clinical phase studies on human subjects in the near future as more preclinical studies demonstrate their enhanced pharmacokinetic properties.

Nanomaterial	Drug	Formulation	Administration	Treatment	Clinical stage	Ref
Microsphere	Triamcinolone acetonide	PLGA (RETAAC)	Intravitreal injection	diabetic macular edema	Launched	[46]
Micelles	Dexamethasone	NPIAAM-VP-MAA	Eye-drop	inflammation	Preclinical	[47]
	Dexamethasone	Pluronic F127-Chitosan	Eye-drop	ocular hypertension	Preclinical	[48]
	Cyclosporin A	MPEG-hexPLA	Eye-drop	dry eye, autoimmune uveitis	Preclinical	[49]
	Dexamethasone	PHEA-PEG	Eye-drop	ocular hypertension	Preclinical	[50]
Hydrogel	Timolol		Topical	ocular hypertension	Randomized human	[37]
			Transceral iontophoresis			Randomized human
Liposomes	Flurbiprofen	stearic acid + castor oil	Eye-drop	inflammation	Preclinical	[51]
	Ciprofloxacin HCl	chitosan coated liposome	Eye-drop	conjunctivitis	Preclinical	[52]
	Fluconazole	liposome	Eye-drop	fungal infection	Preclinical	[53]
	Ciprofloxacin HCl	chitosan coated liposome	Eye-drop	bacterial growth of <i>P. aeruginosa</i>	Preclinical	[54]
	Bevacizumab	liposome	Intravitreal injection	ocular neovascular activity	Preclinical	[55]
	Verteporfin	Liposome (Visudyne®)	Intravitreal injection	classic subfoveal choroidal neovascularization	Launched	[36]
Dendrimer	pilocarpine nitrate and tropicamide carteolol	PANAM	Eye-drop	myosis and mydriasis	Preclinical	[56]
		phosphorus-containing dendrimers	Eye-drop	glaucoma	Preclinical	[57]
Cyclodextrin	Methazolamide	HP $\beta$ CD and HPMC	Eye-drop	ocular hypertension	Randomized human	[45]
	Latanoprost		Eye-drop	open-angle glaucoma	Randomized human	[44]

**Table 1. List of preclinical and clinical studies using nanomaterials in ocular drug delivery system**

## 2.6 Recent developments of nanomaterials in ophthalmic formulations

### 2.6.1 Polymeric micelles

Polymeric micelles are core-shell structured nanoparticles formed by the self-assembly of amphiphilic copolymers. Polymeric micelles have been investigated extensively in the field of drug delivery as they present numerous advantages. Polymeric micelles can be fabricated through the simple self-assembly process, usually involving techniques such as nanoprecipitation, emulsion, or dialysis, in aqueous medium. In addition, the core-shell structure enables encapsulation of hydrophobic drugs in its hydrophobic core. Because the hydrophobic core is shielded by the hydrophilic corona, the stability and the half-life of the drug is significantly prolonged in the circulation. Moreover, biodegradable and biocompatible polymers are selected for formulation of micellar carriers, which would prevent any adverse effects caused in the physiological system by the carriers. With these benefits, polymeric micelles have attracted great interest in the field of drug delivery[42, 58-63], including drug delivery in ocular routes in the past several decades.

Several groups in the past have used polylactide (PLA) or poly(lactide-co-glycolide) (PLGA) drug carriers to enhance the delivery of different types of drugs.[64-69] PLGA copolymers form micro- or nanoparticles in aqueous medium by self-assembly phenomena and can be used to encapsulate the drugs. However, the challenge with using PLGA carriers is that the polymer is unstable in aqueous medium: the ester backbone of the PLGA polymer is prone to hydrolytic degradation, which ultimately lowers the shelf-life of PLGA encapsulated drug complexes. Thus, many scientists have turned to investigating copolymers with hydrophilic chains, such as polyethylene glycol (PEG) or polyethylene oxide (PEO) in order to increase the stability of the nanoparticles by shielding the hydrophobic cores from hydrolytic degradation. In one study, the effect of PEG versus chitosan surface modification on polymeric micelles was compared in terms of the ability to penetrate and deliver drugs across the corneal membrane.[70] Chitosan was electrostatically anchored to the surface of PCL nanocapsules, whereas PCL-b-PEG was synthesized. The results showed both nanocapsules increased the permeability of encapsulated drugs through the corneal epithelium compared to free drug suspension, with Chitosan coated nanocapsules increasing the amount of drug permeation up to three folds at 4 hour interval. However, the mechanism of transport enhancement remains to be completely dissected. A triblock copolymer poly(oxyethylene)-poly(oxypropylene)/poly(oxyethylene) (PEO-PPO-PEO, trade name: Pluronic F127) was suggested by Pepic et al. for encapsulation and delivery of pilocarpine.[71] The triblock copolymer is comprised of a central hydrophobic chain (PPO) with two hydrophilic chains

on either side (PEO) which was shown to self-assemble into a micellar structure in aqueous environment with sizes ranging from 16 to 30 nm having pilocarpine encapsulated. Although the drug encapsulation efficiency was very low (maximal 1.9 wt%), the authors demonstrated that the miotic response (area under curve of miotic response vs. time) using micellar solution of pilocarpine base showed 64% increase compared to standard pilocarpine eye-drop solution. PEO-PPO-PEO triblock copolymer was also used by two other studies. Liaw et al. developed eye drop solution containing the polymeric micelles of Pluronic F127 to deliver DNA plasmids for gene therapy in order to increase the stability of DNA plasmids *in vivo*. [72] More recently, Kadam et al. used the micellization of Pluronic F127 in aqueous environment to encapsulate anti-epileptic drug carbamazepine to increase the water solubility of the drug. [73]

A stimuli-responsive micellar drug delivery system has also been developed. A triblock copolymer comprising N-isopropylacrylamide (NIPAAM), vinyl pyrrolidone (VP) and acrylic acid (AA) was cross-linked with N,N-methylene bis-acrylamide (MBA) to form NPs. [74] The micellar NPs were analyzed for the delivery of anti-inflammatory drug Ketorolac. The polymeric micellar system possesses a unique thermosensitivity since the lower critical solution temperature (LCST) of triblock copolymer was found near the physiological temperature. Therefore, the micellar system showed temperature-dependent release phenomena which can be utilized to control the release of the drugs to specific targeting tissues.

Other types of block copolymers were also exploited by various research groups. Due to the small sizes and the stable suspension in aqueous environment, polymeric micelles have also been injected into the vitreous cavities using intravitreal delivery route. Roy et al. was able to demonstrate intravitreal delivery of antisense oligonucleotides to the retina of a rat using polyoxyethylene-polyspermine (PEO-*b*-PSP) carrier to decrease the fibronectin expression in retinal vascular cells. [75] The block copolymer formed an effective diameter of 12 nm with the oligonucleotides embedded in the matrix. The NPs persisted up to 6 days in the retinal microvessels without showing any toxic effects after being delivered intravitreally. The study provided that the NP delivery method successfully reduced the expression of fibronectin mRNA level to 86.7% 2 days after injection, and down to 46.7% at day 6. An *in vivo* study carried out by Bourges et al. demonstrated that nanoparticles injected through intravitreal means showed tendency to migrate through the retinal layers and accumulate in RPE cells. They observed the presence of the nanoparticles in RPE cells up to 4 months after the initial single intravitreal injection, which provides a promising long term drug delivery tool to the posterior segment of the eye. [76]

Various types of amphiphilic copolymers have also demonstrated their ability to improve the *in vivo* bioavailability of the encapsulated drugs. Qu et al. synthesized chitosan-based amphiphilic copolymer, quaternary ammonium palmitoyl glycol chitosan (GCPQ).[77] The modified amphiphilic copolymer encapsulated hydrophobic drugs by forming micellar clusters, and showed encapsulation of up to 20 – 200 times more hydrophobic drugs compared to that of Pluronic block copolymers. Upon both intravenous injection and topical ocular application of GCPQ with prednisolone, the bioavailability of prednisolone increased 10-fold compared to a commercial emulsion formulation of the same drug. Shen et al. utilized thiolated PEG stearate as a surfactant to modify the surface of nanostructured lipid carrier (NLC) in order to render mucoadhesiveness for the nano drug carriers.[3] The Mucoadhesion was achieved by the disulfide linkage between the thiol groups of the nanocarrier and the mucin particles (Figure 4). When topically administered to the rabbit eye, the thiolated NLC improved the drug concentration and the precorneal retention time of the encapsulated cyclosporine, which remained in the cul-de-sac for up to 6 h. A number of studies have also focused on using prodrugs for enhanced penetration through ocular barriers.[78, 79] An amphiphilic prodrug of tilisolol, *O*-palmitoyl tilisolol, was developed by Kawakimi et al. in order to improve the ocular adsorption of the drug through cornea.[80] Upon topical instillation, the prodrug form of tilisolol showed prolonged retention and high drug concentration in both tear fluid and cornea compared to the tilisolol suspension.

Micellar drug carriers have also shown increased ocular permeability of various drugs, when compared to their pure drug solution forms.[50, 81] From these studies, it is evident that polymeric micellar drug carriers have great potential not only in improving the drug stability and release mechanism to prolong the therapeutic activity of the encapsulated drugs, but they also show promise in increasing the permeability of the drugs through various ocular barriers.



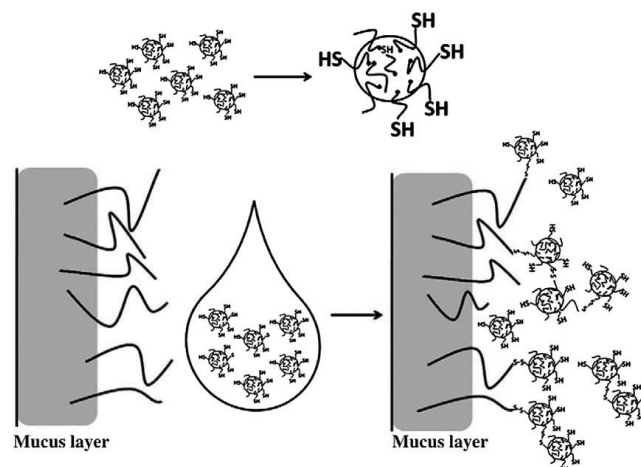


**Figure 4. Schematic representation of the interaction between the thiolated NLCs and mucus (Reproduced with permission from [3]).**

### 2.6.2 Hydrogels

Hydrogels are defined as water-soluble polymeric network that has the ability to absorb more than 20% of its weight of water and still maintain its 3D structure.[82] Hydrogels have been studied extensively in medicinal applications such as tissue engineering and drug delivery due to their unique properties.[83] The chemical and physical properties of hydrogels can be easily modified simply by changing choice of polymers since hydrogels can be fabricated from any hydrophilic polymer. Hydrogel networks are extensively studied as controlled and sustained drug delivery system since their porosity of the matrix can be tailored by modifying the crosslinking density, or using external stimuli such as pH or temperature, to control the diffusivity of the drugs in the matrix.

Barbu et al. fabricated nanoparticulate hybrid polymeric hydrogels with size range from 10 to 70 nm to investigate their feasibility of employing different ophthalmic drugs.[84] The copolymers used for fabricating the nano-sized hydrogels combined chitosan or acrylic acid-functionalized chitosan which has been copolymerized with either 2-hydroxyethyl methacrylate (HEMA), or with N-isopropylacrylamide (NIPAM) to impart thermosensitivity to the nanoparticulate system. Chitosan-based nanomaterials have been widely studied for diverse applications in medicine due to its biocompatible, biodegradable, mucoadhesive and non-toxic properties.[85] Chitosan's mucoadhesive property is especially important in topical ocular drug delivery system since it prolongs the retention of the delivery system on the mucus, which further increases the duration of drug activity. The *in vitro* drug release results demonstrated that the nanoparticulate system showed sustained-release phenomena

and the release rate of various drugs depended on the % content of chitosan materials in the hydrogels. More recent studies have focused on using in-situ gelation properties of some of the hydrogel materials in order to enhance the ocular bioavailability of the drugs and the *in vivo* drug activity. Pluronic F127, in addition to forming micellar structures due to its amphiphilic nature, has been used to fabricate hydrogel network system. Due to its temperature sensitive nature, Pluronic F127 was studied by different groups as an in-situ gelling agent for ocular delivery applications.[86, 87] The sol-gel transition temperature of Pluronic F127 was below the human physiological temperature of 37 °C. The property was utilized by preparing a liquid solution of Pluronic F127 with drugs of interest at low temperatures. Subsequently, upon administration into the physiological environment, the solution undergoes gelation to create a polymeric matrix where the drug is entrapped and released slowly through the gel by diffusion mechanism.

### **2.6.3 Liposomes**

Liposomes are biocompatible and biodegradable particles consisting of membrane-like lipid bilayers composed mostly of phospholipids.[88] Formed by amphiphilic phospholipids, liposomes have hollow spherical structures (vesicles) with both lipophilic (lipid bilayer) and hydrophilic (aqueous compartment) phases. Due to this biphasic nature, liposomes can encapsulate both hydrophilic and/or lipophilic therapeutic agents in each of the compartment. The properties of liposomes, such as surface charge, can be tuned substantially by varying the lipid composition. Since the sialic acid moieties in the mucous membrane of the corneal surface is negatively charged, positively charged liposomes are preferentially captured at the corneal surface compared to neutral or negatively charged liposomes.[32] In addition, a recent study showed that positively charged liposomes also increased the extent of absorption of the encapsulated drugs across corneal membranes.[89] To achieve this characteristic, numerous studies have focused on coating the liposomal surface with mucoadhesive polymer chitosan.

Diebold et al. investigated the cellular uptake effects of liposome-chitosan nanoparticle complexes (LCS-NP) in the precorneal moieties. Strong cellular uptake of LCS-NP in the conjunctiva and less intense uptake by corneal epithelium suggested that the NPs were first retained by mucus layer, and subsequently enter through the conjunctival cells. They also showed that ocular drug delivery system liposome-chitosan nanoparticle complexes (LCS-NP) showed negligible *in vitro* toxicity and acceptable *in vivo* tolerance.[90] Li et al. proposed using low molecular weight chitosan (LCH) coating on liposomes and investigated their *in vitro* and *in vivo* properties.[91] The coating of LCH not only modified the surface to have positive charge, which enhanced its interaction with the mucous membrane

of the corneal surface, but it also showed increased transcorneal penetration of the LCH coated liposomes. The effect of surface coating subsequently led to prolonged retention of the encapsulated drugs at the corneal surface, and also provided potential of using the liposomal carriers as transcorneal drug delivery system to increase bioavailability of the drugs in the aqueous compartment. However, chitosan has shown precipitation phenomena near physiological pH, and therefore, some studies used a modified version of chitosan to solve the precipitation issue. Wang et al. also explored using N-trimethyl chitosan (TMC)-coated liposomes to delivery Coenzyme Q<sub>10</sub> to the human lens epithelial cells to protect against oxidative damages.[92] Chitosan chains were modified to the quaternized derivative TMC in order to overcome issues such as precipitation of chitosan at neutral pH. The study also demonstrated that the TMC-coated liposomes exhibited excellent corneal permeation – increasing the permeability coefficient more than two times in comparison with values obtained from control study.

Other studies have used different coating materials on the liposomes to achieve enhanced pharmacokinetic properties. Hosny developed ofloxacin encapsulated liposomes which were further incorporated into *in situ* thermosensitive hydrogel system composed of chitosan/ $\beta$ -glycerophosphate in order to enhance the transcorneal permeation of ofloxacin.[93] The liposomal hydrogel system improved the transcorneal permeability of ofloxacin sevenfold compared to that of the aqueous solution. In addition, the drug delivery system ensured steady and prolonged permeation of the drugs improving the bioavailability. Bochot et al. used PEG coating on the surface of liposomal formulation to sterically stabilize the liposomes. Intravitreal methods were used to inject the liposomal formulation into the vitreous humor, where the liposomes showed favored biodistribution at retina-choroid moieties compared with non-target tissues such as sclera or lens. The administration of liposome-encapsulated phosphodiester (16-mer oligothymidylate) oligonucleotides in the vitreous humor also showed sustained release phenomenon, which offers prospect that the liposomes can be used as intravitreal delivery system targeting retina and choroid where most of the ocular diseases occur. Hironaka et al. studied the effect of size and rigidity of the liposomes on the delivery performance of the liposomes to the posterior segment of the eye.[94] It was shown that rigid liposomes with size ranges in the nano-scale showed potential as ocular delivery system targeting the posterior segment of the eye.

Despite the recent advancement of using liposomal formulations for ocular drug delivery showing improvements in precorneal retention, sustained drug release and transcorneal permeation, liposomes

still face challenges in their limited long term structural stability and drug loading capacity due to the inherent complex nature of their structures.

#### **2.6.4 Niosomes**

Niosomes, a type of liposomes, are comprised of amphiphilic non-ionic surfactants to form vesicle structures. Niosomes, like liposomes, can entrap both hydrophilic and hydrophobic drugs. Niosomes are generally preferred over other vesicular systems as topical ocular drug delivery systems due to several reasons: they are chemically more stable, less toxic because of the non-ionic nature of the surfactants, easier to handle without special precautions, able to improve the performance of the drug via better bioavailability and controlled delivery at a specific site, and they are also biodegradable, biocompatible, and non-immunogenic.[95, 96]

Abdelbary et al. investigated niosomes as potential topic ocular drug delivery system for local antibiotic gentamicin.[95] The *in vitro* results showed that the encapsulation efficiency were as high as 92%, and the encapsulation of gentamicin showed prolonged release compared to the control study. The encapsulation efficiency and the release rate varied depending on the cholesterol content, the type of surfactant used, and the presence of charge inducer dicetyl phosphate. Ocular irritancy test of niosomes also showed no sign of redness, inflammation or increased tear production, indicating that the niosomes can be used as enhanced and safe topical ocular drug delivery system. Prabhu et al. studied the feasibility of vesicular formulation, using both liposome and noisome, as drug delivery system for brimonidine tartrate in order to improve its intraocular pressure (IOP) lowering activity for treatment of glaucoma.[97] The vesicle formulations were in the size range of 210-245 nm, with drug payload up to 42 w/w%. Although the vesicular formulations did not show as high of IOP-lowering activity as that of marked formulation of pure drug solution, they extended the duration of the activity up to 6 to 8 fold compared to the marketed formulation. Niosomes coated with mucoadhesive materials, chitosan, were developed by Kaur at el. to investigate its potential as drug delivery system for timolol maleate (TM), which is another treatment drug for glaucoma having IOP lowering effect.[98] The chitosan coated noisome showed higher and prolonged corneal permeation of TM into the aqueous humor compared to the pure drug solution. Consequently, the IOP lowering effect of the niosomal formulation of TM was maintained up to 8 hrs, compared to 1.5 hrs of the drug solution.

## 2.6.5 Dendrimers

Dendrimers are three-dimensional, highly branched, and tree-structured macromolecules. Dendrimers have nanoscale sizes due to their well-organized synthesis strategy. In addition, because of their highly branched structure, the surface of the dendritic macromolecules can be easily functionalized with desired properties. Dendrimers can also encapsulate hydrophobic drug molecules since they possess internal empty cavities and open conformations for low generation dendrimers. Due to these properties, dendrimers are very attractive system for drug delivery applications.[99]

One of the most widely studied dendrimer for ocular drug delivery system is poly(amidoamine) (PAMAM). Vandamme and Brobeck used PAMAM dendrimers to improve ocular residence time.[56] They have demonstrated that the use of 0.25 w/v% PANAM solution mixture with pilocarpine prolonged ocular residence time of pilocarpine up to 5 hours, which is comparable to Carbopol® (a commercial bioadhesive polymer for ophthalmic dosage forms) but without causing the irritation that was observed in Carbopol® administration. The study also showed that residence time was longer for dendrimers with hydroxyl or carboxyl surface groups. Puerarin-PAMAM complexes were developed by Yao et al. through hydrogen-bond interactions.[100] Similar to the previous study, they have demonstrated prolonged ocular residence time of the puerarin by having the complex formulation, compared to puerarin eye drops. It was also reported that, although the puerarin-PAMAM complex did not increase the corneal permeability coefficient, the physical mixture of cationic G4 PAMAM dendrimer with puerarin was found to have enhanced corneal permeability coefficient and increased cumulative amount of puerarin permeating across the cornea. Durairaj et al. used complex formation between dendrimeric polyguanidylated translocators (DPTs) and gatifloxacin (GFX) antibiotic to improve the permeation across sclera-choroid-retinal pigment epithelium (SCRPE) membranes.[101] The complex improved the permeation of GFX across SCRPE 40% in 6 hours. *In vivo* studies showed that the topical administration of the complex was able to maintain higher drug concentration for up to 24 hours, compared to pure drug solution. New phosphorus-containing dendrimers, with quaternary ammonium salt as core and carboxylic acid terminal groups have been synthesized.[57] These cationic dendrimers were able to physically associate with amino groups of carteolol (an ocular anti-hypertensive drug) by forming ion pairs. The generation 2 dendrimer-carteolol formulation improved the corneal penetration 2.5 times compared to carteolol alone. However, the generation 2 dendrimer showed poor water solubility and therefore the amount of instilled carteolol was limited.

The ease of surface functionalization and the ability to encapsulate hydrophobic drugs render dendrimers an attractive ocular drug delivery system. In some animal studies however, vision blurring effect was observed after the administration of dendrimer on the ocular surface.[14] This issue must be addressed in the future studies using dendrimers before proceeding to clinical trial studies.

### **2.6.6 Cyclodextrins**

Cyclodextrins (CDs) are a family of cyclic oligosaccharides, composed of 6 to 8 glucose units which have been shown to improve pharmacokinetic properties of many drugs through formation of inclusion complex.[102] The application of cyclodextrins in ophthalmic formulations has been reviewed extensively in the past decade.[102-104] The complex inclusion of hydrophobic drugs with CDs can increase the aqueous solubility of those drugs. Toxicity studies in the past have shown that orally administered CDs are practically non-toxic, due to the lack of absorption from gastrointestinal tract.[105] One of the most extensively reported cyclodextrin used as ocular drug delivery enhancement is 2-hydroxypropyl  $\beta$ -CD (HP $\beta$ CD) which is modified with hydroxypropyl derivative to increase its water solubility. Topical administration of CDs have also shown no toxic effects, and eye drop solutions containing 45% of HP $\beta$ CD showed no irritation effects in rabbits.[106] Similar to other types of nanomaterials described in this report, CDs also act as a permeation enhancer at biological barriers, such as cornea, by increasing the drug retention at the surface of the corneal epithelium.

Wang et al. used inclusion complex between disulfiram (DSF) and HP $\beta$ CD in eye drop formulation in order to increase the bioavailability of the drug across the corneal membrane.[107] Along with the addition of penetration enhancer hydroxypropylmethylcellulose (HPMC), the eye drop formulation successfully suppressed the cataract effect (i.e. lens opacity) for up to 48 hours in rabbits. Similarly, Zhang et al. also used HP $\beta$ CD with complex inclusion of ketoconazole (KET) in topical eye drop formulation.[108] The incorporation of HP $\beta$ CD increased the aqueous solubility of KET. Compared to the KET suspension, the HP $\beta$ CD/KET complex significantly increased the bioavailability of KET; over 8-fold in aqueous humor, and 12-fold in cornea. More recently, another group has investigated the complex between HP $\beta$ CD and indomethacin and found delayed release and high drug stability effect.[109] While showing no signs of irritation after administration to rabbits, HP $\beta$ CD-indomethacin complex showed significant improvement in therapeutic efficacy in healing corneal wounds. Mahmoud et al. developed ionically crosslinked chitosan/sulfobutylether- $\beta$ -cyclodextrin nanoparticles as ocular drug delivery system.[110] The nanoparticle system showed sustained release behavior of encapsulated econazole nitrate. Furthermore, the incorporation of chitosan on the surface of the nanoparticles also

significantly improved the ocular mucoadhesiveness which enable the nanoparticle as promising carrier for controlled ocular drug delivery system.

## **2.7 Future perspectives**

The field of ocular drug delivery has taken a significant stride forward with the advent of nanotechnology. Numerous recent studies have focused on using various types of nanomaterials, such as polymeric micelles, hydrogels, liposomes, niosomes, dendrimers, and CDs as drug carriers, to increase the ocular bioavailability of various therapeutic agents. Topical administration of the drugs associated with the nanomaterials showed sustained release of the drug which increased the duration of therapeutic activity, consequently reducing the need for frequent administration. To date, demonstrating an enhancement in the extent of absorption into the vitreous cavity across corneal membranes, the topical administration of nanomaterial/drug complexes to target the posterior segment of the eye has yet to be proven to be therapeutically effective compared to intravitreal or periocular injections. However, due to the invasive nature of intravitreal and periocular injections, further studies utilizing nanomaterials to overcome the various ocular barriers are expected. Although several in vivo studies have shown that the nanodrug carriers did not induce any signs of irritation or inflammatory responses, the long-term effect of these nanomaterials in both the ocular region and the systemic circulation must be rigorously analyzed. There is no doubt that pharmaceutical researchers will continue improving the performance of ocular drug delivery systems with the help of nanotechnology, to achieve therapeutically effective, patient-compliant, and low cost systems with negligible side-effects.

## Chapter 3

# Development of nanoparticle drug carriers using PLA-Dex block copolymers

### 3.1 Summary

NP drug delivery carriers formed by the self-assembly process of linear block copolymer PLA-Dex have been developed. The characterization of the NPs formed by the self-assembly process of PLA-Dex showed some unique properties that are desirable for drug delivery system. The NPs sizes were tuneable from 15 to 70 nm simply by changing the molecular weights of the PLA and/or Dextran used. In addition to the abundant functional hydroxyl groups on the Dextran surface, the high surface area-to-volume ratio provides effective surface functionalization for targeted therapy. The NPs were also able to encapsulate large dose of hydrophobic therapeutic agent, Doxorubicin, and showed sustained release phenomenon for up to 8 days. These results demonstrate that PLA-Dex is a promising new biomaterial for drug delivery purposes, which can be further explored as a topical ocular drug delivery system for targeted therapy through surface functionalization with specific targeting ligands.

### 3.2 Introduction

Nanomedicine – the fusion of nanotechnology and medicine – is one of the most promising approaches to address challenges associated with conventional drug delivery methods [111]. In the past decade, drug delivery systems constructed from polymeric nanoparticles (NPs) have been the cornerstone of progress in the field of nanomedicine [61, 112, 113]. Various types of polymeric materials composed of poly(D,L-lactide) (PLA), poly(glycolide) (PGA), poly(lactide-co-glycolide) (PLGA), and poly( $\epsilon$ -caprolactone) (PCL), have been studied extensively for NP drug delivery applications [38, 114, 114]. To date, masking the NP surface with poly(ethylene glycol) (PEG) has been the most effective strategy to improve the stabilities of NP drug delivery systems *in vitro* and *in vivo* [115-121]. PEGylated NPs with sizes under 70 nm in diameter have the potential of bypassing the reticuloendothelial system (RES), which leads to prolonged circulation half-life of the particles [122]. Particles with size smaller than 100 nm preferentially accumulate at the tumor site by enhanced permeation and retention (EPR) effect and also evade the organs of the RES [123]. Once the NPs reach the intended tumor site, the rate of NP uptake by the tumor cells is largely influenced by the particle size. It has been demonstrated that rapid cellular uptake of NPs can be achieved when particle size falls below 50 nm [124]. PLGA-PEG



is the most widely used polymer for making biodegradable drug delivery system. However, the self-assembly of PLGA-PEG block copolymer generally yields NPs of sizes greater than 150 nm [125]. Although smaller particles can be synthesized, they suffer from low drug encapsulation and rapid drug release [125]. An emerging strategy for making PLGA-PEG NPs under 100 nm is by rapidly mixing the block copolymers in a microfluidics device [125].

Here, we synthesized a linear block copolymer using PLA and Dextran (Dex-*b*-PLA), and demonstrated that NPs composed of Dex-*b*-PLA can self-assemble into core-shell structured NPs with sizes less than 40 nm without using any flow-focusing devices. We further showed the size of Dex-*b*-PLA NPs can be precisely fine-tuned between 15-70 nm by altering the MW of the compositional blocks. Dextran, a natural polysaccharide composed of 1→6 linked  $\alpha$ -D-glucopyranosyl units, was selected as a model hydrophilic block because of its high hydrophilicity and biocompatibility. Studies have shown that Dextran coated NPs showed superior colloidal stability compared to those coated with PEG chain [126]. Dextran and PLA have been explored together in the synthesis of PLA-*graft*-Dex [127]. However, Dextran-grafted copolymer has a major limitation because grafting density (i.e. the number of PLA per Dextran backbone) is difficult to control, and the grafting is limited only to low MW PLA as opposed to high MW PLA. In this study, linear block copolymers composed Dextran and PLA were synthesized, and the size and morphologies of the NPs formed from Dex-*b*-PLA were systematically controlled by varying their composition. The drug encapsulation efficiencies of the NPs and their release kinetics were also evaluated using Doxorubicin as a model hydrophobic anti-cancer drug. The hemolytic activity of the NPs was tested to profile the biocompatibility of the NPs in systemic circulation, and the blood circulation half-life and biodistribution of the NPs in rats were assessed.

### 3.3 Experimental Section

#### 3.3.1 Materials

Acid-terminated poly(D,L-lactide) (PLA,  $M_w \sim 10, 20$  and 50 kDa) and PLGA-PEG (PLGA  $M_w \sim 40$  kDa, PEG  $M_w \sim 6$  kDa) were purchased from Lakeshore Biomaterials (Birmingham, AL, USA). PLA was purified by dissolving in dimethyl sulfoxide (DMSO) and precipitating in methanol to remove residual monomers. Dextran (Dex,  $M_r \sim 1.5, 6,$  and 10 kDa), hydrochloric acid (HCl), triethylamine (TEA), *N*-(3-dimethylaminopropyl)-*N*-ethylcarbodiimide (EDC), and sodium cyanoborohydride (NaCNBH<sub>3</sub>) were purchased from Sigma Aldrich (Oakville, ON, Canada), and used without further purification. *N*-Hydroxysulfosuccinimide (Sulfo-NHS) and *N*-Boc-ethylenediamine were purchased

from CNH Technologies (Massachusetts, USA). Doxorubicin-HCl (MW = 580 Da, Intatrade GmbH, Bitterfeld, Germany) was deprotonated by adding TEA (2M equivalent) in the aqueous solution of Doxorubicin-HCl, and the hydrophobic form of Doxorubicin was extracted using Dichloromethane (DCM).[128] Borate buffer was prepared at a concentration of 0.05M with pH of 8.2 by mixing boric acid and sodium hydroxide. Whole sheep blood (in Alsever's) was purchased from Cedarlane (Burlington, ON, Canada). Veronal Buffer solution (VBS, 5x) was purchased from Lonza Walkersville Inc (Walkersville, MD, USA). Tritium [<sup>3</sup>H]-PLA-radiolabeled nanocrystals were purchased from PerkinElmer (Boston, MA, USA).

### 3.3.2 Synthesis of PLA-Dex block copolymer

The synthesis of the linear block copolymer was divided into three stages: 1) reductive amination between Dextran and *N*-Boc-ethylenediamine, 2) deprotection of the Boc group, and 3) conjugation of the end modified Dextran with PLA (Figure 5). The first step of the synthesis involves reductive amination between the aldehyde on the reducing end of Dextran and the amine group of *N*-Boc-ethylenediamine cross-linker. In a typical reaction, Dex6 ( $M_r \sim 6$  kDa, 6 g) was dissolved in 15 mL of borate buffer (0.05 M, pH 8.2) with excess *N*-Boc-ethylenediamine. The reducing agent, NaCNBH<sub>3</sub> (1 g, 15 mmol), was added to the borate buffer solution and the mixture was stirred for 72 hours in dark conditions at room temperature. The mixture was then washed in methanol to remove any unreacted molecules or catalysts. The end-modified Dextran was dried overnight *in vacuo* and re-dissolved in de-ionized water (DI-H<sub>2</sub>O). The deprotection of Boc group was performed first by adding HCl (~ 4 M) for 1 hour to cleave the amide bond between the Boc group and the protected amine moiety. Subsequently, TEA was added to increase the pH of the solution up to 9 to deprotonate the NH<sub>3</sub><sup>+</sup> end groups which were deprotected. The mixture was then washed twice using methanol and dried *in vacuo*. The amine terminated Dextran and carboxyl terminated PLA20 ( $M_w \sim 20$  kDa, 6 g, 0.3 mmol) were dissolved in DMSO. The conjugation between the two polymers was facilitated by adding catalysts EDC (120 mg, 0.773 mmol) and Sulfo-NHS (300 mg, 1.38 mmol) and allowing reaction to proceed for 4 hours at room temperature. The resulting Dex-*b*-PLA was twice precipitated and purified using excess methanol. In order to remove free Dextran, the mixture was dissolved in acetone (30 mL) to form a cloudy suspension. This was centrifuged at 4000 rpm for 10 minutes and the supernatant was extracted carefully. The supernatant was purged with air to remove the solvent and then dried overnight *in vacuo* to obtain the final copolymers. The three stages of the synthesis were verified by <sup>1</sup>H NMR characterization.

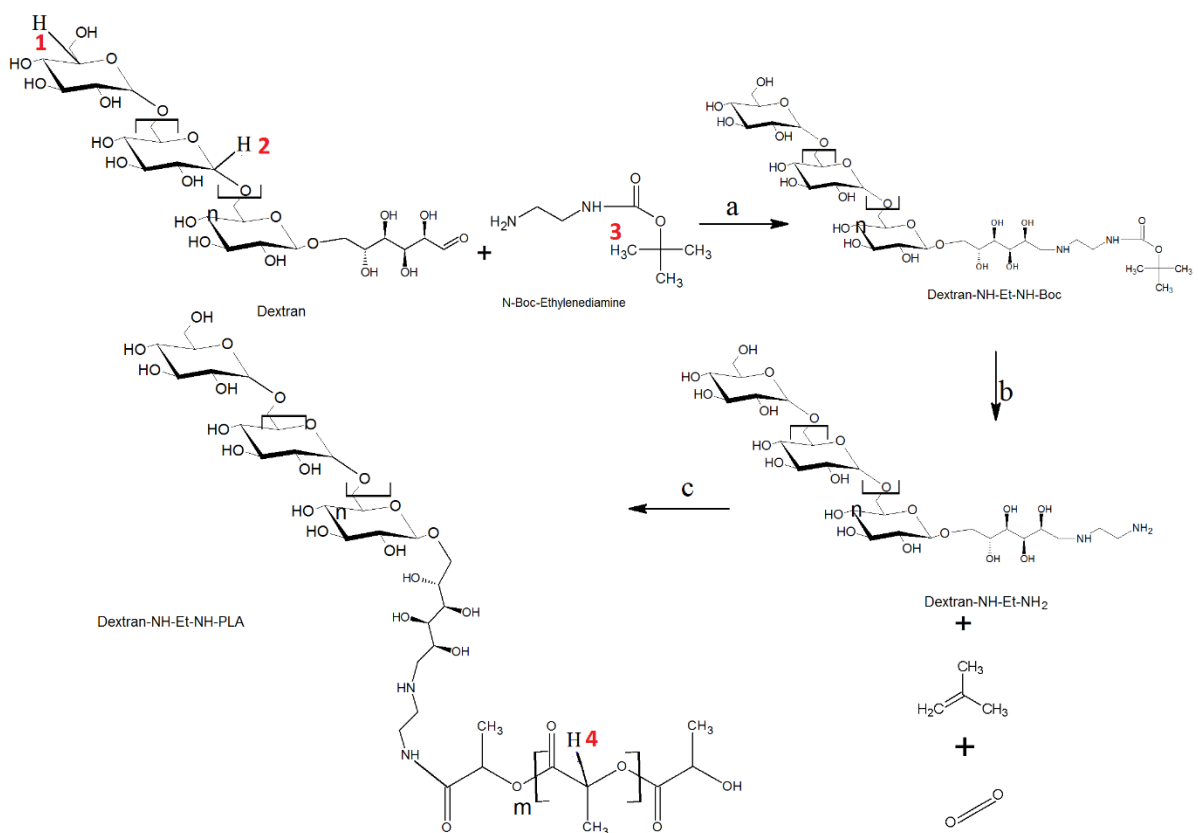


**Figure 5. Synthesis of Dex-*b*-PLA block copolymers. a) Synthesis of Dextran-NH-Et-NH-Boc. Conditions: NaCNBH<sub>3</sub> in Borate buffer (pH 8.2) for 72 hr at RT in dark. b): Synthesis of Dextran-NH-Et-NH<sub>2</sub>. Conditions: HCl/TEA in DI-H<sub>2</sub>O for 1hr each at RT. c): Synthesis of Dextran-NH-Et-NH-PLA. Conditions: EDC/Sulfo-NHS RT for 4hrs.**

### 3.3.3 Characterization of PLA-Dex NPs

The PLA-Dex NPs were prepared using a nanoprecipitation method: 1mL of Dex-*b*-PLA in DMSO (10 mg/mL) was added in a drop-wise manner to 10 mL of DI-H<sub>2</sub>O under constant stirring in order to form NPs. This was stirred for 30 minutes. The sizes of the NPs were analyzed using 90Plus Particle Size Analyzer (Brookhaven,  $\lambda = 659$  nm at 90°). The volume averaged multimode size distribution (MSD) mean diameters were used from the results. The particle size and the morphology of the Dex-*b*-PLA NPs were further verified using Transmission Electron Microscopy (TEM, Philips CM10).

### 3.3.4 Doxorubicin encapsulation in PLA-Dex NPs

The encapsulation of Doxorubicin in the Dex-*b*-PLA NPs was accomplished using a nanoprecipitation method. Dex-*b*-PLA and Doxorubicin were both dissolved in DMSO (Dex-*b*-PLA concentration of 7 mg/mL, with varying drug concentrations). 1 mL of the DMSO solution was added drop-wise into 10 mL of water under stirring and stirring was continued for additional 30 minutes. The NPs in water were filtered through a syringe filter (pore size = 200 nm) to remove the drug aggregates and subsequently filtered through Amicon filtration tubes (MWCO = 10 kDa, Millipore) to further remove any remaining free drugs in the suspension. The filtered NPs containing encapsulated Doxorubicin were resuspended and diluted in DMSO. Consequently, the drug loading (wt%) in the polymer matrix was calculated by measuring concentration of the Doxorubicin in the mixture by obtaining the absorbance of the solution at 480 nm using Epoch Multi-Volume Spectrophotometer System (Biotek). The measurements were obtained in triplicate ( $n = 3$ , mean  $\pm$  S.D). The absorbance measured from the same procedure using the polymers without the drugs was used as the baseline. The absorbance was correlated with the concentration of the Doxorubicin in DMSO by using standard calibration obtained. The same procedure was used for PLGA-PEG to encapsulate Doxorubicin for comparative analysis.

### 3.3.5 *In vitro* release of Doxorubicin from PLA-Dex NPs

Using the procedure described in the previous section, drug encapsulated NPs were prepared and filtered to remove non-encapsulated drug aggregates. A purified sample of NPs-drug suspension was collected to measure the maximum absorbance and this was used as the 100% release point. Subsequently, the NP-drug suspension was injected into a Slide-a-Lyzer Dialysis cassette (MWCO = 20 kDa, Fisher Scientific) and dialyzed against 200 mL of phosphate buffered saline (PBS, pH 7.4) at 37 °C under mild stirring. At predetermined time intervals, 1 mL of the release medium was extracted and the same volume of fresh new PBS was added to the release medium. The extracted release medium was used to perform UV-Vis absorption measurements at 480 nm in triplicates ( $n = 3$ , mean  $\pm$  S.D). The release medium was replaced several times to maintain the concentration of Doxorubicin in the medium below 3  $\mu$ g/mL and to stay below the solubility limit of the Doxorubicin in PBS. The release of Doxorubicin from PLGA-PEG was also obtained with identical procedure for comparative analysis. All experiments were performed in dark environment, and the beakers were sealed with Parafilm to prevent evaporation of PBS.

## 3.4 Results and Discussion

### 3.4.1 $^1\text{H}$ NMR characterization of PLA-Dex

The three steps of the synthesis were verified using Proton Nuclear Magnetic Resonance ( $^1\text{H}$  NMR, 300 MHz) spectroscopy. The conjugation of Dextran with N-Boc-ethylenediamine was confirmed by the presence of multiplets at 1.3 ppm corresponding to the Boc group (Figure 6, II), which then disappears in the deprotection step (Figure 6, III). The last step, the conjugation between Dextran and PLA, was demonstrated by showing both peaks corresponding to the monomers of Dextran (multiplets at 4.86 ppm) and PLA (multiplets at 5.2 ppm).

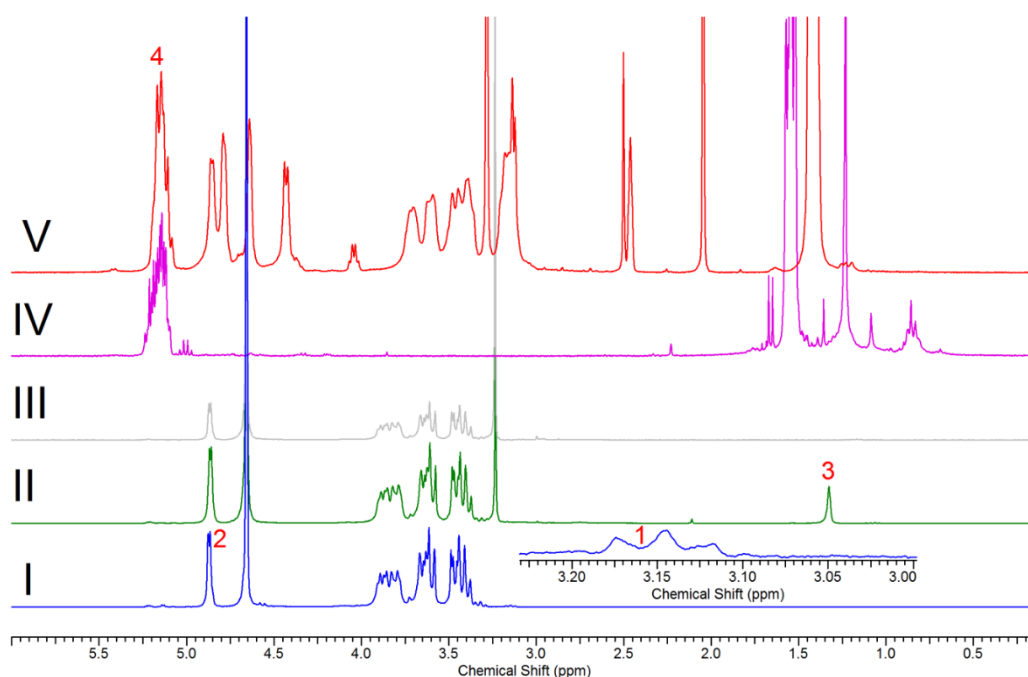


**Figure 6.**  $^1\text{H}$  NMR of I. Dextran (10 kDa), II. Dextran-Ethylenediamine-Boc, III. Dextran-Ethylenediamine, IV. PLA (20 kDa), V. PLA-Dex (PLA20-Dex10).[4]

### 3.4.2 Size and morphology of the PLA-Dex NPs

It is hypothesized that, due to their amphiphilic nature, PLA-Dex block copolymers undergo self-assembly process to form nanoparticles with micellar structure. In aqueous medium, the hydrophobic PLA chains form the core of the nanoparticles while the hydrophilic Dextran form the shell of the nanoparticles, shielding PLA core from the surrounding water. It was shown that varying the molecular weights (MW) of PLA and/or Dextran affected the particle sizes formed by the NPs (Figure 7a).

Increasing the MW of PLA increased the NP size since larger core was formed by higher MW of PLA's. On the other hand, increasing the MW of Dextran decreased the NP size since longer Dextran was more flexible and therefore able to "fold-down" on the particle surface, resulting in smaller hydrodynamic diameters.[129] Transmission Electron Microscopy (TEM) images further verified the sizes and the micellar morphologies of the PLA-Dex NPs (Figure 7b).

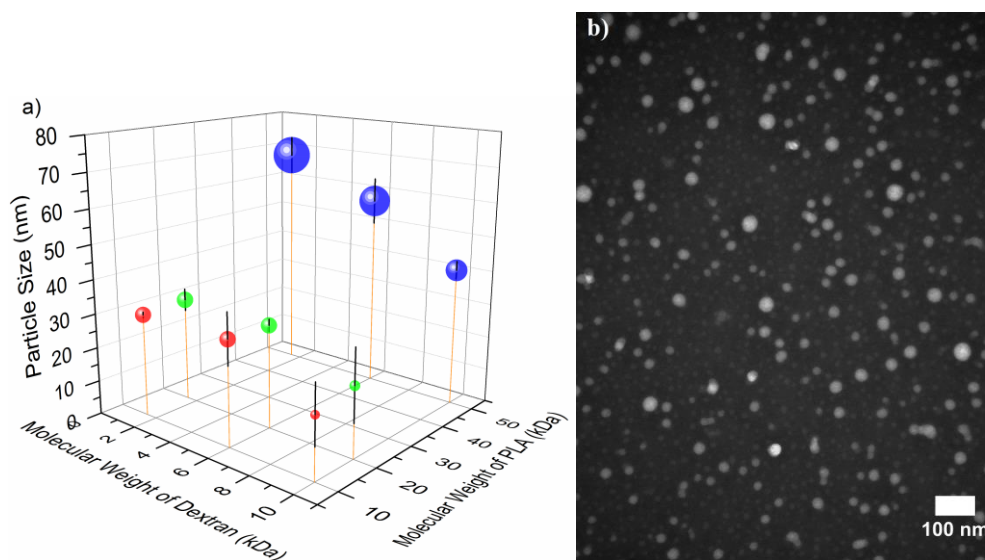


**Figure 7. Particle size and morphology of PLA-Dex NPs: a) Effect of MW's of PLA and Dextran on the sizes of the NPs formed from nine different polymers; b) TEM image of PLA20-Dex6 ( $MW_{PLA} = 20$  kDa,  $MW_{DEX} = 6$  kDa).[4]**

### 3.4.3 Drug encapsulation and release

The ability of the NPs to encapsulate hydrophobic drugs and release them in a sustained manner were also studied. Using anticancer drug Doxorubicin as a model hydrophobic drug, PLA20-Dex6 and PLA20-Dex10 were selected for the study and were also compared with the commercially available biomaterial Poly(lactic-co-glycolic acid)-*b*-Poly(ethylene glycol). The PLA-Dex NPs showed maximum drug loading of 21.2 wt% (PLA20-Dex10), whereas PLGA-PEG NPs showed maximum loading of 7.1 wt% (Figure 8). The maximum loading of PLA-Dex NPs are also comparable to that commercially available liposomal formulation Doxil<sup>®</sup>. In *in vitro* Doxorubicin study, both PLA-Dex NPs and PLGA-PEG NPs showed initial burst release region followed by a sustained release region. The initial burst release region is due to the release of Doxorubicin that is either in the free suspension or loosely bound near the surface of the NPs. On the other hand, the sustained release region is associated

with the diffusion of Doxorubicin that is encapsulated in the PLA core of the NPs. PLGA-PEG NPs exhibited burst release for the first 6 hours of the study followed by a sustained release for up to 4 days, whereas both type of PLA-Dex NPs showed 24 hours of burst release and subsequent sustained release region lasted up to 8 days.

One of the main reasons that PLA-Dex NPs showed more desirable drug encapsulation and release phenomenon compared to PLGA-PEG is hypothesized to be due to the greater hydrophilicity of Dextran over PEG chains. Having greater hydrophilicity than PEG chains, Dextran chains have less chance of being randomly associated with the PLA core of the NPs, thus improving the association of hydrophobic drug with the hydrophobic PLA core. This phenomenon may explain the increased drug loading in PLA-Dex NPs as opposed to PLGA-PEG NPs, which also increase the amount of drug that slowly diffuse from the core of the PLA thus prolonging the duration of sustained release region.

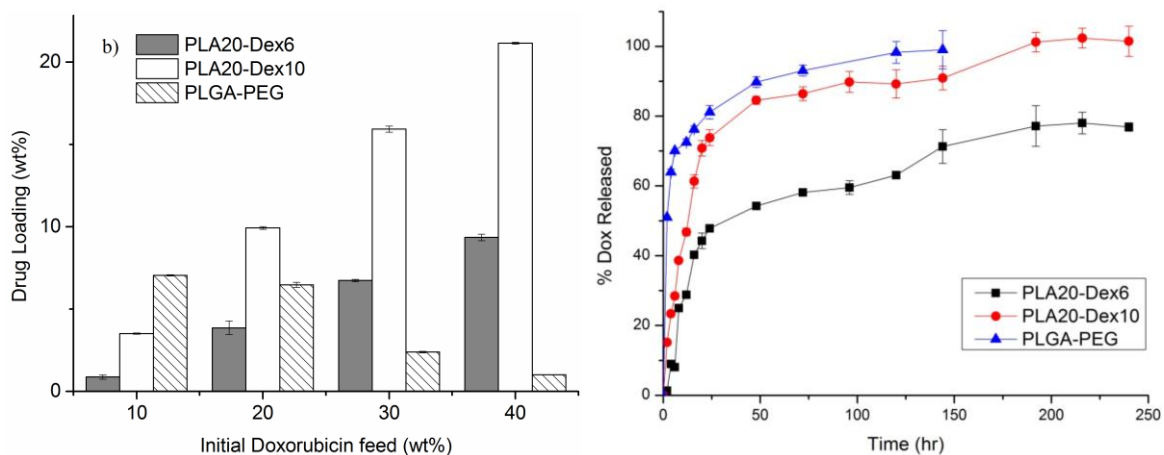


**Figure 8. Drug encapsulation and release: Doxorubicin loading in PLA-Dex and PLGA-PEG NPs (left), and Doxorubicin in vitro release profiles (right).[4]**

### 3.5 Conclusion

A linear block copolymer of Dextran and PLA was synthesized and used for making size tuneable NPs. The size of NPs was controlled under 50 nm, simply by modulating the MW of Dextran and PLA. These NPs demonstrated efficient doxorubicin encapsulation, and controlled drug release. These NPs have provided us with promising tools for developing a controlled drug delivery system for nanomedicine applications.

## Chapter 4

### Mucoadhesive nanoparticles for topical ocular drug delivery

#### 4.1 Summary

Mucoadhesive NP drug carriers have attracted substantial interest as a potential solution to the low bioavailability of topical formulations. In this study, NPs composed of PLA-Dex and surface functionalized with PBA were developed as mucoadhesive NP drug carriers. The NPs encapsulated up to 13.7 wt% Cyclosporine A and exhibited sustained drug release for up to 5 days *in vitro* at a clinically relevant dose. High densities of PBA functionalization were achieved due to the abundance of functional groups on dextran surfaces, and 23 mol% or more functionalization facilitated the mucin-NP interaction in *in vitro* analysis. These data show that PLA-Dex\_PBA NP is a promising new biomaterial to significantly improve the bioavailability of topical formulations.

#### 4.2 Introduction

Topical administration is the most common delivery method employed to treat corneal diseases. Common topical formulations, such as eye drops or ointments, suffer from low ocular bioavailability due to rapid drainage through the naso-lacrimal duct, nearly constant dilution by tear turnover, and low drug permeability across the corneal epithelium[6]. As a result, topical formulations are normally administered multiple times daily in order to achieve therapeutic efficacy, resulting in a higher potential for side effects and lower patient compliance.

Recently, formulations using NPs as drug carriers have been proposed to overcome the limitations associated with topical administration methods. NP carriers have been shown to improve drug stability in water and also prolong drug activity through the controlled release of encapsulated compounds[1, 6, 12, 35]. NPs formulated using biodegradable polymers, such as poly(lactic-co-glycolic acid) (PLGA), have been tested for ocular topical drug delivery applications[1, 7, 9, 33]. Poly(ethylene glycol)-based NPs, or PEGylated NPs, have attracted significant attention due to their ability to improve the stability of drug carrier systems in physiological environments[115, 119, 130, 131]. In chapter 3, we synthesized a dextran-based amphiphilic block copolymer, poly(D,L-lactide)-*b*-dextran (PLA-Dex), that can self-assemble to form core-shell structured NPs. The size of PLA-Dex NPs can be precisely tuned between 20 to 60 nm in diameter by simply adjusting the molecular weight of the two polymer chains[4]. Dextran has an abundance of functional hydroxyl groups on its back bone, as opposed to PEG, which



has one free functional group per chain. The higher density of surface functional groups can improve the efficiency of surface functionalization, and thus, desirable surface properties are more easily achieved with dextran based NPs. Moreover, dextran coated NPs showed excellent colloidal stability in physiological media *in vitro* and long retention in the systemic circulation *in vivo* [4, 132]. We postulate that the abundance of functional groups on dextran can be modified to target the ocular surface, and thus prolong corneal retention.

The surfaces of polymeric NPs have been functionalized with molecular ligands that can selectively bind to the ocular mucosa to increase precorneal drug retention [133-136]. To date, the most widely used method to achieve mucoadhesion exploits electrostatic interactions between the negatively charged sialic acid residues of the corneal mucin and cationic polymers such as chitosan [134, 136]. However, the electrostatic interactions may be hindered by various counter ions in the tear fluid, resulting in the clearance of these NPs by tear turnover. The use of covalent binding via specific targeting ligands can further strengthen the mucoadhesive in order to improve corneal retention of the NPs. Phenylboronic acid (PBA), which contains a phenyl substituent and two hydroxyl groups attached to boron, can form a complex with the diol groups of sialic acid at physiological pH[137-142].

In this study, we aimed to functionalize PLA-Dex NP surfaces with PBA molecules for specific targeting of sialic acid residues of the ocular mucosa. The amount of PBA functionalization on the dextran surface can be varied to analyze its effect on the size of the NPs formed and the extent of their interaction with mucin particles in order to find the optimal formulation at which desirable mucoadhesion is achieved, without compromising the colloidal stability of the NPs formed. Cyclosporine A (CycA), which is prescribed for chronic dry eye syndrome [143, 144], was used as a model hydrophobic drug. The CycA encapsulation and release kinetics were evaluated *in vitro*.

## **4.3 Experimental Section**

### **4.3.1 Materials**

Acid-terminated poly(D,L-lactide) (Mw ~ 20 kDa) was purchased from Lakeshore Biomaterials (Birmingham, USA) and washed with methanol to remove monomer impurities. Dextran (Mr ~ 10 kDa), Cyclosporine A (CycA), 3-Aminophenylboronic acid monohydrate (PBA), sodium periodate (NaIO<sub>4</sub>), glycerol, and sodium cyanoborohydride (NaCNBH<sub>3</sub>) were purchased from Sigma Aldrich (Oakville, Canada). Simulated tear fluid (STF) was prepared for the *in vitro* release experiment using previously known formulation[145]

### **4.3.2 Surface functionalization of PLA-Dex NPs with PBA**

The synthesis of dextran-b-Poly(D,L-lactide) (PLA-Dex) was described in Chapter 3 [4]. PLA-Dex was dissolved in DMSO (30 mg/ml), and added slowly into water under mild stirring. Periodate oxidation of the dextran surface was carried out by adding 60 mg of NaIO<sub>4</sub> and stirring for an hour. Subsequently, glycerol was added to quench the unreacted NaIO<sub>4</sub>. Various amounts of PBA (i.e. 40 mg for PLA-Dex\_40PBA) was added to the mixture along with NaCNBH<sub>3</sub> for 24 hours. All reactions were carried out in dark. The mixture was then dialyzed in H<sub>2</sub>O for 24 hrs to remove any unreacted solutes, changing the wash medium 4 times.

### **4.3.3 Characterization of PLA-Dex\_PBA**

PLA-Dex\_PBA was analyzed using <sup>1</sup>H NMR (Bruker 300 MHz) using DMSO-d<sub>6</sub> as the solvent. The amount of PBA attached to the dextran chain was quantified using UV-Vis absorption at 291 nm after performing the standard calibration of PBA in DMSO. PLA-Dex polymer in DMSO was used as the baseline. The sizes of the NPs were determined using dynamic light scattering (DLS) by measuring the multimode-size distribution (MSD) volume-average mean diameters. The sizes and morphology were further confirmed using transmission electron microscopy (TEM) by drying a sample of NP suspension on a copper grid and using phosphotungstic acid solution as the negative stain [4].

### **4.3.4 Cyclosporine A encapsulation and *in vitro* release**

The determination of encapsulation of CycA in PLA-Dex and PLA-Dex\_PBA NPs was accomplished using methods described previously [4]. Both PLA-Dex and PLA-Dex\_PBA NPs were also used in *in vitro* release study. 10 ml of NP-drug suspension was dialyzed against 200 mL of STF, with 0.1 w/v% sodium dodecyl sulfate, at 35 °C under stirring. At predetermined time intervals, 1 mL of the release medium was extracted and same volume of fresh STF was added to the medium. The amount of CycA was quantified using high-performance liquid chromatography (HPLC) equipment.

### **4.3.5 *In vitro* mucoadhesion**

Mucoadhesion was calculated as the amount of mucin adsorbed per mg of NPs. NP suspension (1ml) was mixed with 1ml of mucin solution (1mg/ml in STF) and incubated at 37°C for 1 hr. The mixture was then centrifuged at 15,000 rpm for 1 hr and free mucin in the supernatant was quantified using the periodic acid/Schiff (PAS) staining method [146]. Mucin adsorption was calculated by subtracting the

free mucin concentration from the initial mucin concentration. Mucin standards (0.1, 0.25 and 0.5 mg/ml) were determined using the same procedure to obtain a calibration curve.

## 4.4 Results and Discussion

### 4.4.1 Synthesis and characterization of PBA functionalized PLA-Dex NPs

The  $^1\text{H}$  NMR spectrum of PLA-Dex\_PBA shows peaks corresponding to both PLA (multiplets at 5.2 ppm) and dextran (multiplets at 4.86 ppm), while also showing multiplet peaks at 6.6 ppm and 6.9 ppm which correspond to carbons from position 2 to 6 in the phenyl group of the PBA (Figure 9). UV absorption at 291 nm was measured to quantify the amount of PBA on the NPs with respect to the dextran monomers. Increasing the amount of PBA in the initial reaction mixture proportionally increased the final PBA conjugation on the dextran surface (Table 2), with highest density of 34.6 mol% (equivalent of about 3.5 PBA conjugated per 10 dextran monomers) achieved for PLA-Dex\_320PBA NPs.

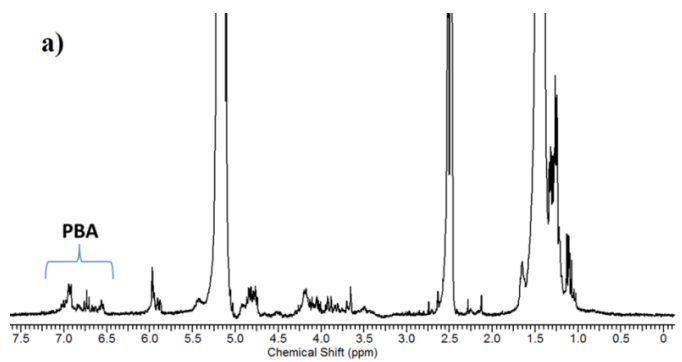


**Figure 9.  $^1\text{H}$  NMR characterization of PLA-Dex\_PBA.**

Upon formation of NPs using nanoprecipitation method, the size and morphology of the PLA-Dex\_PBA NPs were characterized using DLS and TEM respectively. The sizes of the NPs were in the range of 25 to 28 nm, which are smaller than the unmodified NPs of 47.9 nm (Table 2). We postulate that the particle size reduction is attributed by the PBA molecules causing dextran chains to be less hydrophilic, leading to form more compact shells around PLA particle core. TEM images confirmed spherical morphology due to the formation of core-shell structure of the amphiphilic block copolymers (Figure 10). The sizes of PLA-Dex\_PBA NPs obtained are smaller compared to what can normally be achieved with PEG based block copolymers such as PLGA-PEG[125]. We postulate that smaller NPs

may be more desirable for mucoadhesion since they provide greater surface area for interaction mucous membrane.

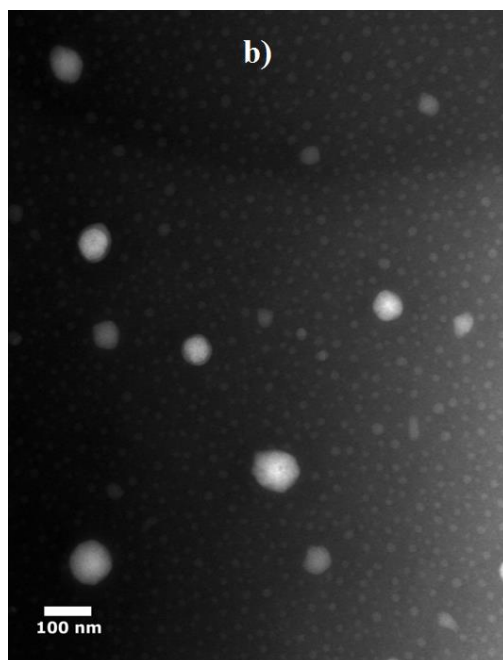


**Figure 10. TEM imaging of PLA-Dex\_320PBA NPs.**

**Table 2. PBA conjugation efficiency and mucin adsorption of PLA-Dex NPs.**

Formulation	PBA:Dex <sup>a)</sup> (mol%)	Diameter <sup>b)</sup> (nm)	Mucin adsorbed/mg of NPs (mg)
PLGA-PEG	0	133.9 ± 6.1	0.177 ± 0.004
PLA-Dex	0	47.9 ± 0.5	0.452 ± 0.007
PLA-Dex_10PBA	2.85 ± 0.03	27.5 ± 0.9	0.575 ± 0.028
PLA-Dex_40PBA	12.2 ± 0.2	26.7 ± 0.1	0.584 ± 0.026
PLA-Dex_160PBA	22.9 ± 0.3	25.2 ± 1.0	0.604 ± 0.016
PLA-Dex_320PBA	34.6 ± 0.2	28.1 ± 0.3	0.471 ± 0.009

<sup>a)</sup>Mol% of PBA with respect to dextran monomers; <sup>b)</sup>NP diameter was determined from DLS

#### **4.4.2 Cyclosporine A encapsulation and *in vitro* release**

The encapsulation of CycA was accomplished through the nanoprecipitation method. Maximum encapsulation of CycA was achieved at initial feed of 40 wt%: PLA-Dex NPs encapsulated up to 10.8

wt% whereas PLA-Dex\_40PBA and PLA-Dex\_320PBA encapsulated up to 11.2 and 13.7 wt% respectively (Figure 11a). The 13.7 wt% encapsulation is equivalent of 2.38  $\mu\text{g}$  of CycA in 28  $\mu\text{L}$  formulation (same as the administration volume of commercially available RESTASIS<sup>®</sup>), whereas the commercial product contains 14  $\mu\text{g}$ . Therefore, a therapeutically relevant dosage can be achieved by simply adjusting the polymer and drug concentration in the formulation. One possibility that PLA-Dex\_PBA NPs encapsulated higher amount of CycA compared to PLA-Dex NPs is that the more hydrophobic dextran chains, due to the PBA conjugation may be able to trap more CycA near the surface of the NPs.

*In vitro* CycA release phenomena from both PBA modified and unmodified PLA-Dex NPs in the STF at 35°C were analyzed by quantifying the CycA in the STF at predetermined time intervals using HPLC. Both PLA-Dex and PLA-Dex\_PBA NPs (PLA-Dex\_40PBA and PLA-Dex\_320PBA) showed total release point at around 120 hrs (Figure 11b), which is significantly longer than some of the previous studies involving *in vitro* release of CycA from micro or nanoparticles [145, 147-149]. Moreover, the release rate may potentially be a significant improvement over commercial product RESTASIS<sup>®</sup> which requires administering twice a day. Whereas PLA-Dex NPs showed sustained release rate for up to 120 hours, PLA-Dex\_PBA NPs showed two regions of slightly different release rate. In the first 48hrs, the PLA-Dex\_PBA NPs released CycA at a faster rate compared to PLA-Dex NPs, which may be due to the release of CycA that were encapsulated near the slightly more hydrophobic surface PLA-Dex\_PBA NPs. The subsequent slower release rate, compared to PLA-Dex NPs, may be due to the release of drugs from the core of the PLA-Dex\_PBA NPs, which need to diffuse through more compact dextran surface. When the volume of PBA modified NP formulation were scaled to the administration volume of RESTASIS<sup>®</sup> (28  $\mu\text{L}$ ), the CycA release rates were in the range of  $\mu\text{g}/\text{day}$ , which is similar to the daily administration dosage of CycA in RESTASIS<sup>®</sup>. Therefore, it is possible to optimize the formulation by changing the concentration of the PBA modified NPs and/or the amount of CycA to achieve clinically effective release rate.

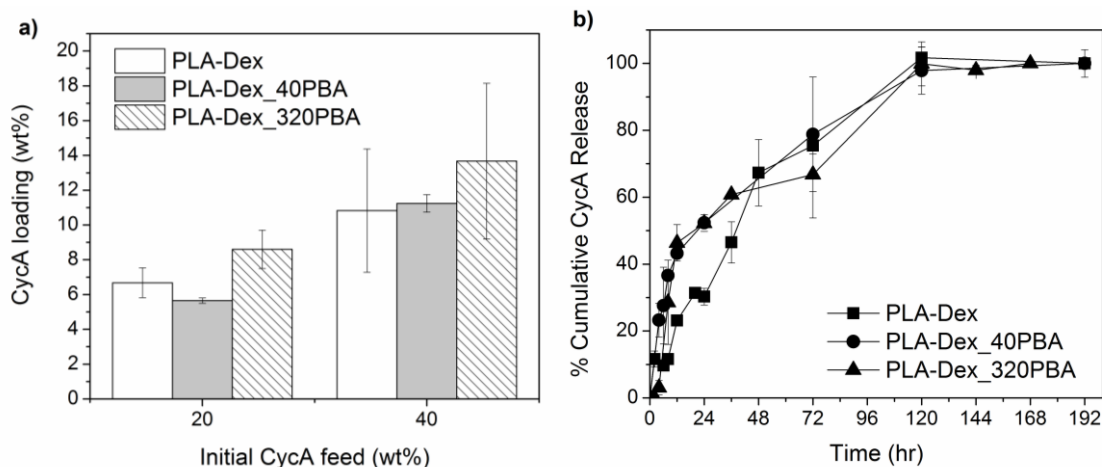


**Figure 11. a) CycA loading and b) In vitro release from PBA modified and unmodified NPs.**

#### 4.4.3 *In vitro* Mucoadhesion

Mucoadhesion of the NPs was measured using the *in vitro* PAS staining method. Compared to the PLA-Dex and the PLGA-PEG NPs, the PLA-Dex\_PBA NPs showed increased mucin adsorption (Table 2). PLA-Dex\_10PBA, PLA-Dex\_40PBA, and PLA-Dex\_160PBA NPs showed a slight increase in mucin adsorption from 0.575 to 0.605 mg/mg of NPs as the degree of PBA surface functionalization increased. However, further increase in PBA surface functionalization (i.e. PLA-Dex\_320PBA) decreased the amount of mucin adsorbed. It is likely that excess functionalization of the NP surfaces with PBA causes the dextran to become more hydrophobic. This would increase the potential for self-aggregation of the NPs, reducing the total available surface area for mucin adsorption. It is therefore ideal to tune the amount of PBA functionalization to achieve optimal mucin-NP interaction without compromising the NP colloidal stability. It is also possible that smaller NPs render higher mucin adsorption due to their larger total surface area, as shown by comparing PLGA-PEG, PLA-Dex, and PLA-Dex\_PBA NPs. However, as each type of NP exhibit different surface properties, the trend is inconclusive. The PLA-Dex\_PBA NPs all exhibited significantly higher mucin adsorption compared to the previous studies involving chitosan based NPs and thiolated NPs, which showed about 0.25 and 0.13 mg/mg of NPs respectively at 1 hr incubation[146]. Although the current study is limited to *in vitro* studies, it shows great promise for PLA-Dex\_PBA NPs as a potential mucoadhesive drug delivery system.

## 4.5 Conclusion

The surface of the nanoparticle formed from a linear block copolymer poly(D,L-lactide)-*b*-dextran was modified with PBA to form a mucoadhesive nanoparticle for topical ocular drug delivery application. The NPs, with sizes around 25 nm and spherical in morphology, encapsulated a therapeutically relevant dosage of Cyclosporine A and demonstrated sustained release for up to 5 days. Moreover, *in vitro* mucin-NP interaction was facilitated when the NPs were functionalized with PBA molecules, which is difficult to achieve using PEG-based systems. Since PBA functionalization also causes dextran to be more hydrophobic, it is ideal to adjust the amount of PBA to achieve optimal mucin-NP interaction without compromising the colloidal stability of the NPs. The current report involving various *in vitro* studies provides promising results for the potential use of PLA-Dex\_PBA NPs to improve the bioavailability of ocular drugs intended to target the anterior segment of the eye.

## Chapter 5

# Phenylboronic acid modified mucoadhesive nanoparticle drug carriers facilitate weekly treatment of experimentally-induced dry eye syndrome

### 5.1 Summary

Topical formulations, commonly applied for treatment of anterior eye diseases, require frequent administration due to rapid clearance from the ocular surface, typically through the lacrimal drainage system or through over-spillage onto the lids. We report on a mucoadhesive nanoparticle drug delivery system that may be used to prolong the precorneal residence time of encapsulated drugs. The nanoparticles were formed from self-assembly of block copolymers composed of poly(D,L-lactide) and dextran. The enhanced mucoadhesion properties were achieved by surface functionalizing the nanoparticles with phenylboronic acid. The nanoparticles encapsulated up to 12 wt% of Cyclosporine A (CycA) and sustained the release for up to 5 days at a clinically relevant dose, which led us to explore the therapeutic efficacy of the formulation with reduced administration frequency. By administering CycA-loaded nanoparticles to dry eye-induced mice once a week, inflammatory infiltrates were eliminated and the ocular surface completely recovered. The same once a week dosage of the nanoparticles also showed no signs of physical irritation or inflammatory responses in acute (1 week) and chronic (12 weeks) studies in healthy rabbit eyes. These findings indicate that the nanoparticles may significantly reduce the frequency of administration for effective treatment of anterior eye diseases without causing ocular irritation.

### 5.2 Introduction

Topical administration of an eye drop solution is the most commonly used drug delivery method for treating anterior eye diseases due to its non-invasiveness, low cost and ease of administration. Such a delivery method, however, suffers from low ocular bioavailability due to rapid clearance from the ocular surface through tear dilution and drainage through the lacrimal drainage system, resulting in less than 5% of the active drug reaching its intended target [6]. As a result, high doses of the formulations must be administered multiple times per day to achieve therapeutic efficacy, ultimately leading to a high risk of adverse effects and low patient compliance.



Much effort has been invested in improving topical formulations to overcome these shortcomings without compromising their benefits. One such approach includes the development of drug carriers developed from polymeric nanoparticles (NPs) [7]. By encapsulating therapeutic agents as their cargo, NP drug carriers enhance the solubility of drugs in water, control the release rates of these drugs, and improve the precorneal retention by targeting the ocular surface moieties [1, 7, 58, 150]. NPs formulated from biodegradable polymers, such as poly(lactic-co-glycolic acid) (PLGA), have been studied in the delivery of ocular therapeutics to the corneal surface [9, 33, 67, 68, 151]. Researchers have also focused on adding poly(ethylene glycol) (PEG) on the surface of the NPs to improve the stability of the NPs in physiological environments as well as precorneal tear fluid [115, 119, 130, 131, 152-154]. In a previous study, we synthesized a dextran based amphiphilic block copolymer, poly(D,L-lactide)-b-dextran (PLA-b-Dex), that self-assembles into NPs with sizes ranging from 20 to 60 nm in diameter by tuning the molecular weights of PLA and Dex [4]. Dextran based NPs have shown colloidal stabilities superior to those of the PEG based NPs previously used [126]. Moreover, dextran has abundant functional groups (i.e. OH groups) on its backbone that can be used for modification, as opposed to the single functional group on the end of PEG chains. As a result, the high density of surface functional groups in dextran based NPs increases the efficiency of surface functionalization and consequently provides greater control over surface properties. In previous studies, researchers functionalized the surfaces of various NP drug carriers with ligands that can target the ocular mucosa to increase the precorneal retention time of the drugs [35, 133-135]. The most common method of achieving mucoadhesive properties was through functionalizing the NPs with cationic polymers, such as chitosan, to take advantage of the electrostatic interaction between the cationic polymers and the negatively charged ocular mucin [52, 91, 110, 147, 155]. However, the electrostatic interaction may be partially impeded by the presence of ions in the tear fluid, resulting in the relatively rapid clearance of the drug carriers. Phenylboronic acid (PBA) molecules form a complex with cis diol groups of sugar residues, such as sialic acids, that are abundant on the mucin structures at physiological pH [137-142]. In addition, several studies have demonstrated biocompatibilities of PBA molecules using both in vitro and in vivo assays [142, 156, 157]. We hypothesize that the PBA functionalized PLA-b-Dex drug carriers will significantly reduce the required dosage of drugs and their administration frequency in treating anterior eye diseases by enhancing the precorneal retention of the encapsulated drugs.

The objective of this study was to develop a mucoadhesive nanoparticle drug delivery system that can reduce the administration frequency of ophthalmic drugs without compromising the therapeutic efficacy. Here, we report the formulation of PLA-b-Dex polymer nanoparticles with surfaces

functionalized with PBA to achieve a mucosal-targeting drug delivery system. We evaluated the ability of these nanoparticles to encapsulate Cyclosporine A (CycA), an immunosuppressant commonly administered for treating dry eye syndrome, and analyzed the subsequent release profile. We then tested the compatibility of these NPs by investigating both the acute and the chronic responses after administration on rabbit eyes. Finally, NP+CycA formulations with reduced administration frequencies were evaluated for treatment of experimental dry eye induced in mice.

## 5.3 Experimental

### 5.3.1 Materials

Acid-terminated poly(D,L-lactide) (PLA; Mw ~20) was purchased from Lakeshore Biomaterials (Birmingham, USA) and washed with methanol to remove monomer impurities. Dextran (Dex; Mw ~10 kDa), hydrochloric acid (HCl), triethylamine (TEA), N-(3-dimethylaminopropyl)-N-ethyl carbodiimide (EDC), 3-Aminophenylboronic acid monohydrate (PBA), sodium periodate (NaIO<sub>4</sub>), glycerol, sodium cyanoborohydride (NaCNBH<sub>3</sub>), and Cyclosporine A (CycA) were purchased from Sigma Aldrich (Oakville, Canada) N-Hydroxysulfosuccinimide (Sulfo-NHS) and N-Boc-ethylenediamine were purchased from CNH Technologies (Massachusetts, USA).

### 5.3.2 Synthesis of PLA-b-Dex and surface modification with PBA

The conjugation of the PLA and Dex polymer chains to form a block copolymer PLA-b-Dex and the surface modification of the PLA-b-Dex NPs with PBA were reported in Chapter 3 [4, 158]. Briefly, the aldehyde end group of the dextran was conjugated with the N-Boc-ethylenediamine linker through reductive amination with NaCNBH<sub>3</sub>. After conjugation with the linker molecule, the Boc group was deprotected using HCl/TEA treatment. The deprotected amine end group is then conjugated with the carboxyl terminal group of the PLA using Sulfo-NHS and EDC as catalysts. The surface of these NPs were modified with PBA molecules by a two-step approach: the hydroxyl groups of the dextran were oxidized to form more reactive aldehyde groups in the presence of NaIO<sub>4</sub>, and the aldehyde groups were conjugated with the amine groups of PBA molecules through reductive amination. The amount of PBA attached to the dextran chain was quantified using UV-Vis absorption at 291 nm after obtaining the standard calibration of PBA in DMSO. The PLA-b-Dex polymers in DMSO were used as the baseline.

### 5.3.3 Characterization of PLA-b-Dex-g-PBA NPs

The NPs of PLA-b-Dex-g-PBA polymers were formed using nanoprecipitation. The sizes of the NPs were determined using dynamic light scattering (DLS) by measuring the multimode-size distribution (MSD) volume-averaged mean diameters using a 90Plus Particle Size Analyzer (Brookhaven,  $\lambda = 659$  nm at  $90^\circ$ ). The zeta potential of the PLA-b-Dex and PLA-b-Dex-g-PBA nanoparticles were measured using Zetasizer Nano ZS (Malvern Instruments Worcestershire, U.K.). The sizes and morphology were further confirmed using Transmission Electron Microscopy (TEM) equipment by drying the PLA-b-Dex-g-PBA NP suspension on 300 Mesh Formvar coated copper grids (Canemco and Marivac) and using phosphotungstic acid solution as the negative stain. The mucoadhesion of the PLA-b-Dex-g-PBA NPs were quantified using an *in vitro* periodic acid/Schiff (PAS) staining method described previously [158]. In brief, the NP suspension and the mucin solution were mixed and incubated at  $37^\circ\text{C}$  for 1 hr. The mixture was then centrifuged and the free mucin in the supernatant was quantified using the PAS method. Mucin adsorption was calculated by subtracting the free mucin from the initial mucin concentration. Mucin standards (0.1, 0.25, 0.5, and 0.75 mg/ml) were also used with the same procedure to obtain a calibration curve.

### 5.3.4 Animal studies

All animal studies performed are in compliance with the guidelines of the Canadian Council on Animal Care (CCAC) and the University of Waterloo (UW) as well as regulations under the Animals for Research Act of Ontario Canada. Female New Zealand White Albino rabbits (2.5 – 3.5 kg, Charles River Laboratories, Canada) were used for both the acute and chronic ocular irritancy tests *in vivo*. Female C57BL/6 mice (Charles River Laboratories, Canada) aged around 6-8 months were used for experimental dry eye model. All animals were acclimated in the animal facility for at least one week prior to the experiments. All formulations used in this study were dialyzed, filtered, and sterilized prior to administration to the animals.

### 5.3.5 *In vivo* ocular irritancy test

The short-term biocompatibility of the NPs was assessed using ocular irritancy tests adapted and modified from previous studies [3, 159]. Three female rabbits were housed individually in cages on a standard laboratory diet. One eye of each of the rabbits was administered with  $28\ \mu\text{l}$  of the PLA-b-Dex-g-PBA NP formulation (containing about  $17\ \mu\text{g}$  of the NPs), while the contra-lateral eye was used as a control. Both eyes were observed using a slit lamp bio-microscope at 0 (before administration), 1, 8,

24, 48, 72, 96, 120, 144, and 168 hours after administration to examine the extent of irritancy on the ocular surface. Upon observation at each time point, both eyes were graded using 7 categories: apparent discomfort, conjunctival redness and swelling, lid swelling, discharge, corneal opacification, and number of infiltrates from 0 (no sign) to 4 (severe) under the supervision of trained optometrists with experience working with animals [90, 160]. After 168 hrs, the rabbits were euthanized and the ocular tissues were extracted for histopathology.

The long-term biocompatibility of the blank NPs and the NPs with Cyclosporine A (NP+CycA) encapsulated were assessed using similar techniques described above at 0, 1, 24, and 48hr each week repeated for 12 weeks. Five female rabbits were used for blank NP irritancy test and four female rabbits were used for NP+CycA irritancy test. Similarly, one eye of each rabbit was administered with 28  $\mu$ l of NP formulation ( $\sim$ 17  $\mu$ g of the PLA-b-Dex-g-PBA NPs) or 28  $\mu$ l NP+CycA formulation ( $\sim$ 17  $\mu$ g of the PLA-b-Dex-g-PBA NPs and  $<$ 8  $\mu$ g of CycA (may also include some freely suspended CycA)), while the contralateral eye served as a control. Similarly, both eyes were examined under a slit lamp bio-microscope on the extent of irritancy based on the 7 categories described above. After 12 weeks, the rabbits were euthanized and the ocular tissues were extracted for histopathology.

### **5.3.6 Histopathology**

The eyes were enucleated and collected immediately after euthanasia for histopathological evaluation by one of the authors (DH), who is a trained pathologist. The entire upper eyelids were also dissected and collected for evaluation of the tarsal conjunctiva and the underlying soft tissues. Consecutive sections of the entire ocular globe and eyelids were processed for microscopic analysis: after initial fixation in 10% neutral buffered formalin, the tissue was embedded in paraffin, serially sectioned into 5  $\mu$ m thick sections, and stained with hematoxylin and eosin (H&E). The histological slides were evaluated using bright field microscopy (Leica DM1000, ICC50 HD, Leica Microsystems Inc, Canada).

### **5.3.7 Experimental dry eye model – *in vivo* efficacy test**

The PLA-b-Dex-g-PBA NPs encapsulating CycA were analyzed for treating experimental dry eye syndrome in a mice model. First, the mice were induced with dry eye conditions using a previously reported method [161]. Transdermal scopolamine patches (Transderm-V, Novartis) were cut into two pieces each, wrapped around the midtails of the mice, and further secured using surgical tape. The patches were replaced every other day throughout the duration of the study. To simulate a desiccating environment, the mice cages (open-top) were placed in a fumehood for 1 hr, 3 times per day throughout

the study (until day 12). After 4 days of this dry eye inducement procedure, the mice were divided into 7 different groups (Table 4) for various types of treatments on both eyes (3 mice per group; 6 eyes per group) for an additional 7 days. On day 1 (before dry eye inducement), 5 (before first administration), 8 (before second administration), and 12 (before euthanasia), tear volume measurements and corneal fluorescein staining were performed to measure the rate of tear production and analyze the ocular surface damage. Note that NP+CycA (1/wk), Saline (1/wk) was only administered on day 5, whereas NP+CycA (2/wk), Saline (2/wk), and Blank NPs were administered on days 5 and 8. Tear volume was measured by holding a phenol red dyed cotton thread (Zone-quick, White Ophthalmic Supply) with jeweler's forceps in the lateral canthus of the ocular surface for 30 seconds. Corneal fluorescein staining was observed and photographed with a slit-lamp bio-microscope using a cobalt blue light 10 minutes after the administration of 1  $\mu$ l of sodium fluorescein solution (10 mg/ml). After the 12 day period, the mice were euthanized and the ocular tissues were collected for histopathological analysis (as described in the previous section).

## 5.4 Results and Discussion

### 5.4.1 Characterization of PLA-b-Dex-g-PBA NPs

We functionalized the surface of PLA-b-Dex NPs, formed from nanoprecipitation, with the mucosal-targeting ligand PBA (Figure 12). The characterization of the PBA functionalization, the CycA loading, and diameters of the NPs are summarized in Table 3. The amount of PBA density on the dextran surface was  $17.6 \pm 2.7$  mol% (mol of PBA/mol of dextran monomers). NP diameter decreased from 45.8 nm to 28.6 nm likely due to the functionalization with PBA, and was also observed in a similar previous study [158]. The size decrease is possibly a result of the reduced hydrophilicity of the dextran surface or the change in the packing density of the nanoparticles due to the volume change of the hydrophilic chains. We found that having excess PBA (i.e. more than 23 mol% PBA/dextran) on the NP surface may cause the NPs to be too hydrophobic and thus compromise its colloidal stability in our previous study [158]. Therefore, PBA density must be tuned to balance between mucoadhesion and colloidal stability. The NPs exhibited a spherical morphology as observed in TEM imaging (Figure 13). The zeta potential of the PLA-b-Dex NPs is close to 0, but when PBA is grafted onto the surface, the potential has dropped to near  $-30$  mV (Table 3). The pKa of the PBA molecules are near 8.6 [162], thus at pH  $\sim 7.4$  (at which the measurements were taken) some percentage of the PBA molecules would be in their deprotonated state, contributing to the overall negative surface charges of the nanoparticles; similar

range of zeta potentials were measured on nanoparticles with PBA molecules on the surface previously [163]. The PBA functionalized NPs showed *in vitro* mucoadhesion properties, resulting in mucin binding of  $1.18 \pm 0.02$  mg/mg of NPs, which is much higher than the values obtained for other types of mucoadhesive NPs such as chitosan based NPs ( $\sim 0.25$  mg/mg of NPs) and thiolated NPs ( $\sim 0.13$  mg/mg of NPs) [146]. From these preliminary findings we postulate that the PBA functionalized NPs may exhibit strong binding affinity toward the ocular mucosa under physiological environment.

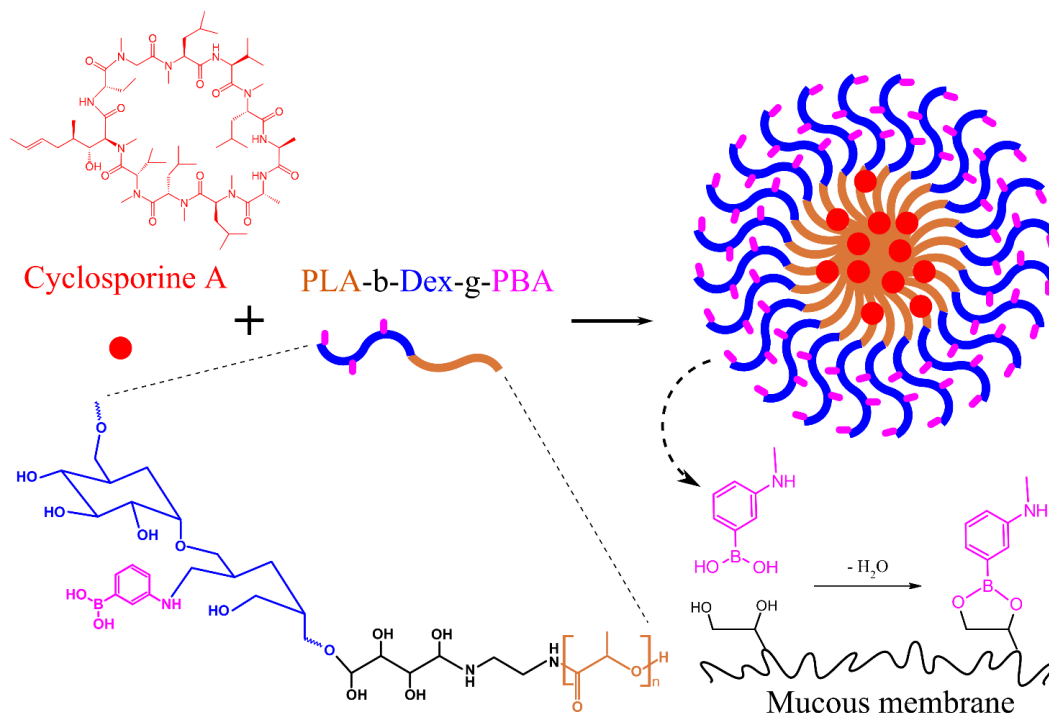


**Figure 12. Schematic illustration of the self-assembly process to form Cyclosporine A loaded PLA-b-Dex-g-PBA nanoparticles, and the mucoadhesion mechanism of the grafted PBA's.**

**Table 3. PLA-b-Dex-g-PBA characterization: PBA surface functionalization, Cyclosporine A loading, and diameter.**

Sample	PBA/Dex (mol%)	CycA load (wt%)	Mean diameter (nm)	$\zeta$ potential (mV)
PLA-b-Dex	0	0	$45.8 \pm 1.5$	$-2.63 \pm 1.55$
PLA-b-Dex-g-PBA	$17.6 \pm 2.7$	0	$28.6 \pm 3.1$	$-31.3 \pm 1.5$

---

PLA-b-Dex-g-PBA with CycA	$17.6 \pm 2.7$	$11.9 \pm 1.6$	$35.6 \pm 7.4$
---------------------------	----------------	----------------	----------------

---

Note that the average and the standard deviations were calculated using measurements of three batches of the nanoparticles

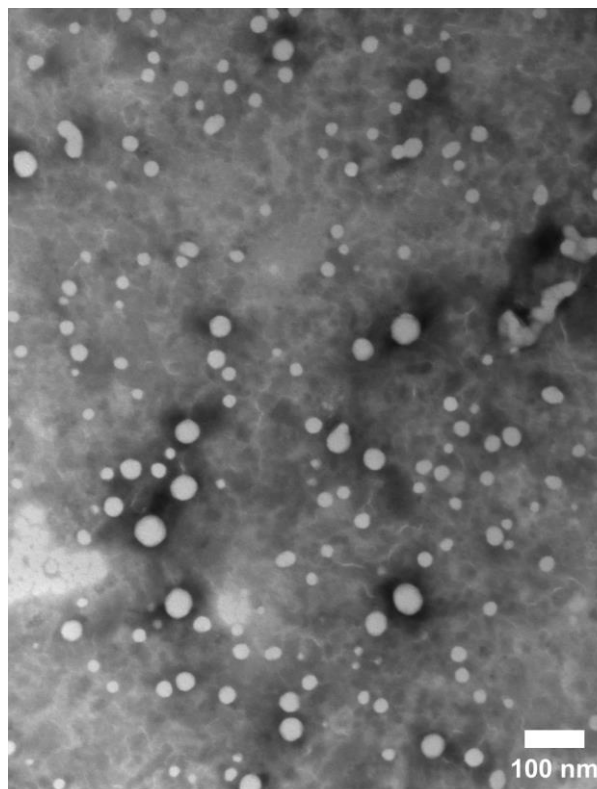


**Figure 13. TEM image of PLA-b-Dex-g-PBA NPs.**

#### **5.4.2 In vivo ocular irritancy test**

Acute responses after one-time administration of PLA-b-Dex-g-PBA NPs were observed using a slit-lamp bio-microscope by grading both the NP administered and contralateral control rabbit eyes for 7 categories over a week (Figure 14). We observed no corneal opacification and infiltrates in any of the eyes throughout the study. All of the other 5 categories—discomfort, conjunctival redness and swelling, lid swelling, and discharge—also showed no significant difference between the administered and the control eyes, similar to what has been observed from chitosan nanoparticles [3]. Most categories showed grades between 0 (no sign) and 1 (mild) with the exception of conjunctival redness. As both the NP administered and control eyes scored relatively higher grades (between 1 and 2) for conjunctival redness, it is highly probably that environmental stress underlies the high scores rather than the

administration of NPs. From the slit-lamp examination alone, the NPs seem well-tolerated by the rabbits' eyes, but closer examination of the ocular tissues is necessary to further validate the findings.

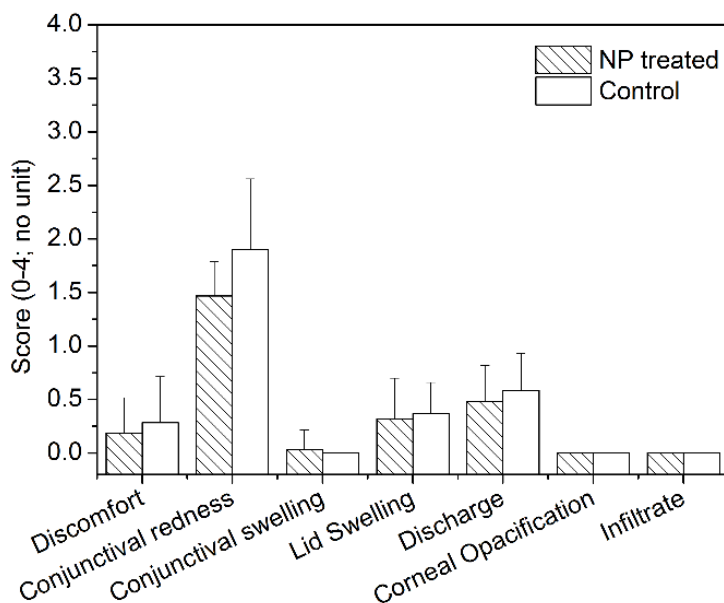


**Figure 14. In vivo acute ocular irritancy test grading obtained through slit-lamp examination.**

After the slit-lamp examination for a week, the ocular tissues of the rabbits were collected for histopathology. Histopathological evaluation revealed the presence of normal ocular surface structures in both control and NP administered eyes (Figure 15). All eyes demonstrated preserved architecture and morphology in the anterior segment. Corneas of NP administered and control eyes displayed normal numbers of cell layers with appropriate morphology (Figure 15, top row). We observed no signs of inflammation, altered layer integrity, or the presence of residual particles in any of the eyes. Hyperplastic changes, hyperkeratosis, or other alterations in the process of normal epithelial maturation and renewal were also not noted. The bulbar and tarsal conjunctiva of both NP administered and control eyes revealed findings within normal limits. NP administered and control eyes also showed adequate numbers of goblet cells with preserved morphology and abundant secretory products (Figure 15, middle and bottom rows). No differences were observed in the size or location of the conjunctiva-associated lymphoid tissues. Individual scattered lymphocytes and single polymorphonuclears and eosinophils were occasionally observed, predominantly in the tarsal conjunctival epithelium and stroma, in both administered and non-administered eyes (Figure 15, bottom row). These findings represent normal variations in the tissue characteristics of exposed mucosal membranes expected for healthy subjects. There were no inflammation, edema, residual particles, epithelial or vascular abnormalities. The ocular



angle demonstrated usual architecture. Both the slit-lamp examination and histopathological evaluations suggest that the NP formulation causes no observable acute irritation on the rabbit eyes. We expected the appropriate compatibility of NPs, as these NPs were composed of a biodegradable polymer chain PLA and a natural polysaccharide dextran, which have both shown *in vitro* and *in vivo* compatibilities previous studies [4]. In addition, the biocompatible nature of PBA targeting ligands has also been demonstrated previously and has since been widely used in *in vivo* molecular targeting of sialic acids expressed on cell surfaces [164]. This study confirms that the combination of the biocompatible NPs surface functionalized with biocompatible PBA does not cause any short term adverse effects on the ocular surface of the rabbits.

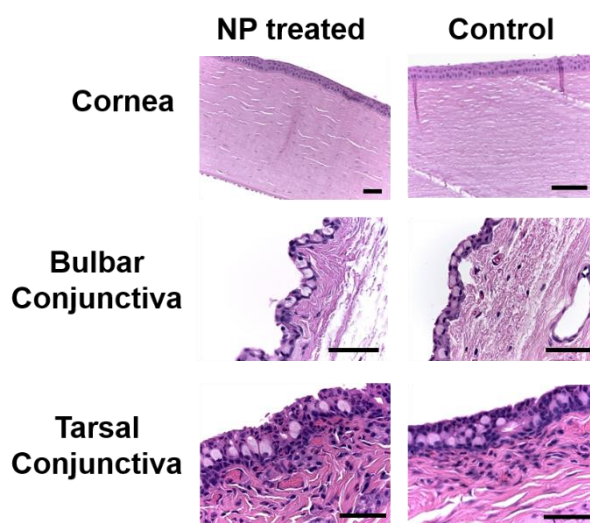


**Figure 15. Histopathology analysis of both NP administered and control eyes in in vivo acute ocular irritancy test reveal no significant differences in the corneal and conjunctival morphological characteristics and architecture. The scale bars (black) are 500  $\mu\text{m}$  in length.**

In addition to the acute irritancy study, it is essential to analyze the chronic ocular response to the repeated administration of NPs since eye drops are often applied periodically for a prolonged duration of treatment. The chronic response on the ocular surface after weekly administration for NPs or NP+CycA for up to 12 weeks was also examined using a slit-lamp bio-microscope and the same grading system of 7 categories described above. No sign of conjunctival swelling, corneal opacification nor infiltrates were observed in any of the eyes throughout the 12 week study. From weekly administration of PLA-b-Dex-g-PBA NPs, discomfort, conjunctival redness, discharge and lid swelling levels were

mostly in the mild region (between score of 0 and 1), with no significant deviation between the NP administered and contralateral control eyes (Figure 16). We also made similar observations after weekly administration of CycA encapsulated NPs (NP+CycA): we observed a slow increase of lid swelling near the end of the study (week 9 to week 12) to moderate scores of about 1.5 with no apparent deviation between the administered and non-administered eyes, suggesting the slow increase was likely due to environmental stress (Figure 17).

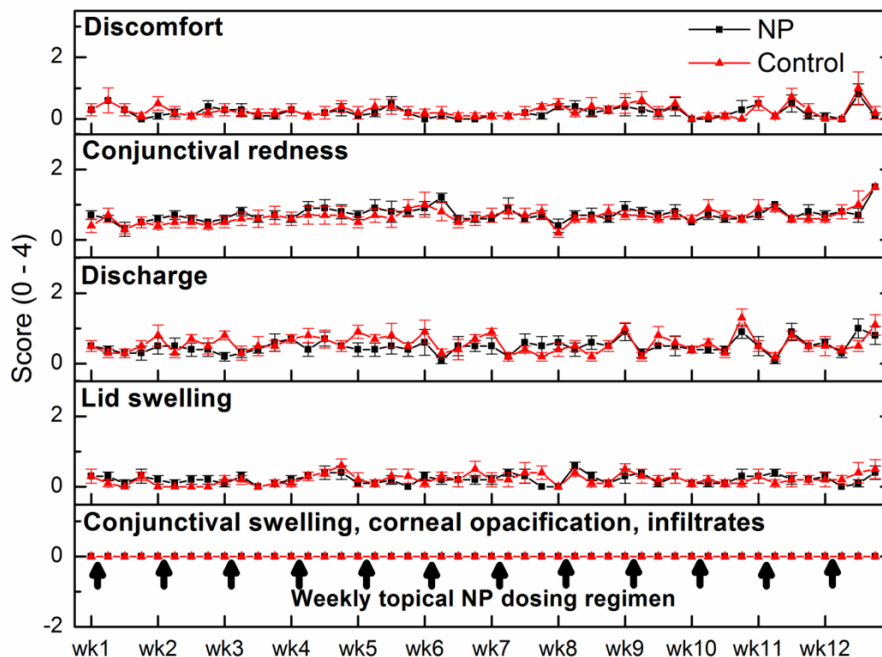


**Figure 16. In vivo chronic ocular irritancy test for weekly administration of NP formulation for up to 12 weeks (each data point shown as mean  $\pm$  s.e.m. (standard errors of mean); n = 5).**

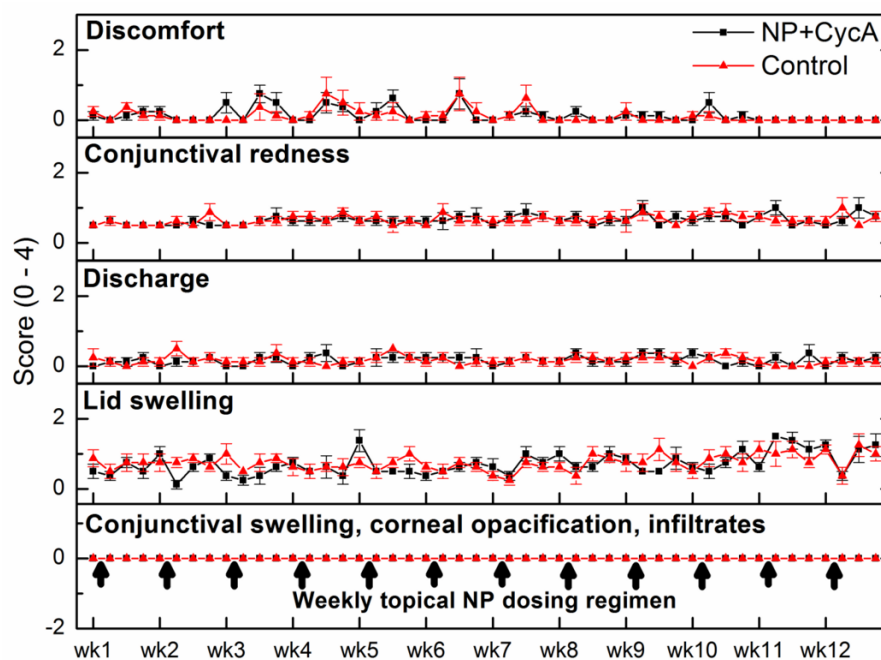


**Figure 17. In vivo chronic ocular irritancy test of weekly administration of NP+CycA formulation for up to 12 weeks (each data point shown as mean  $\pm$  s.e.m.; n = 4).**

Similarly, after the 12 week study, all ocular tissues of the rabbits were collected for histopathological analysis. Histopathological evaluation showed all the signs representative of healthy eyes similar to the acute irritancy test above (Figure 18). Both NP and NP+CycA treated eyes and their corresponding contralateral control eyes demonstrated normal ocular surface structures and anterior eye segments with preserved morphology and architecture. All corneas displayed normal numbers of cell layers with appropriate morphology without any sign of inflammation, altered layer integrity, or presence of residual particles. Hyperplastic changes, hyperkeratosis, or other alterations in the process of normal epithelial maturation and renewal were also not noted. Bulbar and tarsal conjunctiva of all eyes revealed findings within normal limits: they all showed similar adequate numbers of goblet cells with preserved morphology and abundant secretory products. No differences in the size or location of the conjunctiva-associated lymphoid tissues were observed. Individual scattered lymphocytes and single polymorphonuclears and eosinophils were occasionally observed predominantly in the tarsal conjunctival epithelium and stroma in all the eyes. No inflammation, edema, epithelial or vascular abnormalities were found in either set of rabbits.

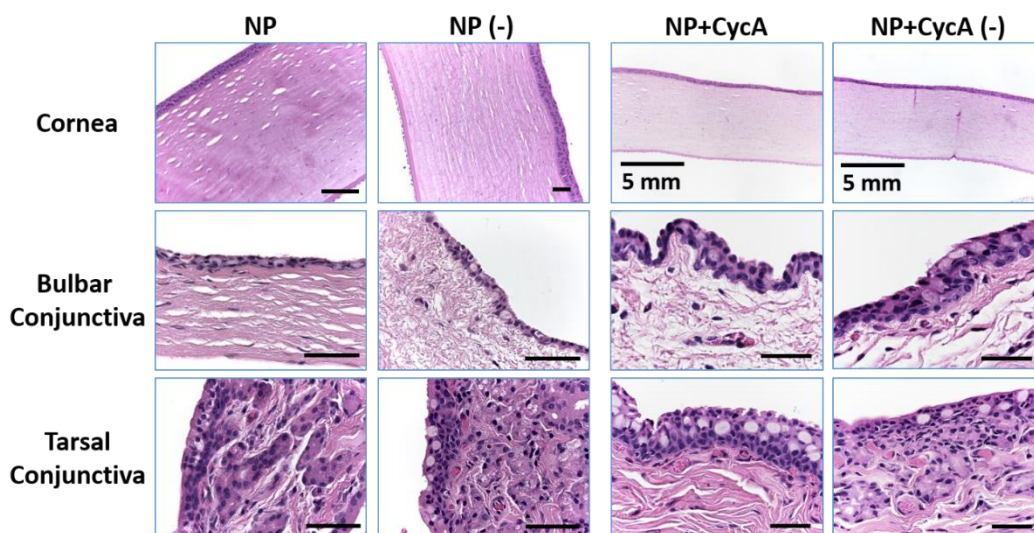


**Figure 18. Histopathology study after in vivo chronic ocular irritancy tests with weekly administration of NP and NP+CycA. NP (-) and NP+CycA (-) represent the contralateral control eyes of the rabbits administered with NP or NP+CycA formulations. The scale bars (black) are 500  $\mu$ m in length unless otherwise specified.**

The repeated dosage of NPs may increase the potential for adverse effects as their corneal exposure time is increased. The study showed that the NPs were well-tolerated for up to 12 weeks, thus demonstrating the long-term compatibility of the carrier system. It was also paramount to perform the same test on NP formulation with the drugs inside, since the drug encapsulating NPs may exhibit an increased diameter due to the increase in the hydrophobic core size, which may or may not lead to a varied ocular response. The current study demonstrated that the inclusion of the drug in the NPs did not significantly alter the ocular response. These two studies indicate that the NP formulation is a promising long term drug delivery system for treating anterior ocular diseases. However, it is not clear how much nanoparticles remain after each dosing of the formulation. Therefore, one of the ongoing studies is to investigate the dosage-dependency of the ocular compatibility of the nanoparticles by studying their ocular biodistribution at predetermined time intervals.

#### **5.4.3 *In vivo* efficacy test – experimental dry eye**

Experimental dry eye was induced in mice and 7 different treatments (Table 4) were applied to the mice groups to analyze the effect of the treatments against dry eye. Tear volume measurements on day 1 and 5 (before DE inducement and before 1st admin) suggest that the tear volumes were significantly reduced ( $p < 0.05$ ) (Figure 19) as a result of the combination of application of anticholinergic drug,

scopolamine, and the simulation of desiccating environment [161]. The dryness of the eyes were also observed in corneal fluorescein staining imaging to varying degrees (Figure 20), between the 1st and 2nd columns): after 4 days of dry eye inducement, less of the administered fluorescein was cleared from the ocular surface compared to day 1 possibly due to the surface damage caused from lack of surface lubrication and/or the reduced tear clearance rate. The healthy group maintained a normal tear volume production rate with minimal or no ocular surface damage, which resulted in clearance of the majority of the fluorescein within 10 mins (Figure 20). Saline (1/wk) and (2/wk) did not show any significant improvement in the tear volume production or the fluorescein clearance from day 5 to 12. NP+CycA (1/wk) and NP+CycA (2/wk) were the only groups that showed a slight increase in tear volume as well as improved fluorescein clearance on day 12 compared to day 5. RESTASIS, administered 3 times per day for 7 days, did not show any improvement in tear production on day 12 compared to day 5. Moreover, the fluorescein images show that less fluorescein was cleared on day 12 compared to day 5, which is most likely due to the ocular surface damage as a result of frequent administration. Blank NPs (2/wk), while showing a certain degree of improvement in terms of fluorescein clearance, were unable to clear as much fluorescein as those administered with NP+CycA (1/wk) and NP+CycA (2/wk) on day 12. The tear volume measurements suggest that NP+CycA formulations showed improved performance in reducing the symptoms of dry eye conditions, however, we note that none of the formulations were able to restore the tear volume production of day 1 by the end of this study (day 12). We postulate that it may be due to the fact that we are constantly inducing dry eye symptoms using anticholinergic agents and therefore it may outweigh the effects of the Cyclosporine A treatment. Similar observations were made in a previous study where they showed that although the treatment of Cyclosporine A itself showed restored lacrimation but when treated alongside anticholinergic agents, the lacrimation was not restored [165]. Thus, closer examination of the immunosuppression, which is the main function of Cyclosporine A, is needed to evaluate the efficacy of the formulations.

**Table 4. Seven different treatment groups applied to the mice for experimental dry eye treatment study in mice.**

<b>Treatment group</b>	<b>Dry eye induced</b>	<b>Admin.</b>	<b>Admin. volume (µl)</b>	<b>NP (µg)</b>	<b>CycA (µg)</b>	<b>Admin. frequency</b>
Healthy	No	N/A	0	0	0	
Saline (1/wk)	Yes	Saline	7	0	0	x1/week

Saline (2/wk)	Yes	Saline	7	0	0	x2/week
Blank NP (2/wk)	Yes	Water	7	4	0	x2/week
NP+CycA (1/wk)	Yes	Water	7	4	<1.5	x1/week
NP+CycA (2/wk)	Yes	Water	7	4	<1.5	x2/week
RESTASIS	Yes	N/A	3	0	1.5	x3/day

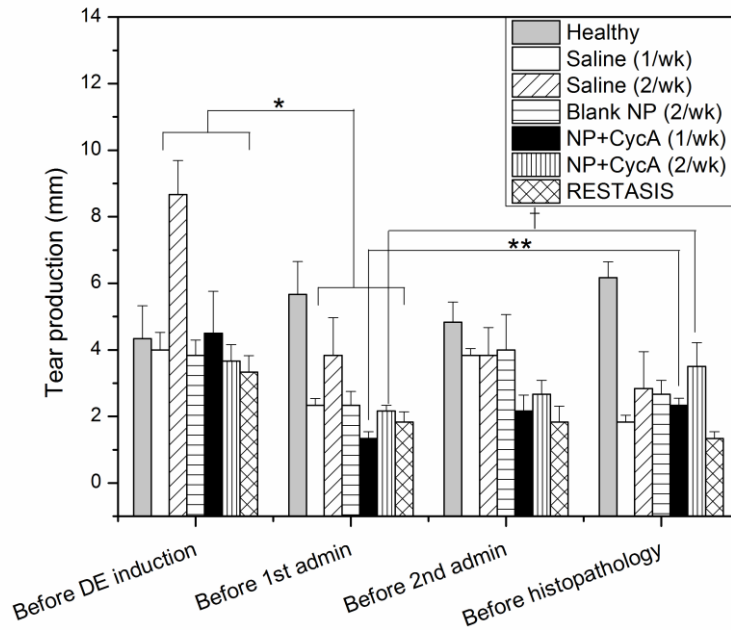


**Figure 19. Tear volume measurements of 7 different treatment groups at 4 time points: before dry eye (DE) induction (day 1), before 1st administration (day 5), before 2nd administration (day 8), and before histopathology (day 12). Each data point is shown as mean  $\pm$  s.e.m., n = 6. Statistical symbols for t-test: † for  $0.05 < p \leq 0.1$ , \* for  $0.01 < p \leq 0.05$ , \*\* for  $0.001 < p \leq 0.01$ , and \*\*\* for  $p < 0.001$ .**

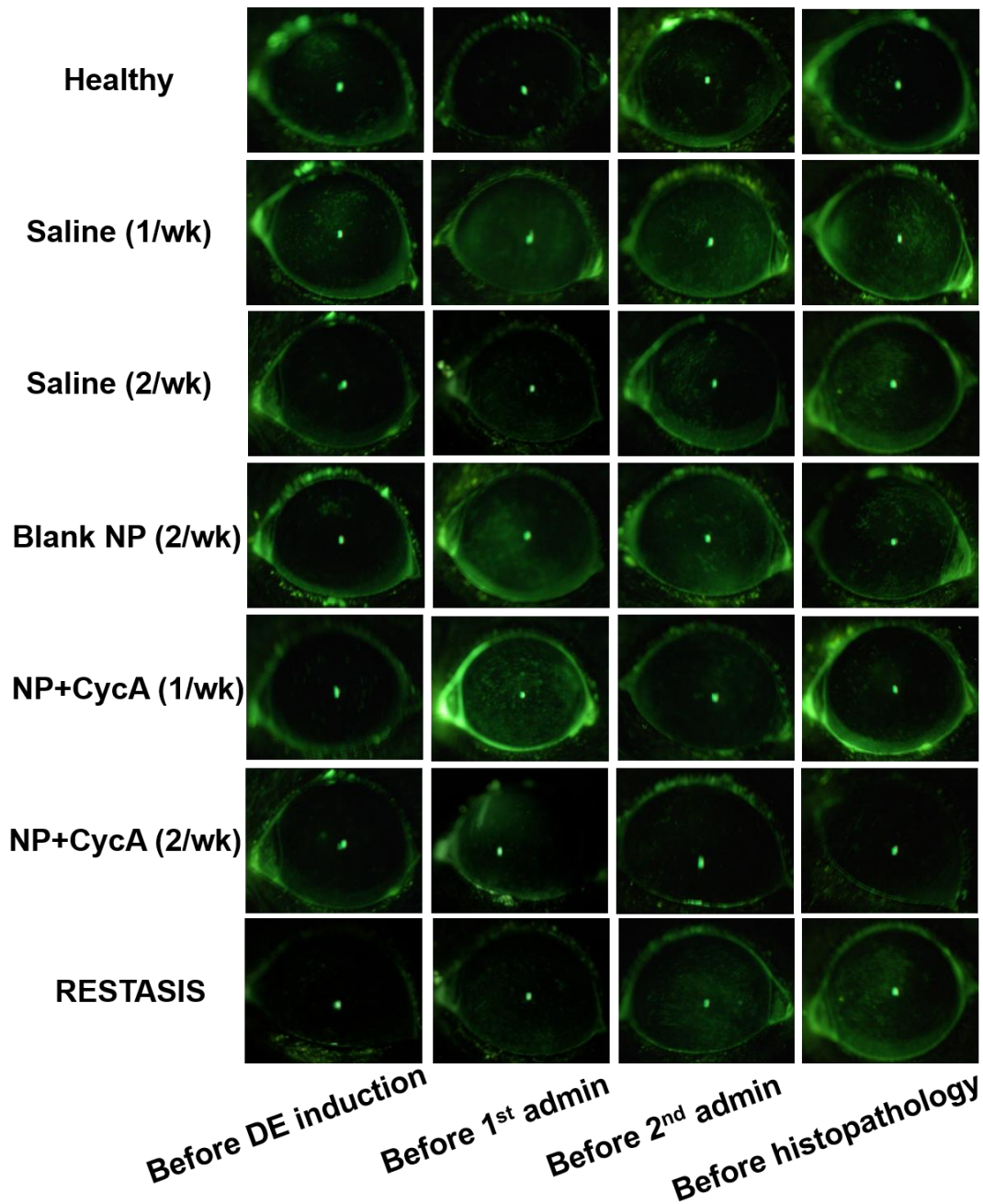


**Figure 20.** Corneal fluorescein staining images of 7 different treatment groups obtained at 4 time points: before dry eye (DE) induction (day 1), before 1st administration (day 5), before 2nd administration (day 8), and before histopathology (day 12). The images were obtained 10 minutes after the application of sodium fluorescein. Note that the corneal fluorescein present on the edges of the lids were due to the local structure and has little to do with the tear production

**or ocular surface damage, thus they were not taken into consideration for the fluorescein clearance analysis.**

Histopathological evaluation of mice in the healthy group showed bulbar and tarsal conjunctiva with stratified squamous epithelium, an adequate number of goblet cells with abundant secretory products, and complete lack of inflammation (Figure 21, A). The stroma showed occasional single lymphocytes and eosinophils within the normal range. The experimental dry eye treated with Saline (1/wk) and (2/wk) groups showed pronounced inflammatory changes ranging from focal mild infiltrates to severe inflammation (Figure 21, B and C). The inflammatory infiltrates, consisting predominantly of lymphocytes with occasional polymorphonuclears and eosinophils, were located in the bulbar and tarsal conjunctiva. The infiltrates involved the conjunctival epithelium as well as the subepithelial stroma of lamina propria. In addition, substantial areas demonstrated a markedly reduced number or complete lack of goblet cells, thereby significantly reducing the mucin secretion and eliminating its lubricating and surface protecting effects [166]. Similarly, mice with experimental dry eye treated with Blank NPs showed mixed inflammatory infiltrates composed of polymorphonuclears and lymphocytes, with occasional plasma cells and eosinophils (Figure 21, D). The bulbar and tarsal conjunctival epithelium both showed markedly reduced number of goblet cells. RESTASIS treatment demonstrated clearing of the intraepithelial and subepithelial inflammatory infiltrates (Figure 21, G). However, substantial residual areas showed complete lack of goblet cells, and goblet cells in isolated areas also exhibited altered morphology with scarce secretory products, which explains why the majority of the fluorescein was not cleared at the end of the treatment (day 12). Treatment with NP+CycA (1/wk) and (2/wk), like RESTASIS, also reversed the inflammatory processes in experimental dry eye induced mice (Figure 21, E and F). No residual particles, epithelial or vascular abnormalities were found. Individual scattered lymphocytes and single polymorphonuclears and eosinophils were observed predominantly in the tarsal conjunctival epithelium and stroma at levels similar to those found in Healthy group. The NP+CycA treated mice showed adequate number of goblet cells on the ocular surface with normal morphology and abundant secretory products.



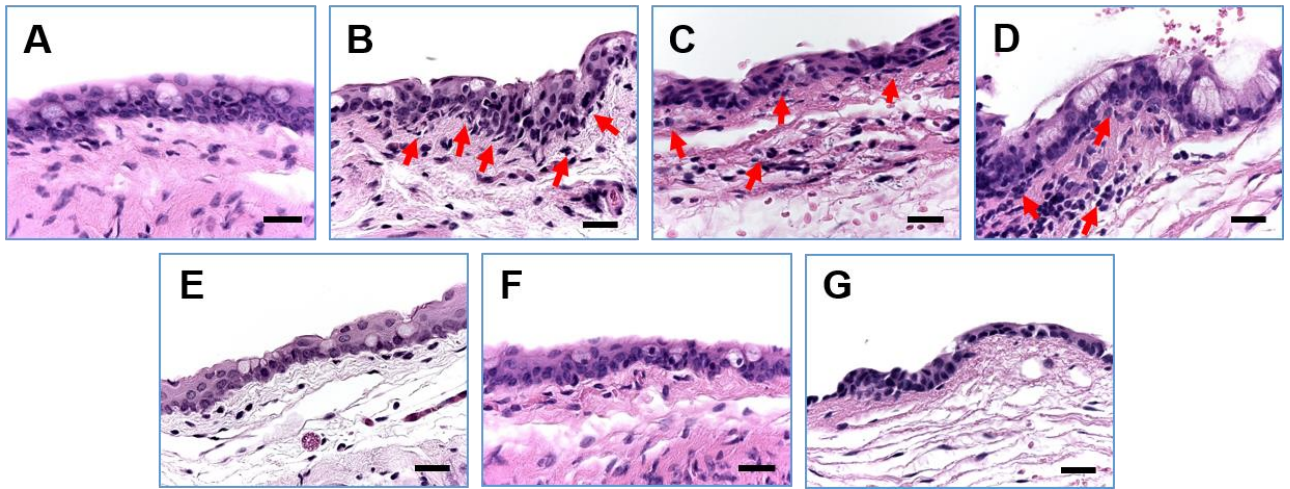


**Figure 21. Histopathology analysis of ocular tissues of mice after 7 different treatment types: A) Healthy, experimental dry eye treated with B) Saline (1/wk), C) Saline (2/wk), D) Blank NPs, E) NP+CycA (1/wk), F) NP+CycA (2/wk), and G) RESTASIS. The scale bars (black) are 300  $\mu\text{m}$  in length. The arrows (red) represent some of the inflammatory infiltrates such as lymphocytes, polymorphonuclears and eosinophils observed.**

Dry eye is characterized as tear deficiency caused by ocular surface inflammation that leads to injury to the ocular surface [166]. The histologic features of dry eye include abnormal proliferation of the ocular surface epithelium, different degrees of inflammatory changes, and decreased production of mucus, manifested by the reduction or absence of goblet cells on the ocular surface epithelium [161]. In all three studies, the tear volume measurement, fluorescein clearance, and histopathology, the Saline (1/wk) and (2/wk) showed no sign of mitigating the symptoms of dry eye conditions such as lowered tear production rate or ocular surface inflammation. This suggests that simple hydration of the ocular surface using saline, at the frequency of the administration specified, was not enough to reduce the inflammation nor recover the integrity of the ocular surface. Blank NP treatment, similar to saline treatment, showed lack of treatment effects of dry eye conditions, but the reduction of goblet cells in the Blank NP group was not as drastic as the reduction of goblet cells in the Saline group. We postulate that the mucoadhesive NPs, once adhering to the ocular mucosa, may improve the hydration of the ocular surface with tear fluid due to the high hydrophilicity of the dextran. This may also explain why the NP+CycA groups also resulted in the preservation of the ocular surface, demonstrated by the abundance of goblet cells, while RESTASIS treated eyes showed insufficient number of goblet cells

and somewhat slower recovery of the ocular surface. Another study reports a significant increase in goblet cell density after 3 months of treatment with RESTASIS [167], so it is likely that the recovery effect was not observable within the time frame of the current study due to insufficient ocular retention of Cyclosporine A from RESTASIS administration. Although the three times daily treatment of RESTASIS effectively eliminated the inflammatory infiltrates from the eyes, the NP+CycA treatment achieved both the elimination of inflammatory infiltrates as well as the complete recovery of the ocular surface with only a single administration per week in the duration of the study. This further implies the long retention of these mucoadhesive NPs on the ocular surface, thus immensely enhancing the ocular bioavailability and efficacy of the encapsulated drugs.

Although the current formulation achieved efficacy in treatment of experimental dry eye, there is room for further improvement. One of the ongoing studies analyzes the effect of PBA surface density on the *in vivo* retention of the NPs on the ocular mucous membrane, to find the optimal PBA density that will maximize its *in vivo* mucoadhesion without compromising the particle stability. In addition, finding the NP:drug ratio that maximizes the total release of the drugs at a therapeutically effective rate is also a significant improvement on the current formulation.

## **5.5 Conclusion**

Nanoparticles (NPs) self-assembled from PLA-b-Dex copolymers and surface functionalized with PBA ligands were formulated as a mucoadhesive drug carrier for topical ocular drug delivery application. The NPs encapsulated large dose of Cyclosporine A and sustained the release at a clinically relevant dose for a prolonged period of time. Neither the blank NP carriers nor NPs encapsulating Cyclosporine A caused any observable irritation or inflammatory responses after weekly administration for up to 12 weeks observed both by slit-lamp examination and histopathology. The NPs encapsulating Cyclosporine A also showed efficacy in treating experimental dry eye in mice: while thrice a day administration of RESTASIS only showed clearance of the inflammatory processes, the once a week administration of Cyclosporine A loaded NPs demonstrated both the elimination of inflammatory infiltrates and the complete restoration of the ocular surface. The current study provides promising results for the potential application of PLA-b-Dex-g-PBA NPs to dramatically improve the efficacy of ocular therapeutics for treating anterior eye diseases.

## Chapter 6

### **Cyclosporine A loaded mucoadhesive nanoparticle eye-drop formulation enhances long term treatment of experimental dry eye in mice using a weekly dosing regimen**

#### **6.1 Summary**

Dry eye syndrome (DES) is characterized by a chronic lack of lubrication on the surface of the eye, with consequences ranging from mild irritation to extensive ocular surface inflammation. Eye drop formulations such as Restasis® (a 0.05% suspension of cyclosporine A, CsA) require frequent dosing at high drug concentrations due to rapid clearance from the ocular surface. We developed a mucoadhesive nanoparticle eye drop delivery platform to prolong the ocular surface retention of topical drugs and studied both its effect on surface retention on the rabbit cornea and its efficacy in treating experimentally-induced dry eye in mice by delivering CsA bound to this delivery system. Ocular surface retention was studied by measuring the amount of fluorescence after topical delivery of nanoparticles encapsulating a near infrared dye, indocyanine green (ICG), to rabbit eyes. Experimental DES was induced in mice by applying scopolamine patches to their midtails and exposing them to desiccating environments. These mice were treated with various formulations including 1) Restasis® (0.05% CsA, thrice daily), 2) CsA-loaded nanoparticles (NPs) with a CsA dosage 1-2% that of Restasis® (NP-CsA 0.005-0.01%, once a week) or 3) NP-CsA 0.025% (once a week) for a month. Dry eye status was evaluated by measuring tear production and clearance, and for inflammation and ocular surface recovery using histopathology analysis. The ICG encapsulated NPs were clearly visible on the ocular surface for up to 24 hrs. Following one month of DES treatment, the once-a-week administration of NP-CsA 0.005-0.01% demonstrated elimination of obvious inflammation and total ocular surface recovery, whereas the administration of Restasis® or NP-CsA 0.025% only showed elimination of inflammatory signs, without recovery of the ocular surface tissues. The mucoadhesive nanoparticle eye-drop platform demonstrated prolonged ocular surface retention of ICG in rabbits, and effective treatment of dry eye conditions in mice with up to 50 to 100 fold reduction in overall dosage of CsA compared to Restasis®, which may significantly reduce side effects and by extending the inter-dosing interval, improve patient compliance.

## 6.2 Introduction

Dry eye syndrome (DES) is defined as a multifactorial disease of the tears and ocular surface that results in symptoms of discomfort, visual disturbance, and tear film instability with potential damage to the ocular surface.[168] DES is also accompanied by increased osmolarity of the tear film and inflammation of the ocular surface. Cyclosporine A (CsA, an immunosuppressant agent) 0.05% ophthalmic emulsion (Restasis®, Allergan Inc., Irvine, CA) is the first commercially available eye drop formulation that showed an increase in natural tear production in dry eye patients, in part by acting to reduce both inflammation and concurrent loss of the conjunctival epithelium and goblet cells.[169] Eye drops, such as Restasis®, are the most popular method of delivering therapeutics to the eye due to their convenience and non-invasiveness, but their biggest challenge is rapid clearance due to tear dilution and turnover: more than 95% of the administered drugs are cleared before they reach their intended target.[6] Hence, eye drop formulations are often administered frequently (twice daily for Restasis®, but up to four times for many topical drugs) at high doses so that the drug concentrations may reach the therapeutic window. However, the high overall dosage of the administered drugs results in increased side effects: approximately 25% of the people in the phase III safety evaluation of Restasis® reported experiencing one or more adverse effects such as burning, stinging and foreign body sensation on the ocular surface.[169, 170] Since DES requires constant long-term treatment of its symptoms and signs, reducing the dosage of CsA using a more efficient drug delivery platform may likely reduce side effects and improve patient compliance, without compromising its therapeutic efficacy. In addition, lower administration rates would reduce the likelihood for adverse reactions to the preservatives that are commonly included in topical drugs and which are a common cause of ocular surface damage.[171-174]

Nanoparticle (NP) as drug carriers have been proposed to address the challenges associated with conventional eye drop delivery methods.[1, 7, 14, 32] By encapsulating drugs as their cargo, NPs may increase the concentration of drugs in the formulation, control the release rates of the drugs, and improve corneal retention by targeting the ocular surface.[58, 150] The controlled release of the drugs from the NP drug carriers may also reduce the total amount of drugs exposed on the ocular tissue at any given time, thus reducing the risk of side effects. Moreover, the small size of the NP (particle sizes  $\leq 10 \mu\text{m}$ ) eliminates discomfort experienced by users from administration of larger particles.[175] The NP formulation may also be tuned to achieve transparency and viscosity similar to that of water. A number of polyester based polymers, such as poly(lactic-co-glycolic acid) (PLGA), poly(glycolic acid)

(PGA), poly( $\epsilon$ -caprolactone) (PCL), and poly(lactic acid) (PLA) have been explored as suitable materials for preparing a NP drug delivery platform for targeting eye diseases.[67, 68, 151, 176-179] These NPs have been coated with polyethylene glycol (PEG) to improve their colloidal stability.[115, 119, 130, 131, 152-154] Recently, we developed an amphiphilic block copolymer composed of poly(D,L-lactic acid) and dextran (PLA-b-Dex) to formulate NP drug carriers.[4] Dextran provides a unique advantage over PEG-based materials due to its greater hydrophilicity and significantly higher density of functional groups for surface modification. Furthermore, dextran based NPs have previously demonstrated superior colloidal stability compared to PEG based NPs.[126] Dextran has three hydroxyl groups per monomer, whereas PEG only has one functional end group per chain: increased functional groups improves the efficiency of surface modification and consequently provides greater control over the surface properties of the NPs. Previously, we modified the surface of PLA-b-Dex NPs with phenylboronic acid (PBA) molecules to achieve mucoadhesion through covalent linkage between PBA and the *cis*-diol groups of carbohydrates abundant on the ocular mucous membrane.[158] By covalent attachment, PBA-modified NPs provide a greater affinity towards mucous membranes compared to the more commonly studied mucous-targeting molecules, such as chitosan, which rely on physical interaction with the mucous membrane.[52, 91, 110, 147, 155] Since the NPs target the surface mucous membrane, the rate of clearance of the NPs is likely reflected by the turnover rate of the ocular mucous membrane. We previously demonstrated significantly improved mucoadhesive properties using PBA-modified NPs, compared to Chitosan-based or thiol-based NPs, and a sustained release of CsA for up to 5 days. We further demonstrated that the CsA-loaded NPs were biocompatible on rabbit eyes, and effective in treating dry eye conditions in a short term study on mice.[180] We hypothesize that the mucoadhesive and controlled release properties of the nanoparticle drug carriers provide a drug delivery platform for long term treatment of dry eye using significantly reduced dosage of the drug, while maintaining treatment efficacy. The objective of this study is to investigate whether the CsA-loaded PBA-modified NPs are able to treat long-term experimental DES using once-a-week dosing (Figure 22).

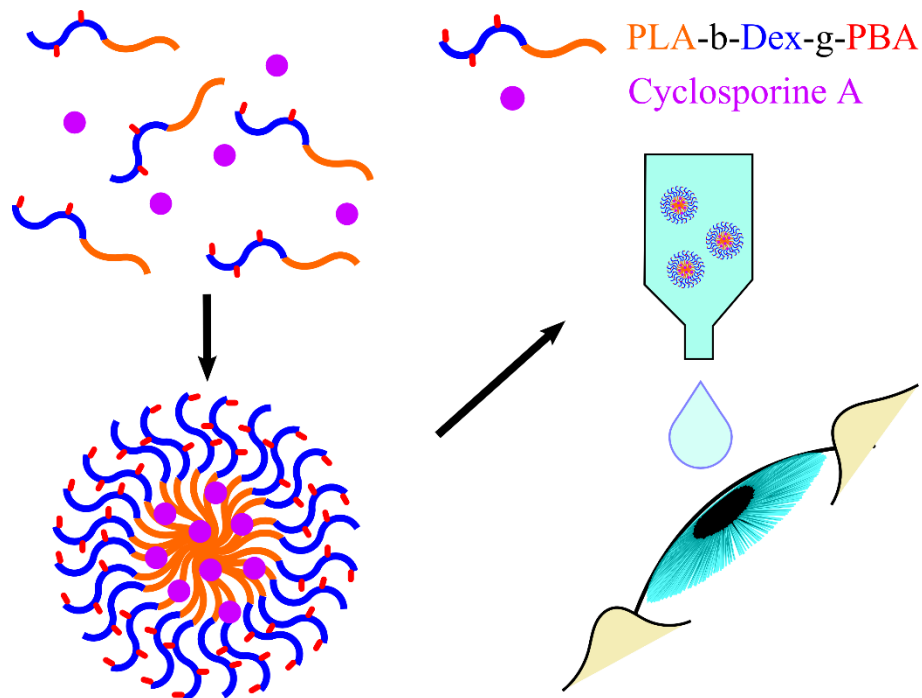


**Figure 22. Preparation of mucoadhesive nanoparticle drug carriers as eye drop formulation.**

In this study, experimental DES was induced in mice and nanoparticle formulations with difference doses of CsA were applied once a week to treat the dry eye signs. Dry eye treatment efficacy was evaluated by measuring for tear production and clearance, and also by evaluating the inflammation and ocular surface recovery using histopathology analysis post-euthanasia. The treatment efficacy of the CsA loaded PBA modified NP formulations were compared with Restasis® applied as a topical drop.

## 6.3 Experimental

### 6.3.1 Materials

Acid-terminated poly(D,L-lactide) (PLA; Mw ~20) was purchased from Lakeshore Biomaterials (Birmingham, USA) and washed with methanol to remove monomer impurities. Dextran (Dex; Mw ~10 kDa), acetonitrile (ACN), 3-Aminophenylboronic acid monohydrate (PBA), sodium periodate (NaIO<sub>4</sub>), glycerol, sodium cyanoborohydride (NaCNBH<sub>3</sub>), sodium fluorescein, and Cyclosporine A were purchased from Sigma Aldrich (Oakville, Canada).

### 6.3.2 Nanoparticle formulation, and encapsulation and *in vitro* release of Cyclosporine A

The amphiphilic block copolymer poly(D,L-lactide)-b-dextran (PLA-b-Dex) polymer was prepared in Chapter 3.[4] NPs were formed by the self-assembly process of the amphiphilic block copolymer through a nanoprecipitation method. To achieve mucoadhesive properties for long retention of ocular drugs on the corneal surface, we modified the surface of the NPs with phenylboronic acid (PBA) in two steps: the hydroxyl groups of the dextran surface of the NPs were oxidized in the presence of  $\text{NaIO}_4$ , and the aldehyde groups were then reacted with the amino groups of PBA using reductive amination in the presence of  $\text{NaCNBH}_3$ . [158]

The encapsulation of raw CsA in the PBA-modified NPs (PLA-b-Dex-g-PBA NPs) was performed using a nanoprecipitation method. 1 ml of DMSO containing polymer (~ 7 mg/ml) and CsA (varied concentration) was slowly added into 10 ml of Millipore water under gentle stirring for self-assembly of NPs carrying the drugs. The NP-drug mixture was then syringe filtered (pore size = 200 nm) to remove NP or drug aggregates, and dialyzed against water to remove some of the free drugs and DMSO from the mixture. The sizes of the nanoparticles were determined using dynamic light scattering (DLS) technique. The amount of CsA in the final mixture was determined using High-performance liquid chromatography (HPLC; C18 HPLC column, ACN/ $\text{H}_2\text{O}$  75:25 as the mobile phase, flow rate = 1 ml/min, UV-absorption detection at 210 nm).

The encapsulation of CsA in the PBA-modified NPs (PLA-b-Dex-g-PBA NPs) was performed using a nanoprecipitation method. 1 ml of DMSO containing polymer (~ 7 mg/ml) and CsA (varied concentration) was slowly added into 10 ml of Millipore water under mild stirring for self-assembly of NPs carrying the drugs. The NP-drug mixture was then syringe filtered (pore size = 200 nm) to remove NP or drug aggregates, and dialyzed against water to remove some of the free drugs and DMSO from the mixture. The sizes of the nanoparticles were determined using dynamic light scattering (DLS) technique. The amount of CsA in the final mixture was determined using High-performance liquid chromatography (HPLC; C18 HPLC column, ACN/ $\text{H}_2\text{O}$  75:25 as the mobile phase with UV-absorption detection at 210 nm).

The CsA *in vitro* release from the NPs was measured using the method reported previously.[158] 8 mL of syringe filtered NP-CsA suspension was injected into a Slide-a-Lyzer Dialysis cassette (MWCO = 20 kDa, Fisher Scientific) and dialyzed against 300 mL of simulated tear fluid (0.654 g of  $\text{NaHCO}_3$ , 2.04 g of NaCl, 0.0189 g of  $\text{CaCl}_2$ , 0.414 g of KCl in 300 mL of Millipore water) at 37 °C. 1 mL of the

release medium was extracted at each predetermined time points to quantify the amount of CsA using HPLC, while 1 mL of fresh simulated tear fluid was added to the release medium

### **6.3.3 Animal studies**

All animal studies adhered to the Association for Research in Vision and Ophthalmology (ARVO) Statement for the Use of Animals in Ophthalmic and Vision Research. The animal studies were also in compliance with the guidelines of the Canadian Council on Animal Care as well as regulations under the Animals for Research Act of Ontario Canada. Ethics approval was obtained from the University of Waterloo prior to the start of the study. Male New Zealand White (NZW) rabbits (Charles River Laboratories, Canada) with average weights of 2.8 to 3.3 kg were used for the ocular surface retention study. Female C57BL/6 mice (Charles River Laboratories, Canada) aged 3-5 months were used experimental dry eye treatment study. All animals were acclimatized in the animal facility for at least one week prior to experimentation. All formulations administered to the mice were sterilized using a sterile syringe filters (pore size = 0.2  $\mu\text{m}$ ) prior to use.

### **6.3.4 Ocular surface retention study on NZW rabbits**

We used ICG as a model drug to estimate change in its retention time as a result of encapsulation and delivery with PBA-modified NPs compared against its retention in aqueous solution. NZW male rabbits were sedated with acepromazine (2mg/kg) and briefly anesthetized using a mask with 2% isoflurane for 10 to 15 minutes for eye drop instillation. After the eye drop instillation, rabbits were transferred back to their cages to blink normally. For each rabbit ( $n = 4$ ), one eye was administered with ICG encapsulated NPs (NP-ICG) while the contralateral eye was administered with equivalent concentration of ICG in water. We used confocal scanning laser ophthalmoscopy (cSLO; Spectralis®: Heidelberg Retinal Angiography 2, Heidelberg Engineering, Germany) for imaging at baseline before administration and at 0, 3, 6, 9 and 24 hrs after the initial administration. To image the fluorescence of ICG, we used an excitation wavelength of 795 nm and an emission wavelength at 810 nm for all images. To achieve standardized images, the power and sensitivity were routinely set at 100% and 90 units, respectively, and the relative brightness of the ocular surface images were analyzed using ImageJ. An octagon shape was drawn on the ocular surface to enclose as much area as possible while avoiding the bright edges between the corneal surface and the eyelids where dye/particles accumulate due to pooling. The average brightness of the area inside the octagon was measured and the background signal was



subtracted from it. All of the means of the fluorescence measurements were normalized with respect to the initial mean fluorescence measurements at time 0 hr, right after instillation of the eye drops.

### 6.3.5 Dry eye induction and nanoparticle administration on C57BL/6 mice

To evaluate the efficacy of NPs carrying CsA in treating DES, an experimental murine dry eye model was used.[161] Transdermal scopolamine patches (Transderm-V, Novartis; 1.5 mg of scopolamine) were cut into two pieces and wrapped around the midtails of the mice and secured with surgical tape. The patches were replaced every other day through the duration of the study. To simulate a desiccating environment, mice cages (open-top) were placed in a fumehood for 1 hr, 3 times a day throughout the study. After 4 days of dry eye induction, the mice were divided into 6 groups of 5 mice and the administration of various formulations were initiated (Table 5). Note that dry eye was not induced in the Healthy group and no drug was administered to that group of mice. Saline, Blank NP, NP-CsA 0.005-0.01% and NP-CsA 0.025% were administered once a week (7  $\mu$ l; on days 5, 12, 19 and 26). RESTASIS® was given 3 times a day (3  $\mu$ ) throughout the study period.[181] On days 5, 12, 19 and 26, before the weekly administrations, tear production measurement and corneal fluorescein staining assessments were performed. On the final day (day 33), the mice were euthanized and the ocular tissues harvested for histopathology.

**Table 5. Six different groups applied to the mice for treatment of experimental dry eye**

Treatment group	Dry eye induced	Admin. volume ( $\mu$ l)	NP ( $\mu$ g)	CsA ( $\mu$ g)	Admin. frequency
Healthy	No	0	0	0	
Saline	Yes	7	0	0	x1/week
Blank NP	Yes	7	4	0	x1/week
NP-CsA 0.005-0.01%	Yes	7	4	0.3/0.6*	x1/week
NP-CsA 0.025%	Yes	7	4	1.5	x1/week
Restasis®	Yes	3	0	1.5	x3/day

### 6.3.6 Tear production measurement

Tear production was measured by holding a phenol red thread (Zone-quick; White Ophthalmic Supply, Canada) with jeweler's forceps in the lateral canthus of the ocular surface for 30 seconds. The length of the dyed segment (red) of the thread was measured and recorded.

### 6.3.7 Corneal fluorescein staining

Corneal fluorescein staining was observed, recorded and photographed with a slit-lamp bio-microscope using a cobalt blue light, 10 minutes after the administration of 1  $\mu$ l of sodium fluorescein solution (10 mg/ml).

### 6.3.8 Histopathology analysis

The eyes were enucleated and collected immediately after euthanasia for histopathological evaluation. The entire upper eyelids were also dissected and collected for evaluation of the tarsal conjunctiva and the underlying soft tissues. Consecutive sections of the entire ocular globe and eyelids were processed for microscopic analysis: After initial fixation in 10% neutral buffered formalin, the tissue was embedded in paraffin, serially sectioned into 5  $\mu$ m thick sections, and stained with hematoxylin and eosin (H&E). The histological slides were evaluated using bright field microscopy (Leica DM1000, ICC50 HD, Leica Microsystems Inc, Canada).

## 6.4 Results

### 6.4.1 Nanoparticle formulation

The nanoparticles were fabricated with approximately  $15.2 \pm 1.0$  mol/mol% of PBA on dextran monomers. The diameter of the raw nanoparticles (Black NPs) was  $25.4 \pm 0.6$  nm (Table 6). With encapsulation of CsA, the diameter increased to  $29.1 \pm 0.3$  nm (NP-CsA 0.025%). [158, 180] From the HPLC analysis, the NP-CsA 0.025% group contained approximately 1.5  $\mu$ g of CsA in a 7  $\mu$ l eye drop (along with approximately 4  $\mu$ g of the PLA-b-Dex-g-PBA NPs) (Table 5). This means that the NP-CsA 0.025% group had the same amount of CsA in a 7  $\mu$ l drop as that in a 3  $\mu$ l drop of Restasis®. Due to the dosing frequency differences between Restasis® and NP-CsA 0.025%, the overall dosage of CsA in NP-CsA 0.025% is approximately 5% that of Restasis® (or 1/21 that of Restasis®). Similarly, the NP-CsA 0.005-0.01% group had 0.3  $\mu$ g of CsA in the 7  $\mu$ l drop for the first two weeks of administration, and 0.6  $\mu$ g for the subsequent two weeks. Thus, the dosage of NP-CsA 0.005-0.01% is approximately 1% that of Restasis® (or 1/105<sup>th</sup> of Restasis®) for the first two weeks, and 2% (2/105<sup>th</sup> of Restasis®) for the subsequent two weeks. The NP-CsA 0.025% and NP-CsA 0.005-0.01% showed total *in vitro* release for up to 4 and 5 days respectively (Supplementary Figure S1), similar to our previous study. [158]

**Table 6. Nanoparticle diameters and their polydispersity measured using dynamic light scattering (DLS).**

	MSD* diameter (nm)	Polydispersity
Blank NPs	25.4 ± 0.6	0.240 ± 0.005
NP-CsA 0.005-0.01%	26.9 ± 1.1	0.317 ± 0.001
NP-CsA 0.025%	29.1 ± 0.3	0.199 ± 0.002

#### **6.4.2 Ocular surface retention study**

To analyze the effect of mucoadhesive NPs on ocular surface retention, ICG was used as a model drug for imaging the corneal surface of rabbit eyes using cSLO. Standardized images SLO (Figure 23) showed that the ICG delivered using NPs (NP-ICGs) demonstrated higher retention of ICG compared to the ICG control, which was especially noticeable at the 6 hr time-point (Figure 23): up to 17.5% of the initial ICG from NP-ICGs administration was still retained after 6 hrs whereas only about 2.81% of the ICG was retained after administration of free ICG solution (Figure 24). At 30 hr, both the ICG and the NP-ICG showed baseline level of fluorescence.

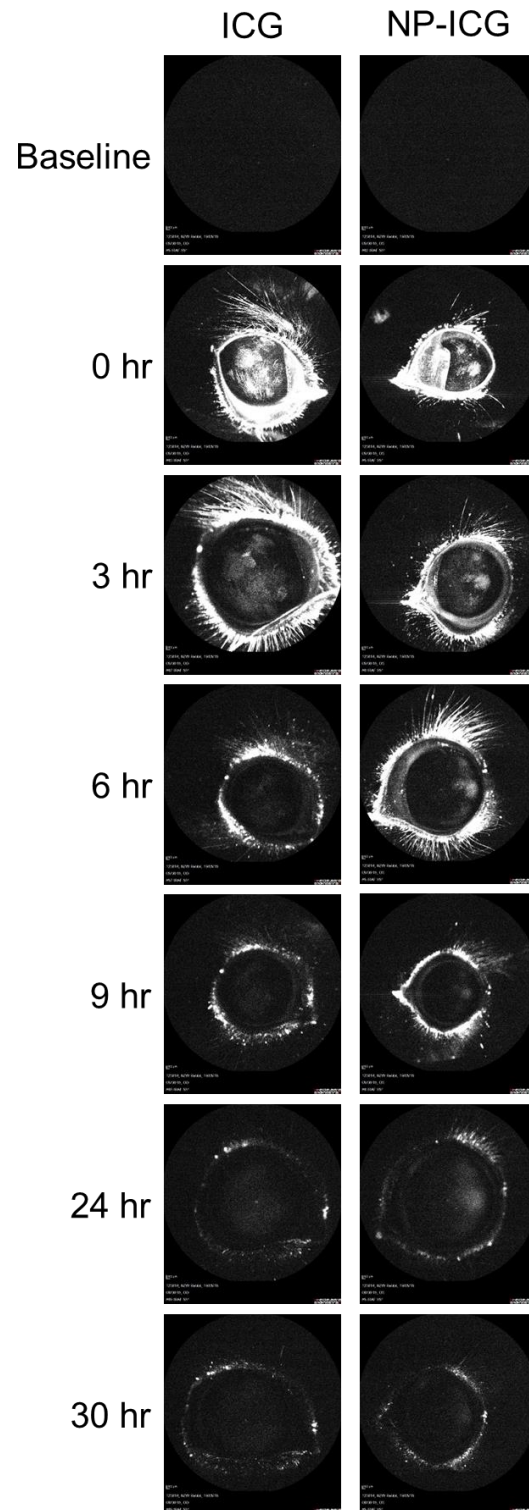


**Figure 23. Fluorescence images of NZW rabbit eyes treated with ICG and ICG-NP taken using confocal Scanning Laser Ophthalmoscopy (cSLO).**

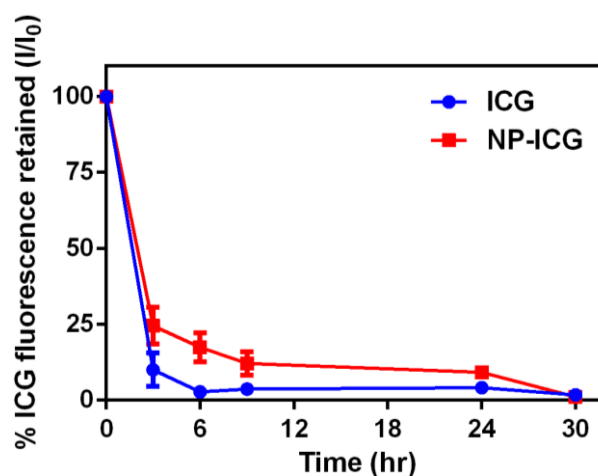


**Figure 24. ImageJ analysis of the fluorescence images taken from rabbit eyes treated with ICG and NP-ICG (n = 4; mean  $\pm$  s.e.m.). I: mean fluorescence intensity measured using ImageJ software;  $I_0$ : initial fluorescence (at 0 hr).**

#### 6.4.3 Tear production and corneal fluorescein clearance on C57BL/6 mice

To evaluate the efficacy of the CsA loaded NPs in treating DES, tear production measurements and corneal fluorescein staining analysis were performed each week right before the dosing of the various formulations on mice. All the groups (with the exception of the Healthy control group) underwent dry eye induction, which was reflected in the sudden drop of tear production after 4 days (i.e., on day 5) (Figure 25). The Healthy group maintained a relatively stable tear production throughout the study except on week 3 (day 26). Interestingly, this slight drop in tear production is also reflected on the reduced corneal fluorescein clearance (Figure 26, top row) observed on day 26, while on all the other measurement time points the fluorescein was rapidly cleared from the corneal surface within 10 minutes. The tear production for all the treatment groups remained at or below half of the initial tear production rate throughout the duration of the study. Only the NP-CsA 0.025% group was able to significantly increase its tear production at the end of the study (day 33) compared to before the start of weekly administrations (day 5) ( $p < 0.05$ ), but it was only able to restore up to about 50% of the initial tear production rate (day 1). These findings were also corroborated by the corneal fluorescein staining analysis. All groups (excluding the Healthy control group) showed a similar dryness on the eye: compared to the Healthy group, all groups showed a relatively high amount of fluorescein staining on the corneal surface due to the ocular surface damage inflicted by the dryness induced by the treatment. Only the NP-CsA 0.005-0.01% group showed an improvement by the end of the study

compared to its earlier measurements in terms of corneal fluorescein staining, whereas the NP-CsA 0.025% group showed improvements up to week 2 (day 19), but showed a worsening effect from day 19 until day 33.

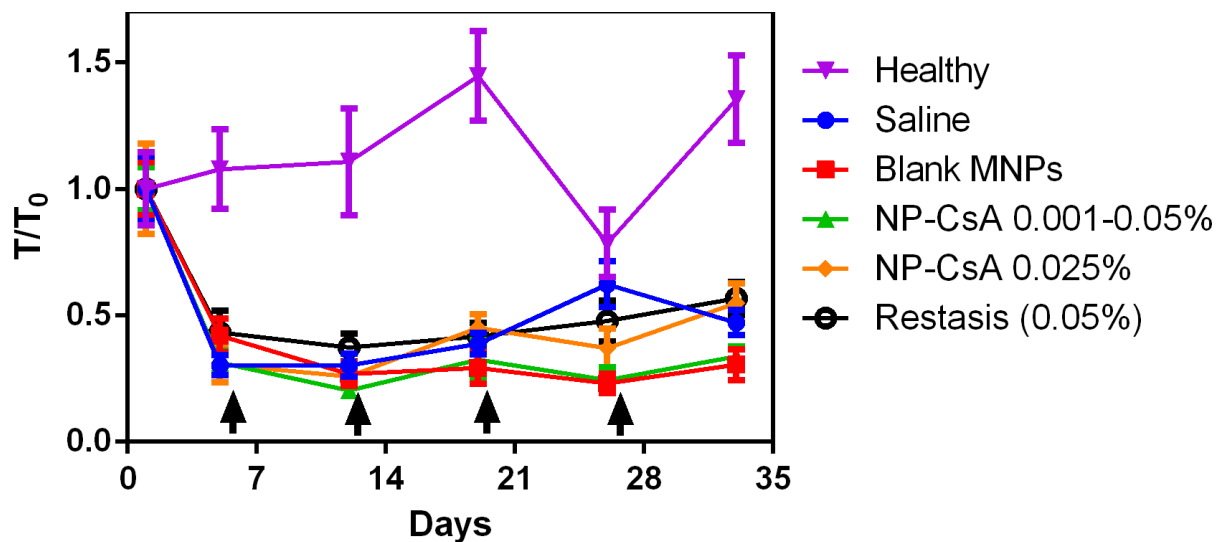


**Figure 25. Tear production measurement of mice with different treatment groups. The tear volumes (T) were normalized with respect to their initial tear volume (T<sub>0</sub>). The arrows represent the weekly dosing regimen of Saline, Blank NPs, NP-CsA 0.005-0.01% and NP-CsA 0.025% groups.**

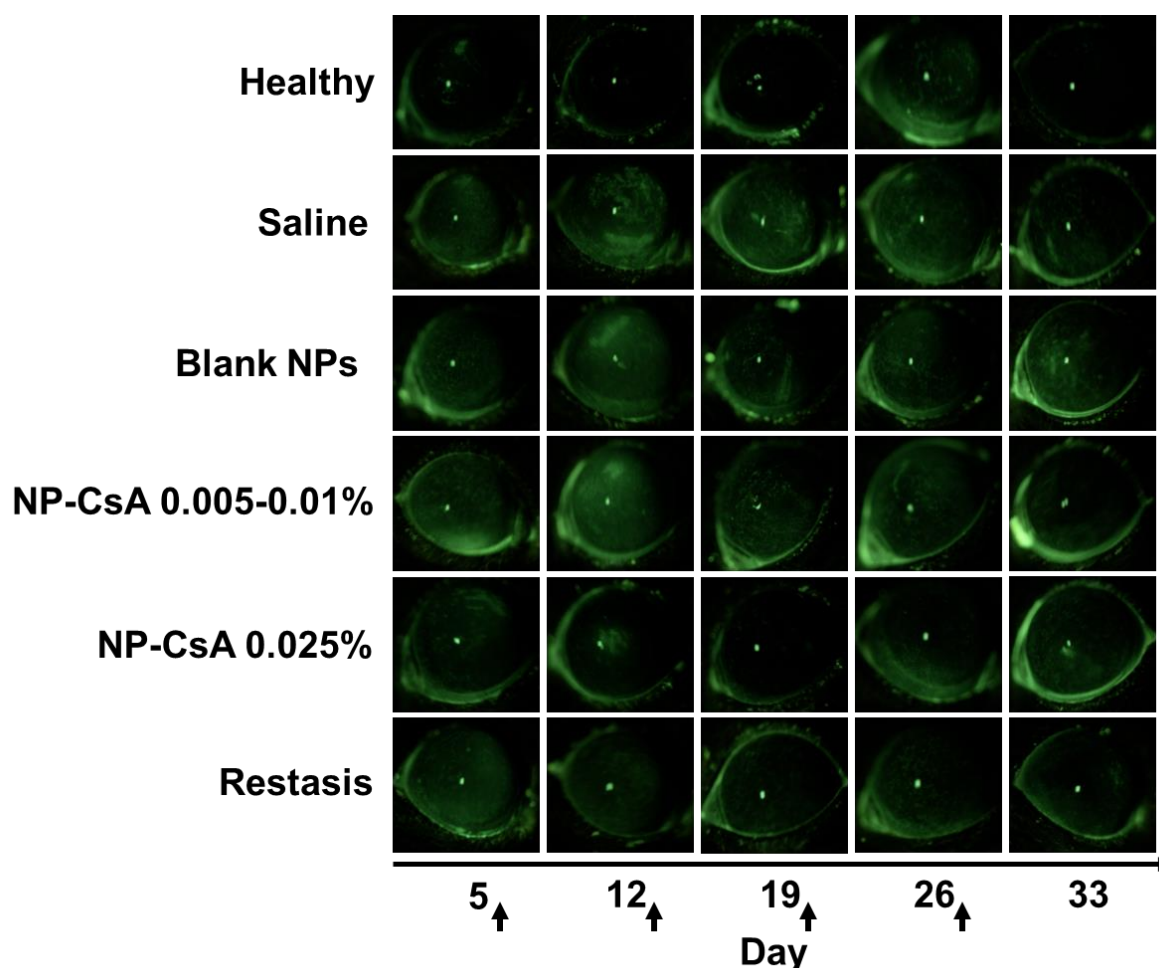


**Figure 26. Corneal fluorescein staining analysis of mice with different treatment groups. The arrows represent the weekly dosing regimen of Saline, Blank NPs, NP-CsA 0.005-0.01% and NP-CsA 0.025% groups. Note that the analysis does not take into account the fluorescein on the lid margins of the eyes.**

#### **6.4.4 Histopathology analysis**

The ocular tissues of the mice in the Healthy group showed all the signs of healthy eyes. The conjunctival epithelium displayed surface epithelium cells with normal morphology and architecture along with abundant goblet cells which indicated the presence of adequate conditions for production and formation of a stable tear film layer on the surface of the ocular mucous membrane (Figure 27, A). The lamina propria were composed of loose connective tissues with occasional lymphocytes, and showed no evidence of acute or chronic inflammation. By contrast, in the DES groups treated with both

the Saline and Blank NPs showed conjunctival epithelium and lamina propria changes consistent with disease (Figure 27, B and C). There were mild to moderate levels of mixed inflammatory infiltrates composed of lymphocytes and occasional polymorphonuclear leucocytes, indicated by the red arrows in the figure. The epithelium was thinned out and showed marked reduction, or in some cases, complete absence of goblet cells. The mice treated with NP-CsA 0.005-0.01% showed conjunctiva with no signs of inflammatory infiltrates (Figure 27, D), displaying morphological features similar to those seen in the Healthy mice group. Moreover, the surface epithelium demonstrated partial to complete recovery of the goblet cells. In terms of the number of goblet cells, the majority of the surface epithelium of the eye samples in this group closely resembled the Healthy group. Similarly, the mice treated with higher dose of CsA loaded NPs (NP-CsA 0.025%) showed no signs of inflammatory infiltrates (Figure 27, E). However, the ocular specimens in this group demonstrated a significantly reduced amount of goblet cells on the surface, and in some cases, complete lack of goblet cells. The mice treated with the commercial form of CsA, RESTASIS®, similarly showed no signs of inflammation, but similar to the NP-CsA 0.025% group, the surface epithelium remained thinned and was completely deprived of goblet cells (Figure 27, F).



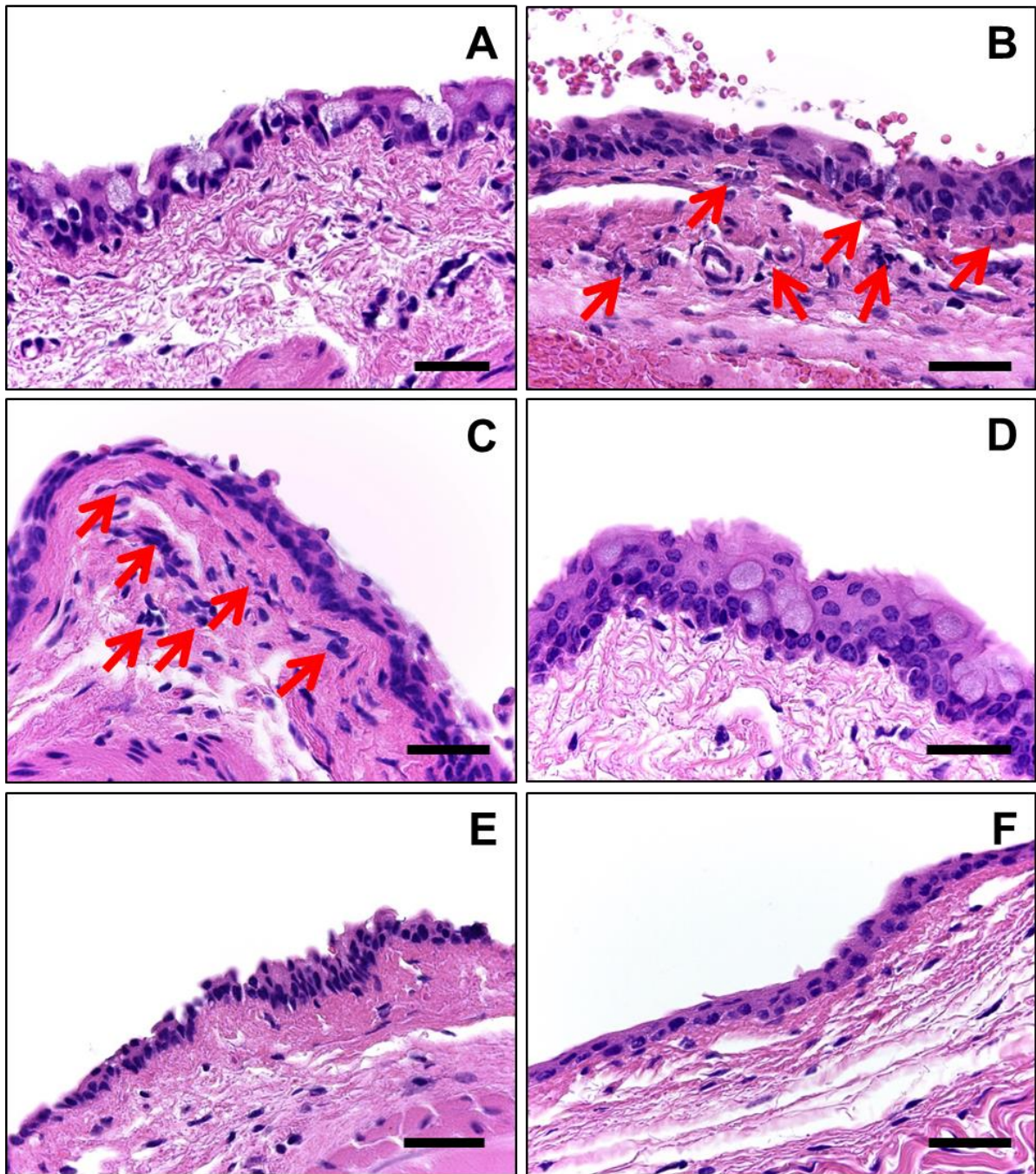


**Figure 27. Histopathology analysis of ocular tissues of mice with different treatments: A) Healthy, B) Saline, C) Blank NPs, D) NP-CsA 0.005-0.01%, E) NP-CsA 0.025%, and F) Restasis®. The scale bars are 100  $\mu$ m in length. The red arrows represent some of the inflammatory infiltrates such as lymphocytes, polymorphonuclears and eosinophils observed.**

## 6.5 Discussion

Mucoadhesive NPs were developed to enhance the delivery of ocular therapeutics to the anterior segment of the eye. PLA-b-Dex NPs, with PBA grafted onto the dextran surface for mucosal targeting, previously showed enhanced *in vitro* mucoadhesion and sustained release of CsA from the NPs for up to 5 days.[158] In a subsequent study, we demonstrated that the CsA loaded NPs showed compatibility on rabbit eyes and efficacy in treating experimental DES in mice using once a week administration.<sup>38</sup> Because the previous studies were limited to a short term treatment period of 1 week, the aim of the current study was to evaluate long term treatment effects administering CsA loaded NPs once a week. The experimental DES was induced in mice using the combination of transdermal application of anticholinergic agents, scopolamine, and the exposure to desiccating environments, as reported in previous studies.[161, 182] From these studies, we hypothesized that the mucoadhesive and sustained release properties of the NPs prolong the retention of CsA, thus allowing for the treatment of dry eye with significantly reduced dosage of CsA in the formulation.

In this study, we visually demonstrated the prolonged retention of the model drug, ICG, when delivered with PBA modified NPs *in vivo* compared against an aqueous solution ICG encapsulated in NPs showed increased retention on the surface of rabbit eyes for up to 24 hrs (Figure 23 & Figure 24). At 30 hr, signals from both the NP-ICG and the aqueous ICG formulations decreased to the baseline levels, implying that the ICG was cleared and/or photobleached (Figure 24). Considering the rapid clearance of Restasis® from the ocular surface within the first 20 minutes of eye drop administration,[183] these data demonstrate that PBA modified NPs significantly prolong the ocular retention of loaded therapeutics by attaching to the ocular mucous membrane. Previous studies demonstrated improved retention of CsA by encapsulating them in non-PBA NPs but the CsA concentration in the lachrymal fluid quickly reached baseline levels after the first few hours.[184, 185] This study further corroborates previous *in vitro* data showing imaging mucoadhesive properties of the PBA modified NPs due to covalent linkage to mucin.[158]

We next studied how prolonged ocular retention of drugs could improve the long term treatment effect of CsA-loaded NPs on dry eye conditions induced in mice. The dry eye induction was confirmed by the drastic drop in tear production rate within 4 days (Figure 25), as well as the increased amount of fluorescein staining on the corneal surface (day 5) compared to the Healthy control group (Figure 26). From both tear production measurements and fluorescein staining analysis, most of the mice in the groups after dry eye induction (excluding the Healthy group) maintained the dry eye conditions

throughout the study (from day 5 to day 33) without much improvement in these clinical parameters. The only groups that showed statistically significant improvements between day 5 and day 33 were the Saline and NP-CsA 0.025% groups ( $p < 0.05$ ), but comparably, the increased tear production is only at 50% of the initial tear production rate. This phenomenon was also observed in our previous short term treatment study.[180] Since the dry eye induction procedures (scopolamine and desiccating environment) were maintained throughout the study, their effects were likely too overwhelming for the treatment effects of CsA. Although the tear production improved for NP-CsA 0.025%, the corneal fluorescein staining only improved up to day 19 and gradually worsened toward the end of the study, implying distinct ocular surface damage. To better understand the treatment effects of the immunosuppressant agent, CsA, closer examination of the ocular surface was conducted using histopathology, to identify signs of inflammation and ocular surface integrity. The ocular tissues of the Saline and Blank NPs group showed that these formulations were unable to treat the symptoms of DES, demonstrating pronounced inflammation and a complete lack of goblet cells on the ocular surface (Figure 27). It is possible that Blank NPs group may further induce inflammation due to the degradation of the PLA chains. However, in our previous study, we showed that the NPs themselves did not cause any inflammation after weekly dosing of up to 12 weeks.[180] It is likely that the timeframe for NP clearance with the mucous membrane is shorter than that of hydrolytic degradation of the PLA polymers.[186, 187] All three formulations containing CsA (NP-CsA 0.005-0.01%, NP-CsA 0.025%, and Restasis®) showed elimination of inflammatory infiltrates, which is the main function of CsA. However, only the NP-CsA 0.005-0.01% group showed recovery of the ocular surface in addition to the lack of inflammatory infiltrates. In our previous study, we observed the elimination of inflammation and full recovery of the ocular surface with NP-CsA 0.025% group for the 1 week treatment study.[180]

In this study, after 4 weeks of treatment, the NP-CsA 0.005-0.01% showed both the elimination of inflammation and the recovery of the ocular surface while NP-CsA 0.025% only showed elimination of inflammation without the full ocular surface recovery. We speculate that NP-CsA 0.025% group likely had sufficient CsA to treat DES in 1 week, but when this dosage was repeated for 4 weeks, the prolonged exposure to this dose may have slowed down or prevented the recovery of the ocular surface. The long term toxicity of CsA on the ocular surface has not been well documented in the past,[188] likely due to rapid ocular clearance of CsA using conventional formulations. We hope to further investigate the long term effect of CsA on ocular surface as a result of mucoadhesion of the drug carriers, especially in terms of recovering the ocular surface tissues. The mice treated with Restasis® also showed similar effects, likely due to the frequent exposure (thrice daily) to the high concentration

CsA in the precorneal tear fluid. Therefore, we believe that it is necessary to lower the dosage of the CsA in the mucoadhesive NPs even further, from 5% of Restasis® (NP-CsA 0.025%) to 1 to 2% (NP-CsA 0.005-0.01%), for long term treatment of DES to facilitate the ocular surface recovery without compromising the therapeutic efficacy.

## **6.6 Conclusion**

PLA-b-Dex NPs surface grafted with PBA ligands were formulated as a mucoadhesive NP eye drop delivery platform. The mucoadhesive nature of the NPs were further demonstrated by showing enhanced ocular retention of the fluorescent dye, ICG, delivered using the NPs compared to ICG delivered without the NPs. Both once a week administration of NPs (NP-CsA 0.025%) and three times daily administration of Restasis® to dry eye induced mice showed elimination of inflammatory infiltrates but failed to fully recover the ocular surface. However, once a week dosing of NPs with an even lower dosage (NP-CsA 0.005-0.01%) showed efficacy in terms of both the elimination of inflammatory infiltrates and the full recovery of the ocular surface, as determined by histopathology. The current study provides promising results for the potential application of PBA-grafted mucoadhesive NPs to dramatically prolong the dosing interval, increase compliance and improve the efficacy of CsA and other ocular therapeutics for treating anterior eye diseases.

## Chapter 7

### A novel method for chemically modifying carbohydrates using a semi-solid state reaction

#### 7.1 Summary

Carbohydrates are abundantly used in drug delivery applications – often as the shell material in designing drug delivery vehicles. However, chemically modifying the carbohydrates to achieve desired surface functionality for the drug delivery vehicles requires long reaction time and numerous steps. Here we propose a novel semi-solid state reaction to chemically modify carbohydrates. The method avoids degradation or caramelization of the carbohydrates by avoiding the use of high temperatures, which is normally associated with solid-state chemistry, by incorporating a small amount of water to act as a “plasticizer”. We used dextran as our model carbohydrate and conjugated 4-(bromomethyl)phenylboronic acid (BPBA) onto dextran using this new approach. NMR analysis demonstrated that the conjugation reaction may have reached saturation level by as early as 10 minutes at temperatures from 70 to 110 °C. By tuning the reaction temperature and the ratio of the reactants, we achieved conjugation efficiency of 42.4 mol/mol% for BPBA/dextran(monomer), which is unattainable using same conditions in a solvent reaction. We believe that this novel semi-solid state reaction will significantly improve the utility of carbohydrates for diverse applications in the field of biomedical engineering.

#### 7.2 Introduction

Carbohydrates are extensively used in drug delivery and tissue engineering applications due to their biocompatible nature [189, 190]. Recently, numerous researchers used carbohydrates as the shell material for nanoparticle (NP) drug delivery systems for their hydrophilic nature and also because of the numerous functional groups on their backbone [120]. These functional groups on the NP drug carriers can be chemically modified with a molecule to achieve specific surface functionality such as targeted therapy. However, surface modification of NPs frequently requires multiple steps, long reaction times, and/or organic solvents that may not be regarded as safe.

Recently, solid state chemistry has gained much attraction as an alternative method to the conventional solvent chemistry due to their rapid reaction rates [191]. A typical solid state reaction requires melting of the reactants together for the reaction to proceed, without the need for a liquid

reaction medium. This is also advantageous for biomedical application since there is no organic solvent, that may be unsafe, to be purified from the final products. Nevertheless, it is difficult to carry out conventional solid state reactions for carbohydrates since the high temperatures required for the reaction may lead to caramelization and/or degradation of the carbohydrates.

Here we propose a slight variation of the solid state reaction to address this issue. By adding a small amount of water to the carbohydrate reaction mixture, we believe that we can significantly lower the temperature for effective reaction, thus maintaining the integrity of the carbohydrates for the reaction. Since carbohydrates are soluble in water, water may act as a “plasticizer” in this reaction to lower the reaction temperature without affecting the reactivity of the process. The addition of water causes the solid reactants to become a paste-like material, which then phase-transitions into a viscous gel-like mixture at an elevated temperature to facilitate the reaction. We hypothesize that this new semi-solid reaction can be utilized to chemically modify carbohydrates with rapidity and simplicity.

To demonstrate the semi-solid state reaction, we used dextran as our model carbohydrate in this study, and we modified it with a 4-(bromomethyl)-phenylboronic acid using Williamson ether synthesis mechanism. Dextran, a polysaccharide made of glucose units, is one of the many carbohydrate materials extensively used in various biomedical applications [192-194]. Straight chains of dextran consists of  $\alpha$ -1,6 glycosidic linkages, while the branched dextran forms  $\alpha$ -1,3 linkages. Previously, we surface modified dextran based NPs with phenylboronic acid molecules to develop a mucosal targeting NP drug delivery platform [158, 180].

## **7.3 Experimental**

### **7.3.1 Materials**

Acid-terminated poly(D,L-lactide) (PLA; Mw ~ 20 kDa) was purchased from Lakeshore Biomaterials (Birmingham, USA) and washed with methanol to remove monomer impurities. dextran (Dex; Mw ~ 10 kDa, mostly linear), sodium tert-butoxide (tBuONa), 4-(bromomethyl)phenylboronic acid (BPBA), hydrochloric acid (HCl), triethylamine (TEA), N-(3-dimethylaminopropyl)-N-ethylcarbodiimide (EDC), and sodium cyanoborohydride (NaCNBH<sub>3</sub>) were purchased from Sigma Aldrich (Oakville, Canada). N-Hydroxysulfosuccinimide (Sulfo-NHS) and N-Boc-ethylenediamine were purchased from CNH Technologies (Massachusetts, USA).

### 7.3.2 A semi-solid state chemistry to chemically modify dextran with 4-(bromomethyl)phenylboronic acid

The Williamson ether synthesis between dextran and BPBA were performed in semi-solid state by adding a small amount of water to the mixture. We used dextran as the model carbohydrate and BPBA as the small molecule with bromo functional group, and to catalyze the Williamson ether conjugation between BPBA and dextran, we used tBuONa as the strong base (Figure 28). To perform the conjugation, we added all three ingredients, dextran, tBuONa, and BPBA, in a mortar and used a pestle to mix the powders as thoroughly as possible. During mixing, water drops (125 wt% of dextran) were added to create a paste-like mixture. The mixture was then transferred to a scintillation vial with a sealed cap and placed inside a pre-heated oven. The samples after reaction were washed with methanol multiple times to remove tBuONa and unreacted BPBAs. The samples were dried overnight in a vacuum desiccator before characterization with  $^1\text{H}$  NMR. The conjugation efficiency of BPBA on dextran was calculated by integrating the peaks in NMR spectra after baseline adjustment: the peaks that correspond to the protons in the phenyl group of the BPBA (near 7.4 ppm and 7.8 ppm) were normalized against the peak corresponding the protons on dextran carbon 1 in the monomer (near 5.2 ppm).

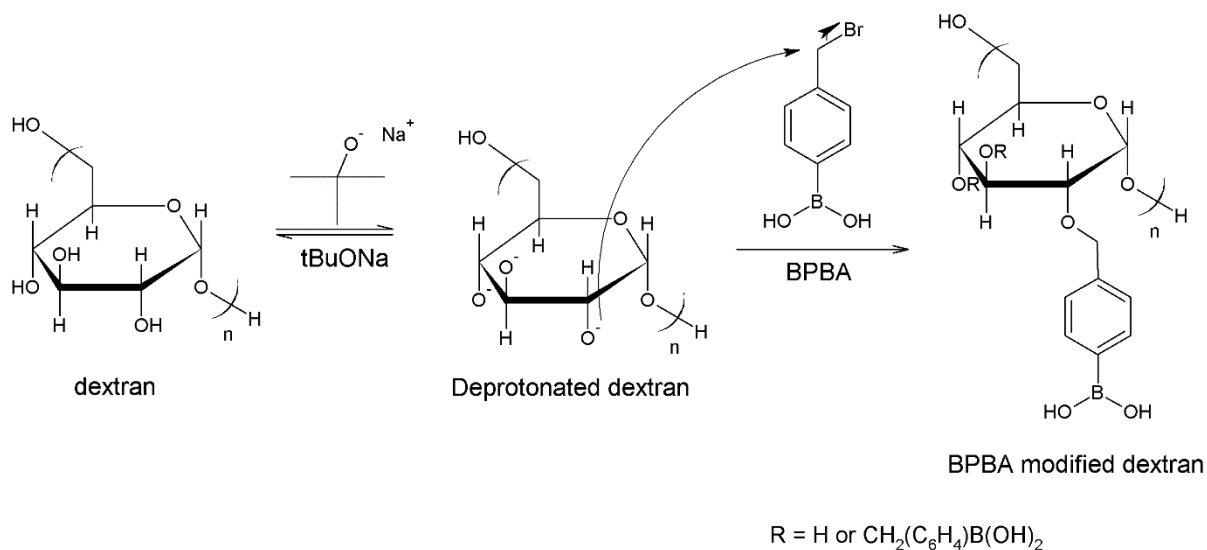


**Figure 28. Reaction scheme for the Williamson ether synthesis between dextran and 4-bromomethylphenylboronic acid (BPBA), using sodium tert-butoxide (tBuONa) as the catalyst. Note that the BPBA is shown to have reacted with the hydroxyl group on C2 of the dextran repeating unit, but BPBA may also attach to the hydroxyl groups on C3 and C4.**

## **7.4 Application of the semi-solid state chemistry in synthesizing BPBA modified dextran based nanoparticles**

The semi-solid Williamson ether conjugation method described above was applied in synthesizing a block copolymer between poly(D,L-lactide) and BPBA modified dextran. The current semi-solid state conjugation method was incorporated into the previous procedure for synthesizing PLA-Dex block copolymer [4, 158]. Briefly, the dextran end group was conjugated with N-Boc-ethylenediamine through reductive amination. The semi-solid state conjugation method was incorporated in the next step to conjugate BPBA to the hydroxyl groups of dextran backbone using dextran(monomer):tBuONa:BPBA molar ratio of 1:2:1 with reaction temperature of 110 °C for 10 mins. Subsequently the amine group protected by the Boc group was deprotected through HCl and TEA treatments. Finally, the amine group of the PBA-dextran end group was conjugated with the carboxyl group of PLA terminal group using EDC and Sulfo-NHS as catalysts. The intermediate and the final product from all 4 steps were analyzed and verified using <sup>1</sup>H NMR.

## **7.5 Results and discussion**

### **7.5.1 Conjugation of BPBA onto dextran using semi-solid state chemistry**

We performed semi-solid state reaction to chemically modify the dextran with BPBA using Williamson ether synthesis mechanism and we evaluated the BPBA/dextran conjugation efficiency using <sup>1</sup>H NMR after removing unreacted BPBAs from the mixture. The <sup>1</sup>H NMR spectrum obtained from the procedure of this reaction showed the presence of peaks near 7.4 ppm which corresponds to the protons at C2 and C6 of BPBA, and 7.8 ppm which corresponds to the protons on C3 and C5 (Figure 29).



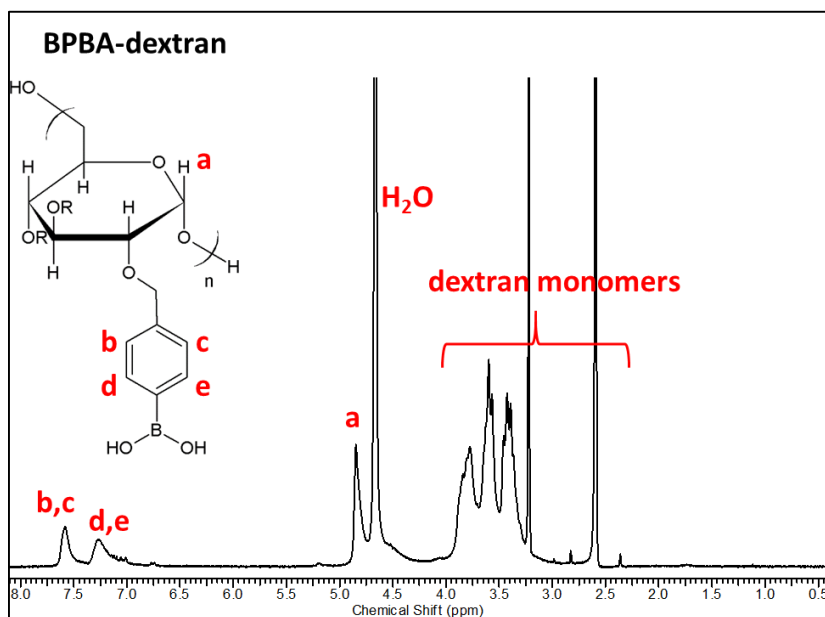


**Figure 29.**  $^1\text{H}$  NMR analysis of the semi-solid state chemistry on BPBA modified dextran in  $\text{D}_2\text{O}$  after purification of unreacted BPBA and  $\text{tBuONa}$ .

### 7.5.2 Effect of the reaction time and the temperature

Semi-solid state reactant mixtures were placed in an oven with varying temperatures and reaction times to determine their effects on the conjugation efficiency between BPBA and dextran. The conjugation of BPBA on dextran increased with increasing reaction temperature but it was unaffected by the reaction time (Figure 30): there was no significant difference among the conjugation efficiencies from 10 min to 2 hrs of reaction time for each reaction temperature of 70, 90 or 110 °C (student t-test:  $p < 0.05$ ). This result is in agreement with the fast nature of solid-state reactions [191]. Increasing the reaction temperature increased the BPBA-Dextran conjugation efficiency, which suggests that higher temperature directly translates to higher reaction kinetics of the Williamson ether mechanism. We observed that the all the reaction mixtures coming out of the oven exhibited a gel-like viscous nature, which implies that the initial paste-like mixtures went through a phase-transition into a supersaturated liquid mixture at the elevated reaction temperatures. Thus, we avoided increasing the reaction temperature near the melting point of at least one of the reactants, which in this case is at least 170 °C, by adding a small amount of water. At 130 °C, the samples turned brown after 10 mins and 30 mins which implies the caramelization of the dextran [195] and no further reaction durations were examined.

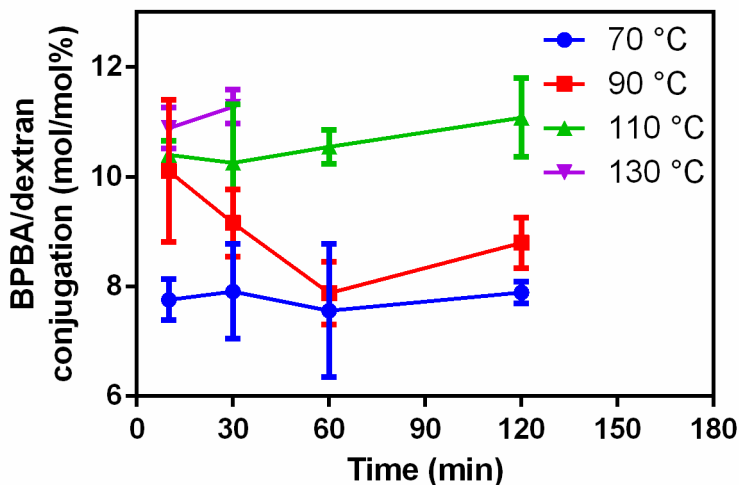


**Figure 30. Effect of reaction time and temperature on the BPBA:dextran conjugation efficiency.**

### 7.5.3 Effect of the ratio of the reactants

We investigated the effect of the molar ratios BPBA:dextran (note that mole of dextran throughout this study represents the mole of the dextran repeating units) and tBuONa:dextran on the conjugation efficiency between BPBA and dextran using the semi-solid state method. While keeping the tBuONa:dextran molar ratio constant (1:1) and using the optimal reaction conditions of 10 mins at 110 °C, we varied the ratio of BPBA:dextran to study its effect on the BPBA/dextran conjugation efficiency. Conjugation efficiency decreased with the increasing amount of BPBA with respect to dextran in the mixture (Figure 31). It is likely due to the side reactions that BPBA undergo among themselves to form trimeric anhydrides, boroxines, especially under dehydrating conditions [196]. The excess BPBA's in the mixture may promote the formation of these boroxine complexes rather than forming ether linkages with deprotonated hydroxyl groups of dextran. We believe that the use of an alternative targeting ligand which do not undergo side reactions among themselves may still increase the conjugation efficiency linearly with increasing molar ratio of the targeting ligand to dextran monomers. On the other hand, the conjugation efficiency of BPBA on dextran increased with increasing ratio of tBuONa:dextran while keeping the BPBA:dextran molar ratio constant at 1:1 (Figure 32). With tBuONa:dextran ratio of 4:1, the BPBA/dextran conjugation reached 42.4 mol/mol %. The result implied that the more tBuONa added, the more hydroxyl groups were deprotonated, leading to higher number of ether linkages formed with BPBA's present in the mixture. When we performed the Williamson ether synthesis using the same reaction temperature and the same duration in a solvent condition (using water as the solvent),

the conjugation efficiency was in the range of 1 to 3 mol/mol%. These result provide us with a great flexibility in tuning the desired conjugation efficiency using this semi-solid state reaction chemistry.

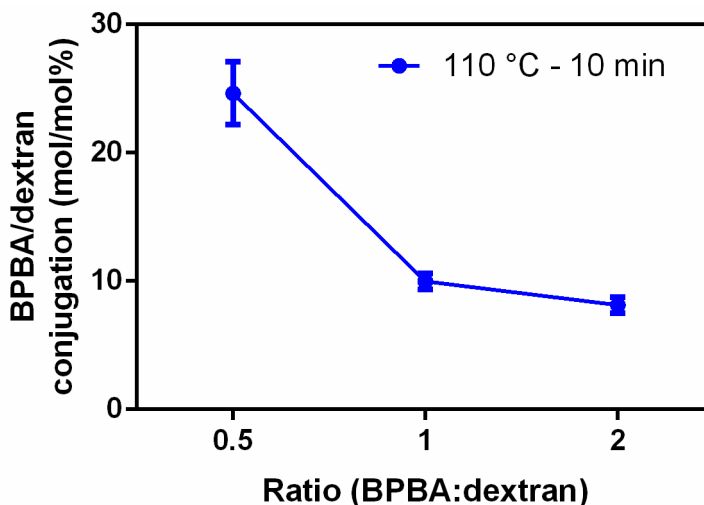


**Figure 31.** Effect of the molar ratio of BPBA to dextran repeating unit on the BPBA:dextran conjugation efficiency. The molar ratio of tBuONa to dextran repeating unit is kept constant at 1.

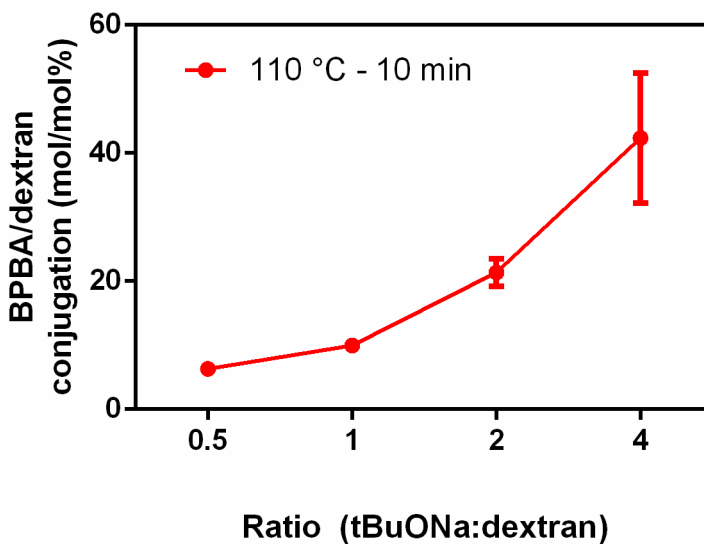


**Figure 32.** Effect of the molar ratio of tBuONa to dextran repeating unit on the BPBA:dextran conjugation efficiency. The molar ratio of BPBA to dextran repeating unit is kept constant at 1.

#### **7.5.4 Application of the semi-solid state chemistry in synthesizing BPBA modified dextran based nanoparticles**

After obtaining the results on the effect of various parameters on the conjugation efficiency of BPBA on dextran, we employed this method into synthesizing a poly(D,L-lactide)-b-dextran (PLA-Dex) block copolymer with BPBA groups grafted onto the dextran. Previously, we developed a method for synthesizing a PLA-Dex block copolymer [4], and subsequently modifying the dextran surfaces with phenylboronic acid derivatives after forming the nanoparticles using the PLA-Dex block copolymers [158]. The previous method required multiple reaction and purification steps as well as long reaction times to graft 3-amino-phenylboronic acid onto periodate oxidized dextran monomers. The current semi-solid state method uses a single step approach to graft BPBA onto the hydroxyl groups of dextran without the need for pre-treatment of the dextran molecules (i.e. periodate oxidation). The simplicity of the reaction combined with the short reaction time (i.e. 10 mins at 110 °C) of the semi-solid state chemistry provides a significant improvement in the synthesis of PLA-Dex-g-PBA block copolymers. Using the optimal reaction conditions of 110 °C for 10 mins and 1:2:1 as the molar ratio for dextran-NH-Boc:tBuONa:BPBA, we synthesized the dextran-NH-Boc (prepared from step 1 in Figure 33) with about 17.6 mol/mol% of BPBA grafted onto the dextran backbone in step 2 of the proposed reaction scheme (Figure 33), which was within the range of values obtained using the previous method with a much longer reaction time and many more steps [158]. The four steps of the reaction to synthesize PLA-Dex-g-PBA involving the semi-solid state chemistry were verified using NMR (Figure 34). The semi-solid state method provides an alternative approach in chemically modifying carbohydrates that is fast, simple, and tunable. We demonstrated that this new method can be incorporated into existing block copolymer synthesis methods to significantly speed up and simplify the fabrication process without compromising the conjugation efficiency of grafting the ligands onto the backbone of carbohydrates.

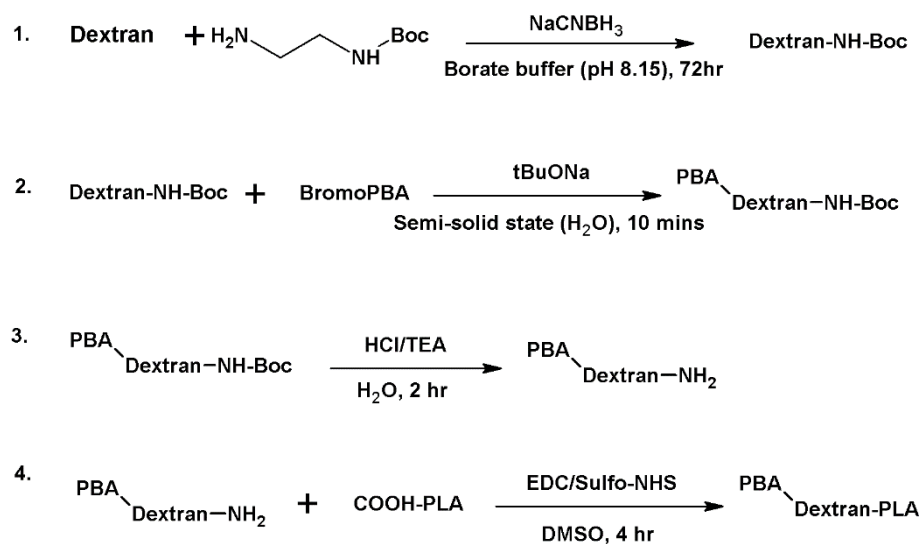


**Figure 33. Reaction scheme: application of the semi-solid state method in synthesizing a block copolymer between BPBA modified dextran and poly(D,L-lactide) (PLA).**

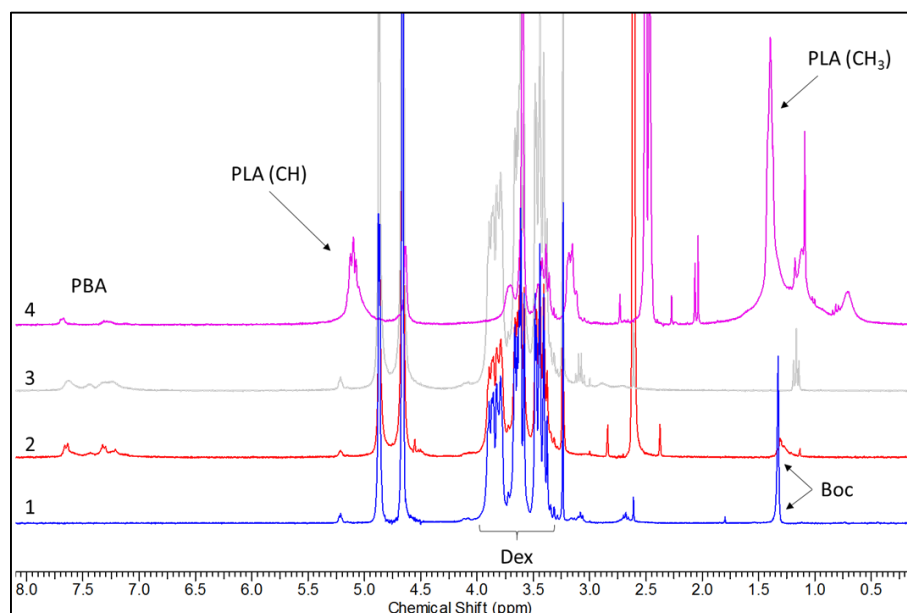


**Figure 34.  $^1\text{H}$  NMR analysis of the all 4 steps on the PLA-Dex block copolymer synthesis with BPBA grafted dextran. Note that  $\text{D}_2\text{O}$  was used for analysis on the products of steps 1 to 3, and  $\text{DMSO-d}_6$  was used for the analysis of product on step 4.**

## 7.6 Conclusion

Due to the rapid advances in the use of carbohydrates in a wide range of biomedical applications, there is a need for simple and rapid method to chemically modify the carbohydrates to achieve various functionalities. We developed a semi-solid state reaction method to chemically modify carbohydrates in a simple and rapid manner. The method benefits from the rapid reaction rates associated with conventional solid-state chemistry while avoiding the need of high reaction temperatures by adding a small amount of water to act as “plasticizer”. By using dextran as a model carbohydrate, we demonstrated conjugation of BPBA onto dextran within 10 minutes of the reaction at temperatures between 70 to 110 °C. By tuning the reaction temperature and the ratios of the reactants, we showed that the semi-solid state method provides a wide range of tunability to achieve desired conjugation densities on dextran. To demonstrate the applicability of this new method, we incorporated the semi-solid state reaction into our existing block copolymer synthesis between PLA and BPBA modified dextran. The new method achieved similar properties using much shorter reaction duration with significantly reduced number of steps. We believe that this novel semi-solid state chemistry can be used for many different carbohydrates to significantly broaden their scope of application in the field of biomedical engineering.

## Chapter 8

### Conclusions and Future Work

#### 8.1 Summary

This thesis presents the development of a nanoparticle (NP) drug delivery system to enhance the ocular surface retention of therapeutics delivered to the anterior segment of the eye. The NPs were comprised of amphiphilic block copolymers formed between dextran and poly(D,L-lactide). The surfaces of the NPs were chemically modified with phenylboronic acid, which can covalently bind to diol groups that are commonly found in ocular mucous membranes, for mucoadhesive targeting. The NPs showed mucoadhesive properties and were able to release the therapeutically relevant dosage of Cyclosporine A (CsA), a drug commonly used to treat dry eye syndrome, for up to 5 days *in vitro*. The weekly administration of NPs containing CsA showed biocompatibility and efficacy in treating experimental dry eye in animal models. The dosage of CsA in the NP formulation was optimized to 50- to 100-fold less than the commercial product, Restasis®, in the long term treatment of experimental dry eye in mice, successfully eliminating inflammation as well as recovering the ocular surface goblet cells. Thrice daily treatments using Restasis® in the same experiment were only able to eliminate the inflammation without recovering the ocular surface integrity. The mucoadhesive property of the NPs was further demonstrated in animal models by showing prolonged ocular retention of a fluorescent dye delivered topically to the eyes using the same NPs. Finally, to demonstrate the feasibility of the NP formulation to advance to clinical trials, we developed a semi-solid state reaction process to synthesize the building block of the NPs – the block copolymer with phenylboronic acid grafted on the dextran – in a simple, fast, and scalable manner.

#### 8.2 Conclusions

NP drug carriers were formed by a self-assembly process of an amphiphilic block copolymer in a controlled environment. For this thesis, we synthesized an amphiphilic block copolymer by covalently linking two polymers: poly(D,L-lactide) (PLA), a biodegradable biomaterial, and dextran, a natural polysaccharide that has an abundance of functional groups for surface modification of the NPs to achieve desired surface properties. The sizes of the NPs were in the sub-100 nm range and were tuneable based on the molecular weight of the PLA and/or dextran used to form the block copolymer.

The surfaces of the self-assembled polymeric NPs were chemically modified using phenylboronic acid (PBA) for mucous membrane targeted delivery of nanoparticle drug carriers. The amount of PBA per dextran monomer was tuneable by changing the initial reaction conditions. The PBA-modified nanoparticles demonstrated two to five times improvement in mucoadhesion compared with other types of mucoadhesive particles reported in the literature, such as chitosan or thiol-modified particles, in an *in vitro* study. The PBA-modified NPs encapsulated clinically relevant doses of CsA and released them in a sustained manner for up to 5 days *in vitro*. The results from this study demonstrated the potential of the mucoadhesive NPs as a drug delivery platform to drastically improve the ocular retention time of the drugs on the ocular surface.

After demonstrating the feasibility of the PBA-modified NPs as a potential eye drop delivery platform, we further evaluated the performance of these nanoparticles using an *in vivo* environment as a proof-of-concept demonstration. The once weekly dosing of CsA-encapsulating, PBA-modified NPs to rabbits showed no physical signs of irritation or discomfort, and also did not show any inflammatory responses in post-euthanasia histopathology analysis. The same once weekly dosing of PBA-modified NPs with CsA demonstrated effective treatment of dry eye in mice by eliminating ocular inflammation as well as restoring ocular surface goblet cells. In the same study, the commercial product of CsA, Restasis®, only showed elimination of ocular inflammation without showing the recovery of ocular surface goblet cells. These promising results led us to further investigate the pharmacokinetic properties of these formulations to find the optimal dosage of the NP formulation for long term treatment of dry eye.

In a subsequent study, we studied the ocular surface retention of drugs following delivery through the PBA-modified NPs. A near-infrared fluorescent dye, indocyanine green (ICG), was used as a model drug to mimic the topical delivery of drugs using PBA-modified NPs. ICG delivered using the PBA-modified NPs demonstrated ocular retention for up to 24 hours, whereas the ICG delivered without the NPs only remained for up to 3 hours.

We further reduced the dosage of the Cyclosporine A in the NPs to determine their effect on the long term treatment of dry eye in mice. Restasis® and NPs carrying 21-fold lower dosage of CsA compared to that of Restasis® both showed elimination of ocular inflammation but also failed to recover ocular surface integrity. NPs carrying 50- to 100-fold lower dosage of CsA with respect to Restasis® showed both the elimination of ocular inflammation and the full recovery of ocular surface integrity, including



restoration of ocular surface goblet cells. All the results thus far demonstrate the feasibility of the PBA-modified NPs to move forward into clinical trials.

One of the key requirements to meet to go into clinical trials is to have a scalable manufacturing process that can meet the standards posed by the Food and Drug Administration (FDA). Since the procedure that we introduced in Chapter 4 is not easily scalable, we developed a new process that can synthesize the PBA modified PLA-Dex block copolymer in a fast, simple, and scalable manner using a semi-solid reaction mechanism. The amount of PBA grafted onto the dextran backbone was tuneable by changing the reaction temperature and the duration, as well as the ratio of ingredients in the reaction. Within 10 minutes of reaction, the semi-solid state process yielded PBA/dextran with a conjugation efficiency comparable to the method developed in Chapter 4.

### **8.3 Recommendations for future work**

The following research and development tasks are recommended based on the conclusions drawn from this thesis to further advance this project into clinical trials and beyond:

1. Demonstrate the manufacturing process of the NP-drug eye drop formulation with an acceptable shelf-life. Chapter 7 describes the process for synthesizing the block copolymers in a scalable manner. The next task is to develop a manufacturing process for the final NP-drug eye drop formulation in a scalable process with an acceptable shelf-life, depending on the drug of choice.
2. Investigate the pharmacokinetic and ocular biodistribution of drugs delivered through mucoadhesive NPs. In addition to investigating the ocular surface retention of drugs delivered using the NP formulation, we must also investigate how the drugs are distributed on the ocular surface and how much of it penetrates deep into the ocular tissues and perhaps ends up in the blood stream. These are key questions to address in order to understand the biocompatibility of the formulation and to optimize the dosage of the drugs in the formulation to treat various ocular diseases.
3. Demonstrate good manufacturing practice (GMP) process for formulating the NP eye drops as well as good laboratory practice (GLP) level safety and efficacy studies using the NP eye drop formulation. GMP level production of the formulation and GLP studies to demonstrate the biocompatibility and the efficacy in treatment are key factors in determining the approval of the formulation to advance to the clinical stage.

4. Optimize the drug dose and the dosing frequency of the NP formulation from the GLP studies. Once GLP studies have demonstrated the safety and efficacy, another key question to address is the optimal drug concentration and its administration frequency to treat ocular diseases.
5. Submit an investigational new drug (IND) application to obtain approval to perform clinical trial phases I, II, and III. With the successful completion of all the studies described above, we can submit the IND application with all the necessary data for approval from the appropriate government agencies to proceed to the clinical trials.

## Appendix A

### Covalent linkage between phenylboronic acid and sialic acid for mucoadhesive targeting

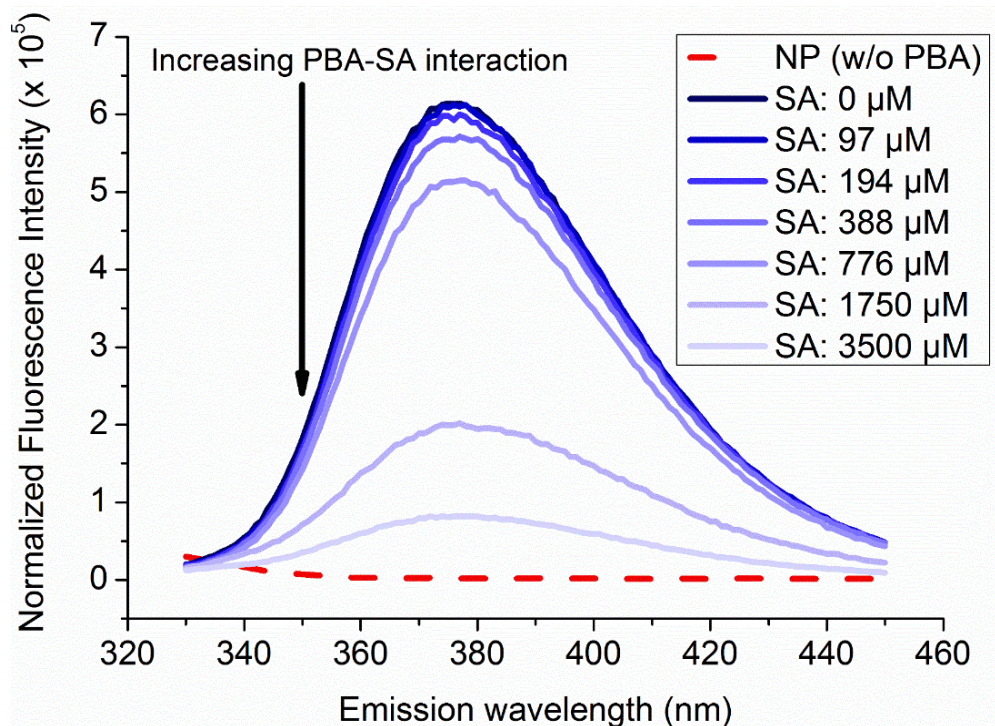


**Figure 35. Verification of covalent complexation between the phenylboronic acid (PBA) on the PLA-Dex NPs with sialic acid. The intrinsic fluorescence of PBA (excitation: 288 nm; emission 376 nm) is quenched in the presence of sialic acid (SA) due to the covalent complexation between PBA and sialic acid.**

## Bibliography

- [1] Liu, S.; Jones, L.; Gu, F. X. Nanomaterials for ocular drug delivery. *Macromol Biosci.* **2012**, *5*, 608-620.
- [2] Gulsen, D. and Chauhan, A. Dispersion of microemulsion drops in HEMA hydrogel: A potential ophthalmic drug delivery vehicle. *Int. J. Pharm.* **2005**, *1-2*, 95-117.
- [3] Shen, J.; Wang, Y.; Ping, Q.; Xiao, Y.; Huang, X. Mucoadhesive effect of thiolated PEG stearate and its modified NLC for ocular drug delivery. *J. Controlled Release* **2009**, *3-4*, 217-223.
- [4] Verma, M. S.; Liu, S.; Chen, Y. Y.; Meerasa, A.; Gu, F. X. Size-tunable nanoparticles composed of dextran-b-poly(D,L-lactide) for drug delivery applications. *Nano Res.* **2012**, *1*, 49-61.
- [5] Dogru, M. and Tsubota, K. Pharmacotherapy of dry eye. *Expert Opin. Pharmacother.* **2011**, *3*, 325-334.
- [6] Gaudana, R.; Jwala, J.; Boddu, S. H. S.; Mitra, A. K. Recent perspectives in ocular drug delivery. *Pharm Res.* **2009**, *5*, 1197-1216.
- [7] Diebold, Y. and Calonge, M. Applications of nanoparticles in ophthalmology. *Prog Retin Eye Res.* **2010**, *6*, 596-609.
- [8] Lee, V. H. and Robinson, J. R. Topical ocular drug delivery: Recent developments and future challenges. *J. Ocul. Pharmacol.* **1986**, *1*, 67-108.
- [9] Lee, V. H. L. Review - new directions in the optimization of ocular drug delivery. *J. Ocul. Pharmacol.* **1990**, *2*, 157-164.
- [10] Zimmer, A. and Kreuter, J. Microspheres and nanoparticles used in ocular delivery systems. *Adv. Drug Deliv. Rev.* **1995**, *1*, 61-73.
- [11] Bejjani, R. A.; Behar-Cohen, F.; Benezra, D.; Gurny, R.; Delie, F. Polymeric nanoparticles for drug delivery to the posterior segment of the eye. *Chimia* **2005**, *6*, 344-347.
- [12] Nagarwal, R. C.; Kant, S.; Singh, P. N.; Maiti, P.; Pandit, J. K. Polymeric nanoparticulate system: A potential approach for ocular drug delivery. *J. Controlled Release* **2009**, *1*, 2-13.
- [13] Tong, Y.; Chang, S.; Liu, C.; Kao, W. W. -; Huang, C. H.; Liaw, J. Eye drop delivery of nanopolymeric micelle formulated genes with cornea-specific promoters. *J. Gene Med.* **2007**, *11*, 956-966.
- [14] Wadhwa, S.; Paliwal, R.; Paliwal, S. R.; Vyas, S. P. Nanocarriers in ocular drug delivery: An update review. *Curr Pharm Des.* **2009**, *23*, 2724-2750.
- [15] Zarbin, M. A.; Montemagno, C.; Leary, J. F.; Ritch, R. Nanomedicine in ophthalmology: The new frontier. *Am. J. Ophthalmol.* **2010**, *2*, 144-162.
- [16] Hughes, P. M.; Olejnik, O.; Chang-Lin, J. E.; Wilson, C. G. Topical and systemic drug delivery to the posterior segments. *Adv. Drug Deliv. Rev.* **2005**, *14*, 2010-2032.
- [17] Peng, C. C.; Bengani, L. C.; Jung, H. J.; Leclerc, J.; Gupta, C.; Chauhan, A. Emulsions and microemulsions for ocular drug delivery. *Journal of Drug Delivery Science and Technology* **2011**, *1*, 111-121.
- [18] del Amo, E. M. and Urtti, A. Current and future ophthalmic drug delivery systems. A shift to the posterior segment. *Drug Discov. Today* **2008**, *3-4*, 135-143.
- [19] Yasukawa, T.; Ogura, Y.; Tabata, Y.; Kimura, H.; Wiedemann, P.; Honda, Y. Drug delivery systems for vitreoretinal diseases. *Prog. Retin. Eye Res.* **2004**, *3*, 253-281.
- [20] Harder, B. C.; Baltz, S.; Jonas, J. B.; Schlichtenbrede, F. C. Intravitreal bevacizumab for retinopathy of prematurity. *J Ocul Pharmacol Ther.* **2011**, *9/1/2011*,

- [21] Kolomeyer, A. M.; Roy, M. S.; Chu, D. S. The use of intravitreal ranibizumab for choroidal neovascularization associated with vogt-koyanagi-harada syndrome. *Case reports in medicine* **2011**, 747648.
- [22] Ranta, V.; Mannermaa, E.; Lummeppuro, K.; Subrizi, A.; Laukkanen, A.; Antopolsky, M.; Murtomaki, L.; Hornof, M.; Urtili, A. Barrier analysis of periocular drug delivery to the posterior segment. *J. Controlled Release* **2010**, *1*, 42-48.
- [23] Ciolino, J. B.; Dohlman, C. H.; Kohane, D. S. Contact lenses for drug delivery. *Semin. Ophthalmol.* **2009**, *3*, 156-160.
- [24] Lavik, E.; Kuehn, M. H.; Kwon, Y. H. Novel drug delivery systems for glaucoma. *Eye* **2011**, *5*, 578-586.
- [25] Weiner, A. L. and Gilger, B. C. Advancements in ocular drug delivery. *Vet. Ophthalmol.* **2010**, *6*, 395-406.
- [26] Fonn, D. Targeting contact lens induced dryness and discomfort: What properties will make lenses more comfortable. *Optometry Vision Sci.* **2007**, *4*, 279-285.
- [27] Li, C. C. and Chauhan, A. Modeling ophthalmic drug delivery by soaked contact lenses. *Ind Eng Chem Res* **2006**, *10*, 3718-3734.
- [28] Ciolino, J. B.; Hoare, T. R.; Iwata, N. G.; Behlau, I.; Dohlman, C. H.; Langer, R.; Kohane, D. S. A drug-eluting contact lens. *Invest. Ophthalmol. Vis. Sci.* **2009**, *7*, 3346-3352.
- [29] Gulsen, D.; Li, C. C.; Chauhan, A. Dispersion of DMPC liposomes in contact lenses for ophthalmic drug delivery. *Curr. Eye Res.* **2005**, *12*, 1071-1080.
- [30] Jimenez, N.; Galan, J.; Vallet, A.; Egea, M. A.; Garcia, M. L. Methyl trypsin loaded poly(D,L-lactide-coglycolide) nanoparticles for contact lens care. *J. Pharm. Sci.* **2010**, *3*, 1414-1426.
- [31] Kapoor, Y. and Chauhan, A. Drug and surfactant transport in cyclosporine A and brij 98 laden p-HEMA hydrogels. *J. Colloid Interface Sci.* **2008**, *2*, 624-633.
- [32] Sahoo, S. K.; Diinawaz, F.; Krishnakumar, S. Nanotechnology in ocular drug delivery. *Drug Discov Today.* **2008**, *3-4*, 144-151.
- [33] Zimmer, A. and Kreuter, J. Microspheres and nanoparticles used in ocular delivery systems. *Adv. Drug Deliv. Rev.* **1995**, *1*, 61-73.
- [34] Hamidi, M.; Azadi, A.; Rafiei, P. Hydrogel nanoparticles in drug delivery. *Adv. Drug Deliv. Rev.* **2008**, *15*, 1638-1649.
- [35] Ludwig, A. The use of mucoadhesive polymers in ocular drug delivery. *Adv. Drug Deliv. Rev.* **2005**, *11*, 1595-1639.
- [36] Kuno, N. and Fujii, S. Recent advances in ocular drug delivery systems *Polymers* **2011**, *1*, 193-221.
- [37] Volotinen, M.; Maenpaa, J.; Kautiainen, H.; Tolonen, A.; Uusitalo, J.; Ropo, A.; Vapaatalo, H.; Aine, E. Ophthalmic timolol in a hydrogel vehicle leads to minor inter-individual variation in timolol concentration in aqueous humor. *European Journal of Pharmaceutical Sciences* **2009**, *2-3*, 292-296.
- [38] Parkinson, T. M.; Ferguson, E.; Febbraro, S.; Bakhtyari, A.; King, M.; Mundasad, M. Tolerance of ocular iontophoresis in healthy volunteers. *Journal of Ocular Pharmacology and Therapeutics* **2003**, *2*, 145-151.
- [39] Eljarrat-Binstock, E. and Domb, A. J. Iontophoresis: A non-invasive ocular drug delivery. *J. Controlled Release* **2006**, *3*, 479-489.
- [40] Eljarrat-Binstock, E.; Orucov, F.; Frucht-Pery, J.; Pe'er, J.; Domb, A. J. Methylprednisolone delivery to the back of the eye using hydrogel iontophoresis. *Journal of Ocular Pharmacology and Therapeutics* **2008**, *3*, 344-350.

- [41] Eljarrat-Binstock, E.; Orucov, F.; Aldouby, Y.; Frucht-Pery, J.; Domb, A. J. Charged nanoparticles delivery to the eye using hydrogel iontophoresis. *J. Controlled Release* **2008**, *2*, 156-161.
- [42] Gaucher, G.; Marchessault, R. H.; Leroux, J. Polyester-based micelles and nanoparticles for the parenteral delivery of taxanes. *J. Controlled Release* **2010**, *1*, 2-12.
- [43] Molokhia, S. A.; Jeong, E.; Higuchi, W. I.; Li, S. K. Transscleral iontophoretic and intravitreal delivery of a macromolecule: Study of ocular distribution in vivo and postmortem with MRI. *Exp. Eye Res.* **2009**, *3*, 418-425.
- [44] Gonzalez, J. R.; Baiza-Duran, L.; Quintana-Hau, J.; Tornero-Montano, R.; Castaneda-Hernandez, G.; Ortiz, M.; Alarcon-Oceguera, F.; Beltran-Loustaunau, M.; Cortez-Gastelum, M.; Garciduenas-Mejia, J., et al. Comparison of the stability, efficacy, and adverse effect profile of the innovator 0.005% latanoprost ophthalmic solution and a novel cyclodextrin-containing formulation. *J. Clin. Pharmacol.* **2007**, *1*, 121-126.
- [45] Gudmundsdottir, E.; Stefansson, E.; Bjarnadottir, G.; Sigurjonsdottir, J. F.; Gudmundsdottir, G.; Masson, M.; Loftsson, T. Methazolamide 1% in cyclodextrin solution lowers IOP in human ocular hypertension. *Invest. Ophthalmol. Vis. Sci.* **2000**, *11*, 3552-4.
- [46] Cardillo, J. A.; Souza-Filho, A. A.; Oliveira, A. G. Intravitreal bioerudivel sustained-release triamcinolone microspheres system (RETAAC). preliminary report of its potential usefulness for the treatment of diabetic macular edema. *Arch. Soc. Esp. Oftalmol.* **2006**, *12*, 675.
- [47] Rafie, F.; Javadzadeh, Y.; Javadzadeh, A. R.; Ghavidel, L. A.; Jafari, B.; Moogooee, M.; Davaran, S. In vivo evaluation of novel nanoparticles containing dexamethasone for ocular drug delivery on rabbit eye. *Curr. Eye Res.* **2010**, *12*, 1081-1089.
- [48] Pepic, I.; Hafner, A.; Lovric, J.; Pirkic, B.; Filipovic-Grcic, J. A nonionic Surfactant/Chitosan micelle system in an innovative eye drop formulation. *J. Pharm. Sci.* **2010**, *10*, 4317-4325.
- [49] Di Tommaso, C.; Torriglia, A.; Furrer, P.; Behar-Cohen, F.; Gurny, R.; Moller, M. Ocular biocompatibility of novel cyclosporin A formulations based on methoxy poly(ethylene glycol)-hexylsubstituted poly(lactide) micelle carriers. *Int. J. Pharm.* **2011**, *2*, 515-24.
- [50] Civiale, C.; Licciardi, M.; Cavallaro, G.; Giammona, G.; Mazzone, M. G. Polyhydroxyethylaspartamide-based micelles for ocular drug delivery. *Int. J. Pharm.* **2009**, *1-2*, 177-186.
- [51] Gonzalez-Mira, E.; Egea, M. A.; Garcia, M. L.; Souto, E. B. Design and ocular tolerance of flurbiprofen loaded ultrasound-engineered NLC. *Colloids and Surfaces B-Biointerfaces* **2010**, *2*, 412-421.
- [52] Abdelbary, G. Ocular ciprofloxacin hydrochloride mucoadhesive chitosan-coated liposomes. *Pharm Dev Technol.* **2011**, *1*, 44-56.
- [53] Habib, F. S.; Fouad, E. A.; Abdel-Rhman, M. S.; Fathalla, D. Liposomes as an ocular delivery system of fluconazole: In-vitro studies. *Acta Ophthalmol.* **2010**, *8*, 901-904.
- [54] Mehanna, M. M.; Elmaradny, H. A.; Samaha, M. W. Mucoadhesive liposomes as ocular delivery system: Physical, microbiological, and in vivo assessment. *Drug Dev. Ind. Pharm.* **2010**, *1*, 108-118.
- [55] Abrishami, M.; Zarei-Ghanavati, S.; Soroush, D.; Rouhbakhsh, M.; Jaafari, M. R.; Malaekheh-Nikouei, B. Preparation, characterization, and in vivo evaluation of nanoliposomes-encapsulated bevacizumab (avastin) for intravitreal administration (vol 29, pg 699, 2009). *Retina-the Journal of Retinal and Vitreous Diseases* **2011**, *1*, 205-205.
- [56] Vandamme, T. F. and Brobeck, L. Poly(amidoamine) dendrimers as ophthalmic vehicles for ocular delivery of pilocarpine nitrate and tropicamide. *J. Controlled Release* **2005**, *1*, 23-38.
- [57] Spataro, G.; Malecaze, F.; Turrin, C.; Soler, V.; Duhayon, C.; Elena, P.; Majoral, J.; Caminade, A. Designing dendrimers for ocular drug delivery. *Eur. J. Med. Chem.* **2010**, *1*, 326-334.

- [58] Cho, H. K.; Cheong, I. W.; Lee, J. M.; Kim, J. H. Polymeric nanoparticles, micelles and polymersomes from amphiphilic block copolymer. *Korean J Chem Eng.* **2010**, *3*, 731-740.
- [59] Gaucher, G.; Dufresne, M. H.; Sant, V. P.; Kang, N.; Maysinger, D.; Leroux, J. C. Block copolymer micelles: Preparation, characterization and application in drug delivery. *J. Controlled Release* **2005**, *1-3*, 169-188.
- [60] Jagur-Grodzinski, J. Polymers for targeted and/or sustained drug delivery. *Polym. Adv. Technol.* **2009**, *7*, 595-606.
- [61] Kim, D. K. and Dobson, J. Nanomedicine for targeted drug delivery. *Journal of Materials Chemistry* **2009**, *35*, 6294-6307.
- [62] Onaca, O.; Enea, R.; Hughes, D. W.; Meier, W. Stimuli-responsive polymersomes as nanocarriers for drug and gene delivery. *Macromolecular Bioscience* **2009**, *2*, 129-139.
- [63] Soppimath, K. S.; Aminabhavi, T. M.; Kulkarni, A. R.; Rudzinski, W. E. Biodegradable polymeric nanoparticles as drug delivery devices. *J. Controlled Release* **2001**, *1-2*, 1-20.
- [64] Ayalasonmayajula, S. P. and Kompella, U. B. Subconjunctivally administered celecoxib-PLGA microparticles sustain retinal drug levels and alleviate diabetes-induced oxidative stress in a rat model. *Eur. J. Pharmacol.* **2005**, *2-3*, 191-198.
- [65] Barcia, E.; Herrero-Vanrell, R.; Diez, A.; Alvarez-Santiago, C.; Lopez, I.; Calonge, M. Downregulation of endotoxin-induced uveitis by intravitreal injection of polylactic-glycolic acid (PLGA) microspheres loaded with dexamethasone. *Exp. Eye Res.* **2009**, *2*, 238-245.
- [66] Cleland, J. L.; Duenas, E. T.; Park, A.; Daugherty, A.; Kahn, J.; Kowalski, J.; Cuthbertson, A. Development of poly-(D,L-lactide-coglycolide) microsphere formulations containing recombinant human vascular endothelial growth factor to promote local angiogenesis. *J. Controlled Release* **2001**, *1-3*, 13-24.
- [67] Gavini, E.; Chetoni, P.; Cossu, M.; Alvarez, M. G.; Saettone, M. F.; Giunchedi, P. PLGA microspheres for the ocular delivery of a peptide drug, vancomycin using emulsification/spray-drying as the preparation method: In vitro/in vivo studies. *Eur J Pharm Biopharm.* **2004**, *2*, 207-212.
- [68] Gupta, H.; Aqil, M.; Khar, R. K.; Ali, A.; Bhatnagar, A.; Mittal, G. Sparfloxacin-loaded PLGA nanoparticles for sustained ocular drug delivery. *Nanomed-nanotechnol.* **2010**, *2*, 324-333.
- [69] Qaddoumi, M. G.; Ueda, H.; Yang, J.; Davda, J.; Labhasetwar, V.; Lee, V. H. L. The characteristics and mechanisms of uptake of PLGA nanoparticles in rabbit conjunctival epithelial cell layers. *Pharm. Res.* **2004**, *4*, 641-648.
- [70] De Campos, A. M.; Sanchez, A.; Gref, R.; Calvo, P.; Alonso, M. J. The effect of a PEG versus a chitosan coating on the interaction of drug colloidal carriers with the ocular mucosa. *European Journal of Pharmaceutical Sciences* **2003**, *1*, 73-81.
- [71] Pepic, I.; Jalsenjak, N.; Jalsenjak, I. Micellar solutions of triblock copolymer surfactants with pilocarpine. *Int. J. Pharm.* **2004**, *1-2*, 57-64.
- [72] Liaw, J.; Chang, S. F.; Hsiao, F. C. In vivo gene delivery into ocular tissues by eye drops of poly(ethylene oxide)-poly(propylene oxide)-poly(ethylene oxide) (PEO-PPO-PEO) polymeric micelles. *Gene Ther.* **2001**, *13*, 999-1004.
- [73] Kadam, Y.; Yerramilli, U.; Bahadur, A. Solubilization of poorly water-soluble drug carbamezapine in pluronic (R) micelles: Effect of molecular characteristics, temperature and added salt on the solubilizing capacity. *Colloids and Surfaces B-Biointerfaces* **2009**, *1*, 141-147.
- [74] Gupta, A. K.; Madan, S.; Majumdar, D. K.; Maitra, A. Ketorolac entrapped in polymeric micelles: Preparation, characterisation and ocular anti-inflammatory studies. *Int. J. Pharm.* **2000**, *1-2*, 1-14.

- [75] Roy, S.; Zhang, K.; Roth, T.; Vinogradov, S.; Kao, R. S.; Kabanov, A. Reduction of fibronectin expression by intravitreal administration of antisense oligonucleotides. *Nat. Biotechnol.* **1999**, *5*, 476-479.
- [76] Bourges, J. L.; Gautier, S. E.; Delie, F.; Bejjani, R. A.; Jeanny, J. C.; Gurny, R.; BenEzra, D.; Behar-Cohen, F. F. Ocular drug delivery targeting the retina and retinal pigment epithelium using polylactide nanoparticles. *Invest. Ophthalmol. Vis. Sci.* **2003**, *8*, 3562-3569.
- [77] Qu, X.; Khutoryanskiy, V. V.; Stewart, A.; Rahman, S.; Papahadjopoulos-Sternberg, B.; Dufes, C.; McCarthy, D.; Wilson, C. G.; Lyons, R.; Carter, K. C., et al. Carbohydrate-based micelle clusters which enhance hydrophobic drug bioavailability by up to 1 order of magnitude. *Biomacromolecules* **2006**, *12*, 3452-3459.
- [78] Sasaki, H.; Yamamura, K.; Mukai, T.; Nishida, K.; Nakamura, J.; Nakashima, M.; Ichikawa, M. Enhancement of ocular drug penetration. *Crit. Rev. Ther. Drug Carrier Syst.* **1999**, *1*, 85-146.
- [79] SaarinenSavolainen, P.; Jarvinen, T.; Suhonen, P.; Urtti, A. Amphiphilic properties of pilocarpine prodrugs. *Int. J. Pharm.* **1996**, *1-2*, 171-178.
- [80] Kawakami, S.; Nishida, K.; Mukai, T.; Yamamura, K.; Nakamura, J.; Sakaeda, T.; Nakashima, M.; Sasaki, H. Controlled release and ocular absorption of tilisolol utilizing ophthalmic insert-incorporated lipophilic prodrugs. *J. Controlled Release* **2001**, *3*, 255-263.
- [81] Tu, J.; Pang, H.; Yan, Z.; Li, P. Ocular permeability of pirenzepine hydrochloride enhanced by methoxy poly(ethylene glycol)-poly(D, L-lactide) block copolymer. *Drug Dev. Ind. Pharm.* **2007**, *10*, 1142-1150.
- [82] Gupta, P.; Vermani, K.; Garg, S. Hydrogels: From controlled release to pH-responsive drug delivery. *Drug Discov. Today* **2002**, *10*, 569-579.
- [83] Hoare, T. R. and Kohane, D. S. Hydrogels in drug delivery: Progress and challenges. *Polymer* **2008**, *8*, 1993-2007.
- [84] Barbu, E.; Verestiuc, L.; Iancu, M.; Jatariu, A.; Lungu, A.; Tsibouklis, J. Hybrid polymeric hydrogels for ocular drug delivery: Nanoparticulate systems from copolymers of acrylic acid-functionalized chitosan and N-isopropylacrylamide or 2-hydroxyethyl methacrylate. *Nanotechnology* **2009**, *22*, 225108.
- [85] Peniche, H. and Peniche, C. Chitosan nanoparticles: A contribution to nanomedicine. *Polym Int.* **2011**, *6*, 883-889.
- [86] El-Kamel, A. H. In vitro and in vivo evaluation of pluronic F127-based ocular delivery system for timolol maleate. *Int. J. Pharm.* **2002**, *1*, 47-55.
- [87] Ma, W.; Xu, H.; Wang, C.; Nie, S.; Pan, W. Pluronic F127-g-poly(acrylic acid) copolymers as in situ gelling vehicle for ophthalmic drug delivery system. *Int. J. Pharm.* **2008**, *1-2*, 247-256.
- [88] du Toit, L. C.; Pillay, V.; Choonara, Y. E.; Govender, T.; Carmichael, T. Ocular drug delivery - a look towards nanobioadhesives. *Expert Opinion on Drug Delivery* **2011**, *1*, 71-94.
- [89] Law, S. L.; Huang, K. J.; Chiang, C. H. Acyclovir-containing liposomes for potential ocular delivery. corneal penetration and absorption. *J. Controlled Release* **2000**, *1-2*, 135-140.
- [90] Diebold, Y.; Jarrin, M.; Saez, V.; Carvalho, E. L. S.; Orea, M.; Calonge, M.; Seijo, B.; Alonso, M. J. Ocular drug delivery by liposome-chitosan nanoparticle complexes (LCS-NP). *Biomaterials* **2007**, *8*, 1553-1564.
- [91] Li, N.; Zhuang, C.; Wang, M.; Sun, X.; Nie, S.; Pan, W. Liposome coated with low molecular weight chitosan and its potential use in ocular drug delivery. *Int J Pharm.* **2009**, *1*, 131-138.
- [92] Wang, S.; Zhang, J.; Jiang, T.; Zheng, L.; Wang, Z.; Zhang, J.; Yu, P. Protective effect of coenzyme Q(10) against oxidative damage in human lens epithelial cells by novel ocular drug carriers. *Int. J. Pharm.* **2011**, *1-2*, 219-229.



- [93] Hosny, K. M. Preparation and evaluation of thermosensitive liposomal hydrogel for enhanced transcorneal permeation of ofloxacin. *Aaps Pharmscitech* **2009**, *4*, 1336-1342.
- [94] Hironaka, K.; Inokuchi, Y.; Tozuka, Y.; Shimazawa, M.; Hara, H.; Takeuchi, H. Design and evaluation of a liposomal delivery system targeting the posterior segment of the eye. *J. Controlled Release* **2009**, *3*, 247-253.
- [95] Abdelbary, G. and El-gendy, N. Niosome-encapsulated gentamicin for ophthalmic controlled delivery. *Aaps Pharmscitech* **2008**, *3*, 740-747.
- [96] Vyas, S. P.; Mysore, N.; Jaitely, V.; Venkatesan, N. Discoidal niosome based controlled ocular delivery of timolol maleate. *Pharmazie* **1998**, *7*, 466-469.
- [97] Prabu, P.; Chaudhari, A. A.; Aryal, S.; Dharmaraj, N.; Park, S. Y.; Kim, W. D.; Kim, H. Y. In vitro evaluation of poly(caporlactone) grafted dextran (PGD) nanoparticles with cancer cell. *Journal of Materials Science-Materials in Medicine* **2008**, *5*, 2157-2163.
- [98] Kaur, I. P.; Aggarwal, D.; Singh, H.; Kakkar, S. Improved ocular absorption kinetics of timolol maleate loaded into a bioadhesive niosomal delivery system. *Graefes Archive for Clinical and Experimental Ophthalmology* **2010**, *10*, 1467-1472.
- [99] Cheng, Y.; Xu, Z.; Ma, M.; Xu, T. Dendrimers as drug carriers: Applications in different routes of drug administration. *J. Pharm. Sci.* **2008**, *1*, 123-143.
- [100] Yao, W.; Sun, K.; Mu, H.; Liang, N.; Liu, Y.; Yao, C.; Liang, R.; Wang, A. Preparation and characterization of puerarin-dendrimer complexes as an ocular drug delivery system. *Drug Dev. Ind. Pharm.* **2010**, *9*, 1027-1035.
- [101] Durairaj, C.; Kadam, R. S.; Chandler, J. W.; Hutcherson, S. L.; Kompella, U. B. Nanosized dendritic polyguanidylated translocators for enhanced solubility, permeability, and delivery of gatifloxacin. *Invest. Ophthalmol. Vis. Sci.* **2010**, *11*, 5804-5816.
- [102] Loftsson, T. and Jarvinen, T. Cyclodextrins in ophthalmic drug delivery. *Adv. Drug Deliv. Rev.* **1999**, *1*, 59-79.
- [103] Conway, B. R. Recent patents on ocular drug delivery systems. *Recent patents on drug delivery & formulation* **2008**, *1*, 1-8.
- [104] Kaur, I. P.; Chhabra, S.; Aggarwal, D. Role of cyclodextrins in ophthalmics. *Current drug delivery* **2004**, *4*, 351-60.
- [105] Totterman, A. M.; Schipper, N. G. M.; Thompson, D. O.; Mannermaa, J. P. Intestinal safety of water-soluble beta-cyclodextrins in paediatric oral solutions of spironolactone: Effects on human intestinal epithelial caco-2 cells. *J. Pharm. Pharmacol.* **1997**, *1*, 43-48.
- [106] Loftsson, T. and Stefansson, E. Effect of cyclodextrins on topical drug delivery to the eye. *Drug Dev. Ind. Pharm.* **1997**, *5*, 473-481.
- [107] Wang, S. L.; Li, D. X.; Ito, Y.; Nabekura, T.; Wang, S. J.; Zhang, J. H.; Wu, C. F. Bioavailability and anticataract effects of a topical ocular drug delivery system containing disulfiram and hydroxypropyl-beta-cyclodextrin on selenite-treated rats. *Curr. Eye Res.* **2004**, *1*, 51-58.
- [108] Zhang, J.; Wang, L.; Gao, C.; Zhang, L.; Xia, H. Ocular pharmacokinetics of topically-applied ketoconazole solution containing hydroxypropyl beta-cyclodextrin to rabbits. *Journal of Ocular Pharmacology and Therapeutics* **2008**, *5*, 501-506.
- [109] Halim Mohamed, M. A. and Mahmoud, A. A. Formulation of indomethacin eye drops via complexation with cyclodextrins. *Curr. Eye Res.* **2011**, *3*, 208-16.
- [110] Mahmoud, A. A.; El-Feky, G. S.; Kamel, R.; Awad, G. E. A. Chitosan/sulfobutylether-beta-cyclodextrin nanoparticles as a potential approach for ocular drug delivery. *Int J Pharm.* **2011**, *1-2*, 229-236.
- [111] Jain, R. K. and Stylianopoulos, T. Delivering nanomedicine to solid tumors. *Nat. Rev. Clin. Oncol.* **2010**, *11*, 653-664.

- [112] Pridgen, E. M.; Langer, R.; Farokhzad, O. C. Biodegradable, polymeric nanoparticle delivery systems for cancer therapy. *Nanomedicine* **2007**, *5*, 669-680.
- [113] Gu, F. X.; Karnik, R.; Wang, A. Z.; Alexis, F.; Levy-Nissenbaum, E.; Hong, S.; Langer, R. S.; Farokhzad, O. C. Targeted nanoparticles for cancer therapy. *Nano Today* **2007**, *3*, 14-21.
- [114] Gref, R.; Minamitake, Y.; Peracchia, M. T.; Trubetskoy, V.; Torchilin, V.; Langer, R. Biodegradable long-circulating polymeric nanospheres. *Science* **1994**, *5153*, 1600-1603.
- [115] Dong, Y. and Feng, S. In vitro and in vivo evaluation of methoxy polyethylene glycol-poly(lactide) (MPEG-PLA) nanoparticles for small-molecule drug chemotherapy. *Biomaterials*. **2007**, *28*, 4154-4160.
- [116] Gursahani, H.; Riggs-Sauthier, J.; Pfeiffer, J.; Lechuga-Ballesteros, D.; Fishburn, C. S. Absorption of polyethylene glycol (PEG) polymers: The effect of PEG size on permeability. *J. Pharm. Sci.* **2009**, *8*, 2847-2856.
- [117] Yang, J.; Cho, E.; Seo, S.; Lee, J.; Yoon, H.; Suh, J.; Huh, Y.; Haam, S. Enhancement of cellular binding efficiency and cytotoxicity using polyethylene glycol base triblock copolymeric nanoparticles for targeted drug delivery. *J. Biomed. Mater. Res. A* **2008**, *1*, 273-280.
- [118] Wei, X.; Gong, C.; Gou, M.; Fu, S.; Guo, Q.; Shi, S.; Luo, F.; Guo, G.; Qiu, L.; Qian, Z. Biodegradable poly(epsilon-caprolactone)-poly(ethylene glycol) copolymers as drug delivery system. *Int. J. Pharm.* **2009**, *1*, 1-18.
- [119] Bazile, D.; Prudhomme, C.; Bassoulet, M. T.; Marlard, M.; Spenlehauer, G.; Veillard, M. Stealth me.peg-pla nanoparticles avoid uptake by the mononuclear phagocytes system. *J Pharm Sci.* **1995**, *4*, 493-498.
- [120] Lemarchand, C.; Gref, R.; Couvreur, P. Polysaccharide-decorated nanoparticles. *Eur. J. Pharm. Biopharm.* **2004**, *2*, 327-341.
- [121] Kailasan, A.; Yuan, Q.; Yang, H. Synthesis and characterization of thermoresponsive polyamidoamine-polyethylene glycol-poly(D,L-lactide) core-shell nanoparticles. *Acta Biomater.* **2010**, *3*, 1131-1139.
- [122] Owens, D. E. and Peppas, N. A. Opsonization, biodistribution, and pharmacokinetics of polymeric nanoparticles. *Int. J. Pharm.* **2006**, *1*, 93-102.
- [123] Cho, K.; Wang, X.; Nie, S.; Chen, Z.; Shin, D. M. Therapeutic nanoparticles for drug delivery in cancer. *Clin. Cancer. Res.* **2008**, *5*, 1310-1316.
- [124] Jiang, W.; Kim, B. Y. S.; Rutka, J. T.; Chan, W. C. W. Nanoparticle-mediated cellular response is size-dependent. *Nat. Nanotechnol.* **2008**, *3*, 145-150.
- [125] Karnik, R.; Gu, F.; Basto, P.; Cannizzaro, C.; Dean, L.; Kyei-Manu, W.; Langer, R.; Farokhzad, O. C. Microfluidic platform for controlled synthesis of polymeric nanoparticles. *Nano Lett.* **2008**, *9*, 2906-2912.
- [126] Goodwin, A. P.; Tabakman, S. M.; Welsher, K.; Sherlock, S. P.; Prencipe, G.; Dai, H. Phospholipid-dextran with a single coupling point: A useful amphiphile for functionalization of nanomaterials. *J Am Chem Soc.* **2009**, *1*, 289-296.
- [127] Nouvel, C.; Frochot, C.; Sadtler, V.; Dubois, P.; Dellacherie, E.; Six, J. L. Poly(lactide)-grafted dextrans: Synthesis and properties at interfaces and in solution. *Macromolecules* **2004**, *13*, 4981-4988.
- [128] Chittasupho, C.; Xie, S.; Baoum, A.; Yakovleva, T.; Siahaan, T. J.; Berkland, C. J. ICAM-1 targeting of doxorubicin-loaded PLGA nanoparticles to lung epithelial cells. *Eur. J. Pharm. Sci.* **2009**, *2*, 141-150.
- [129] Zahr, A. S.; Davis, C. A.; Pishko, M. V. Macrophage uptake of core-shell nanoparticles surface modified with poly(ethylene glycol). *Langmuir* **2006**, *19*, 8178-8185.

- [130] Dhar, S.; Gu, F. X.; Langer, R.; Farokhzad, O. C.; Lippard, S. J. Targeted delivery of cisplatin to prostate cancer cells by aptamer functionalized pt(IV) prodrug-PLGA-PEG nanoparticles. *Proc Natl Acad Sci U. S. A.* **2008**, *45*, 17356-17361.
- [131] Esmaeili, F.; Ghahremani, M. H.; Ostad, S. N.; Atyabi, F.; Seyedabadi, M.; Malekshahi, M. R.; Amini, M.; Dinarvand, R. Folate-receptor-targeted delivery of docetaxel nanoparticles prepared by PLGA-PEG-folate conjugate. *J Drug Target.* **2008**, *5*, 415-423.
- [132] Alpert, A. J. Hydrophilic-interaction chromatography for the separation of peptides, nucleic acids and other polar compounds. *J. Chromatogr.* **1990**, 177-196.
- [133] du Toit, L. C.; Pillay, V.; Choonara, Y. E.; Govender, T.; Carmichael, T. Ocular drug delivery - a look towards nanobioadhesives. *Expert Opin. Drug Deliv.* **2011**, *1*, 71-94.
- [134] Khutoryanskiy, V. V. Advances in mucoadhesion and mucoadhesive polymers. *Macromol Biosci.* **2011**, *6*, 748-764.
- [135] Shaikh, R.; Raj Singh, T. R.; Garland, M. J.; Woolfson, A. D.; Donnelly, R. F. Mucoadhesive drug delivery systems. *J. Pharm. Bioall.* **2011**, *1*, 89-100.
- [136] Sogias, I. A.; Williams, A. C.; Khutoryanskiy, V. V. Why is chitosan mucoadhesive? *Biomacromolecules* **2008**, *7*, 1837-1842.
- [137] Matsumoto, A.; Cabral, H.; Sato, N.; Kataoka, K.; Miyahara, Y. Assessment of tumor metastasis by the direct determination of cell-membrane sialic acid expression. *Angew Chem Int Edit.* **2010**, *32*, 5494-5497.
- [138] Matsumoto, A.; Sato, N.; Cabral, H.; Kataoka, K.; Miyahara, Y. Self-assembled molecular gate field effect transistor for label free sialic acid detection at cell membrane. *Eurosensor Xxiv Conference* **2010**, 926-929.
- [139] Matsumoto, A.; Sato, N.; Kataoka, K.; Miyahara, Y. Noninvasive sialic acid detection at cell membrane by using phenylboronic acid modified self-assembled monolayer gold electrode. *J Am Chem Soc.* **2009**, *34*, 12022-12023.
- [140] Ivanov, A. E.; Eccles, J.; Panahi, H. A.; Kumar, A.; Kuzimenkova, M. V.; Nilsson, L.; Bergenstahl, B.; Long, N.; Phillips, G. J.; Mikhalovsky, S. V., et al. Boronate-containing polymer brushes: Characterization, interaction with saccharides and mammalian cancer cells. *J Biomed Mater Res A.* **2009**, *1*, 213-225.
- [141] Liu, A.; Peng, S.; Soo, J. C.; Kuang, M.; Chen, P.; Duan, H. Quantum dots with phenylboronic acid tags for specific labeling of sialic acids on living cells. *Anal Chem.* **2011**, *3*, 1124-1130.
- [142] Otsuka, H.; Uchimura, E.; Koshino, H.; Okano, T.; Kataoka, K. Anomalous binding profile of phenylboronic acid with N-acetylneuraminic acid (Neu5Ac) in aqueous solution with varying pH. *J. Am. Chem. Soc.* **2003**, *12*, 3493-3502.
- [143] Rao, S. N. Topical cyclosporine 0.05% for the prevention of dry eye disease progression. *Journal of Ocular Pharmacology and Therapeutics* **2010**, *2*, 157-163.
- [144] Utine, C. A.; Stern, M.; Akpek, E. K. Clinical review: Topical ophthalmic use of cyclosporin A. *Ocul. Immunol. Inflamm.* **2010**, *5*, 352-361.
- [145] Shen, J.; Deng, Y.; Jin, X.; Ping, Q.; Su, Z.; Li, L. Thiolated nanostructured lipid carriers as a potential ocular drug delivery system for cyclosporine A: Improving in vivo ocular distribution. *Int. J. Pharm.* **2010**, *1-2*, 248-253.
- [146] Lee, D.; Shirley, S. A.; Lockey, R. F.; Mohapatra, S. S. Thiolated chitosan nanoparticles enhance anti-inflammatory effects of intranasally delivered theophylline. *Resp Res.* **2006**, 112.
- [147] Li, N.; Zhuang, C.; Wang, M.; Sui, C.; Pan, W. Low molecular weight chitosan-coated liposomes for ocular drug delivery: In vitro and in vivo studies. *Drug Deliv.* **2012**, *1*, 28-35.
- [148] Shen, J.; Sun, M.; Ping, Q.; Ying, Z.; Liu, W. Incorporation of liquid lipid in lipid nanoparticles for ocular drug delivery enhancement. *Nanotechnology* **2010**, *2*, 1-025101.

- [149] Yuan, X.; Li, H.; Yuan, Y. Preparation of cholesterol-modified chitosan self-aggregated nanoparticles for delivery of drugs to ocular surface. *Carbohydr. Polym.* **2006**, *3*, 337-345.
- [150] Subbiah, R.; Veerapandian, M.; Yun, K. S. Nanoparticles: Functionalization and multifunctional applications in biomedical sciences. *Curr Med Chem.* **2010**, *36*, 4559-4577.
- [151] Yoncheva, K.; Vandervoort, J.; Ludwig, A. Development of mucoadhesive poly(lactide-co-glycolide) nanoparticles for ocular application. *Pharm Dev Technol.* **2011**, *1*, 29-35.
- [152] Gao, Y.; Sun, Y.; Ren, F.; Gao, S. PLGA-PEG-PLGA hydrogel for ocular drug delivery of dexamethasone acetate. *Drug Dev Ind Pharm.* **2010**, *10*, 1131-1138.
- [153] Vega, E.; Egea, M. A.; Calpena, A. C.; Espina, M.; Garcia, M. L. Role of hydroxypropyl-beta-cyclodextrin on freeze-dried and gamma-irradiated PLGA and PLGA-PEG diblock copolymer nanospheres for ophthalmic flurbiprofen delivery. *Int J Nanomedicine.* **2012**, 1357-1371.
- [154] Yang, J.; Yan, J.; Zhou, Z.; Amsden, B. G. Dithiol-PEG-PDLLA micelles: Preparation and evaluation as potential topical ocular delivery vehicle. *Biomacromolecules.* **2014**, 1346-1354.
- [155] De Campos, A. M.; Sanchez, A.; Alonso, M. J. Chitosan nanoparticles: A new vehicle for the improvement of the delivery of drugs to the ocular surface. application to cyclosporin A. *Int J Pharm.* **2001**, *1-2*, 159-168.
- [156] Cheng, C.; Zhang, X.; Wang, Y.; Sun, L.; Li, C. Phenylboronic acid-containing block copolymers: Synthesis, self-assembly, and application for intracellular delivery of proteins. *New Journal of Chemistry* **2012**, *6*, 1413-1421.
- [157] Deshayes, S.; Cabral, H.; Ishii, T.; Miura, Y.; Kobayashi, S.; Yamashita, T.; Matsumoto, A.; Miyahara, Y.; Nishiyama, N.; Kataoka, K. Phenylboronic acid-installed polymeric micelles for targeting sialylated epitopes in solid tumors. *J. Am. Chem. Soc.* **2013**, *41*, 15501-15507.
- [158] Liu, S.; Jones, L.; Gu, F. X. Development of mucoadhesive drug delivery system using phenylboronic acid functionalized poly(D,L-lactide)-b-dextran nanoparticles. *Macromol Biosci.* **2012**, *12*, 1622-1626.
- [159] Vijay, A. K.; Sankaridurg, P.; Zhu, H.; Willcox, M. D. P. Guinea pig models of acute keratitis responses. *Cornea* **2009**, *10*, 1153-1159.
- [160] Cole, N.; Hume, E. B. H.; Vijay, A. K.; Sankaridurg, P.; Kumar, N.; Willcox, M. D. P. In vivo performance of melimine as an antimicrobial coating for contact lenses in models of CLARE and CLPU. *Invest. Ophthalmol. Vis. Sci.* **2010**, *1*, 390-395.
- [161] Dursun, D.; Wang, M.; Monroy, D.; Li, D. Q.; Lokeshwar, B. L.; Stern, M. E.; Pflugfelder, S. C. A mouse model of keratoconjunctivitis sicca. *Invest Ophthalmol Vis Sci.* **2002**, *3*, 632-638.
- [162] Kitano, S.; Kataoka, K.; Koyama, Y.; Okano, T.; Sakurai, Y. Glucose-responsive complex-formation between poly(vinyl alcohol) and poly(n-vinyl-2-pyrrolidone) with pendent phenylboronic acid moieties. *Makromol. Chem-rapid.* **1991**, *4*, 227-233.
- [163] Wang, Y.; Zhang, X.; Han, Y.; Cheng, C.; Li, C. pH- and glucose-sensitive glycopolymer nanoparticles based on phenylboronic acid for triggered release of insulin. *Carbohydr. Polym.* **2012**, *1*, 124-131.
- [164] Yang, W. Q.; Gao, X. M.; Wang, B. H. Boronic acid compounds as potential pharmaceutical agents. *Med. Res. Rev.* **2003**, *3*, 346-368.
- [165] Toshida, H.; Nakayasu, K.; Kanai, A. Effect of cyclosporin A eyedrops on tear secretion in rabbit. *Jpn. J. Ophthalmol.* **1998**, *3*, 168-173.
- [166] Stern, M. E.; Gao, J. P.; Siemasko, K. F.; Beuerman, R. W.; Pflugfelder, S. C. The role of the lacrimal functional unit in the pathophysiology of dry eye. *Exp. Eye Res.* **2004**, *3*, 409-416.
- [167] Keklikci, U.; Soker, S. I.; Sakalar, Y. B.; Unlu, K.; Ozekinci, S.; Tunik, S. Efficacy of topical cyclosporin A 0.05% in conjunctival impression cytology specimens and clinical findings of severe vernal keratoconjunctivitis in children. *Jpn. J. Ophthalmol.* **2008**, *5*, 357-362.

- [168] Lemp, M. A.; Baudouin, C.; Baum, J.; Dogru, M.; Foulks, G. N.; Kinoshita, S.; Laibson, P.; McCulley, J.; Murube, J.; Pflugfelder, S. C., et al. The definition and classification of dry eye disease: Report of the definition and classification subcommittee of the international dry eye WorkShop (2007). *Ocul Surf.* **2007**, *2*, 75-92.
- [169] Sall, K.; Stevenson, O. D.; Mundorf, T. K.; Reis, B. L.; CsA Phase 3 Study Grp. Two multicenter, randomized studies of the efficacy and safety of cyclosporine ophthalmic emulsion in moderate to severe dry eye disease. *Ophthalmol.* **2000**, *4*, 631-639.
- [170] Barber, L. D.; Pflugfelder, S. C.; Tauber, J.; Foulks, G. N. Phase III safety evaluation of cyclosporine 0.1% ophthalmic emulsion administered twice daily to dry eye disease patients for up to 3 years. *Ophthalmology* **2005**, *10*, 1790-1794.
- [171] Mantelli, F.; Tranchina, L.; Lambiase, A.; Bonini, S. Ocular surface damage by ophthalmic compounds. *Curr Opin Allergy Clin Immunol.* **2011**, *5*, 464-470.
- [172] Iester, M.; Telani, S.; Frezzotti, P.; Motolese, I.; Figus, M.; Fogagnolo, P.; Perdicchi, A.; Beta-Blocker Study Grp. Ocular surface changes in glaucomatous patients treated with and without preservatives beta-blockers. *J Ocul Pharmacol Ther.* **2014**, *6*, 476-481.
- [173] Jee, D.; Park, S. H.; Kim, M. S.; Kim, E. C. Antioxidant and inflammatory cytokine in tears of patients with dry eye syndrome treated with preservative-free versus preserved eye drops. *Invest Ophthalmol Vis Sci.* **2014**, *8*, 5081-9.
- [174] Aydin Kurna, S.; Acikgoz, S.; Altun, A.; Ozbay, N.; Sengor, T.; Olcaysu, O. O. The effects of topical antiglaucoma drugs as monotherapy on the ocular surface: A prospective study. *J Ophthalmol.* **2014**,
- [175] Shinde, U. A.; Shete, J. N.; Nair, H. A.; Singh, K. H. Eudragit RL100 based microspheres for ocular administration of azelastine hydrochloride. *J Microencapsul.* **2012**, *6*, 511-519.
- [176] Kimura, H. and Ogura, Y. Biodegradable polymers for ocular drug delivery. *Ophthalmologica.* **2001**, *3*, 143-155.
- [177] Aliabadi, H. M.; Mahmud, A.; Sharifabadi, A. D.; Lavasanifar, A. Micelles of methoxy poly(ethylene oxide)-b-poly(epsilon-caprolactone) as vehicles for the solubilization and controlled delivery of cyclosporine A. *J Control Release.* **2005**, *2*, 301-311.
- [178] Velluto, D.; Demurtas, D.; Hubbell, J. A. PEG-b-PPS diblock copolymer aggregates for hydrophobic drug solubilization and release: Cyclosporin A as an example. *Mol Pharm.* **2008**, *4*, 632-642.
- [179] Mondon, K.; Zeisser-Labouebe, M.; Gurny, R.; Moeller, M. Novel cyclosporin A formulations using MPEG-hexyl-substituted polylactide micelles: A suitability study. *Eur J Pharm Biopharm.* **2011**, *1*, 56-65.
- [180] Liu, S.; Chang, C. N.; Verma, M.; Hileeto, D.; Muntz, A.; Stahl, U.; Woods, J.; Jones, L.; Gu, F. Phenylboronic acid modified mucoadhesive nanoparticle drug carriers facilitate weekly treatment of experimentally-induced dry eye syndrome. *Nano Res.* **2014**,
- [181] Okanobo, A.; Chauhan, S. K.; Dastjerdi, M. H.; Kodati, S.; Dana, R. Efficacy of topical blockade of interleukin-1 in experimental dry eye disease. *Am. J. Ophthalmol.* **2012**, *1*, 63-71.
- [182] Oh, H. J.; Li, Z.; Park, S.; Yoon, K. C. Effect of hypotonic 0.18% sodium hyaluronate eyedrops on inflammation of the ocular surface in experimental dry eye. *J Ocul Pharmacol Ther.* **2014**, *7*, 533-42.
- [183] Di Tommaso, C.; Valamanesh, F.; Miller, F.; Furrer, P.; Rodriguez-Aller, M.; Behar-Cohen, F.; Gurny, R.; Moeller, M. A novel cyclosporin A aqueous formulation for dry eye treatment: In vitro and in vivo evaluation. *Invest. Ophthalmol. Vis. Sci.* **2012**, *4*, 2292-2299.
- [184] Cholkar, K.; Patel, S. P.; Vadlapudi, A. D.; Mitra, A. K. Novel strategies for anterior segment ocular drug delivery. *Journal of Ocular Pharmacology and Therapeutics* **2013**, *2*, 106-123.

- [185] Yavuz, B.; Pehlivan, S. B.; Unlu, N. An overview on dry eye treatment: Approaches for cyclosporin A delivery. *Scientific World Journal* **2012**, 194848.
- [186] Tracy, M. A.; Ward, K. L.; Firouzabadian, L.; Wang, Y.; Dong, N.; Qian, R.; Zhang, Y. Factors affecting the degradation rate of poly(lactide-co-glycolide) microspheres in vivo and in vitro. *Biomaterials* **1999**, *11*, 1057-1062.
- [187] Kim, K.; Yu, M.; Zong, X. H.; Chiu, J.; Fang, D. F.; Seo, Y. S.; Hsiao, B. S.; Chu, B.; Hadjiargyrou, M. Control of degradation rate and hydrophilicity in electrospun non-woven poly(D,L-lactide) nanofiber scaffolds for biomedical applications. *Biomaterials* **2003**, *27*, 4977-4985.
- [188] Lallemand, F.; Felt-Baeyens, O.; Besseghir, K.; Behar-Cohen, F.; Gurny, R. Cyclosporine A delivery to the eye: A pharmaceutical challenge. *European Journal of Pharmaceutics and Biopharmaceutics* **2003**, *3*, 307-318.
- [189] Liu, Z.; Jiao, Y.; Wang, Y.; Zhou, C.; Zhang, Z. Polysaccharides-based nanoparticles as drug delivery systems. *Adv. Drug Deliv. Rev.* **2008**, *15*, 1650-1662.
- [190] Shu, S.; Sun, L.; Zhang, X.; Wu, Z.; Wang, Z.; Li, C. Polysaccharides-based polyelectrolyte nanoparticles as protein drugs delivery system. *Journal of Nanoparticle Research* **2011**, *9*, 3657-3670.
- [191] Toda, F. Solid state organic chemistry: Efficient reactions, remarkable yields, and stereoselectivity. *Acc. Chem. Res.* **1995**, *12*, 480-486.
- [192] Boddohi, S. and Kipper, M. J. Engineering nanoassemblies of polysaccharides. *Adv Mater* **2010**, *28*, 2998-3016.
- [193] Sun, G. and Mao, J. J. Engineering dextran-based scaffolds for drug delivery and tissue repair. *Nanomedicine* **2012**, *11*, 1771-1784.
- [194] Coviello, T.; Matricardi, P.; Marianecchi, C.; Alhaique, F. Polysaccharide hydrogels for modified release formulations. *J. Controlled Release* **2007**, *1*, 5-24.
- [195] Cote, G. and Willet, J. Thermomechanical depolymerization of dextran. *Carbohydr. Polym.* **1999**, *2*, 119-126.
- [196] Korich, A. L. and Iovine, P. M. Boroxine chemistry and applications: A perspective. *Dalton Transactions* **2010**, *6*, 1423-1431.